STUDYING THE EVOLUTIONARY HISTORY AND CONSERVATION OF THE COMMON PIPISTRELLE IN TÜRKİYE BY USING ACOUSTIC AND PHYLOGENETIC ANALYSES, AND ECOLOGICAL NICHE MODELING

by

Maha Salameh

B.Sc. in Life Sciences, Lebanese University, 2017

M.Sc. in Biodiversity, Ecology and Evolution, University of Bordeaux, 2019

Submitted to the Institute of Environmental Sciences

in partial fulfillment of the requirements for the degree of

Doctor of Philosophy

in

Environmental Sciences

Boğaziçi University

2026

STUDYING THE EVOLUTIONARY HISTORY AND CONSERVATION OF THE COMMON PIPISTRELLE IN TÜRKİYE BY USING ACOUSTIC AND PHYLOGENETIC ANALYSES, AND ECOLOGICAL NICHE MODELING

APPROVED BY:

Prof. Dr. Raşit Bilgin Dissertation Advisor	. . . . .
Prof. Dr. Andrzej Furman	. . . . .
Prof. Dr. Ferhat Matur	. . . . .
Prof. Dr. Arpat Özgül	. . . . .
Assist. Prof. Dr. Hugo Rubelo	. . . . .

DATE OF APPROVAL: 23/01/2026

ACKNOWLEDGEMENTS

First and foremost, I want to thank my supervisor, Raşit Bilgin. I am grateful to him for giving me the opportunity to work on this project and welcoming me into his lab, where I never once felt like a stranger. I am thankful for his knowledge, kindness, and never-ending positive attitude, which has been a source of inspiration far beyond scientific research. He is truly exceptional, and I cannot thank him enough. I am also grateful to him for introducing me to his friends Kerem and Arpat. Kerem deserves special thanks for welcoming me into his company, where I have been collaborating for the past five years. His kindness, constructive feedback, and supportive nature make him the best boss anyone could wish for. I thank Arpat for being part of my jury and for his incredibly kind, insightful, and valuable feedback. Together, this remarkable trio made my PhD journey not only less stressful, but genuinely enjoyable. I am also grateful to Andrej for his critical comments and for always pushing me to know more and think more critically.

I am extremely thankful to my lab mates, who created such a wonderful working and living environment: Aygün, Onur, Nehir, and all the visiting students and young researchers with whom I have shared an office, ideas, teas, lab work, and much more. I especially want to thank my best friend and lab organizing partner, sometimes my therapist and sometimes my Thai food explorer companion, Merve, who has been more than welcoming from the very first day, generously sharing her knowledge and advice, and lifting my spirits on my hardest days.
I am also grateful to my colleagues at work for tolerating my stress, with special thanks to Serap and Dilara for always being my strongest supporters.

During my PhD, I had the opportunity to travel to Prague to collect samples from the National Museum, and I would like to thank Petr Benda for welcoming me there and showing me around. His love of bats was truly inspiring. I also had the wonderful opportunity to collaborate with the talented artist Gökçe Akgül, another introduction I owe to my supervisor. Gökçe brought *Pistrella* to life, the story I wrote for my Rufford Foundation-funded project. His remarkable creativity and artistic vision transformed my words into something truly magical and far beyond what I had imagined.

I am grateful to the Rufford Foundation for their financial support of the research presented in the second chapter of this thesis. This work was made possible through the 1st Rufford Small Grant.

I want to thank my family and friends who have given me confidence and support for as long as I can remember, long before this academic journey began. Special thanks to Hassan my best friend, my brother Rami for his perfectly timed check-ins to see if I was okay or spiraling into a breakdown, my sister Mona and her daughter Ward, the absolute love of my life, for bringing pure joy and unconditional love every time we video call, and my favorite cousin Lama for her thoughtful and love-filled messages that always arrived exactly when I needed them most. I also thank my best person, my biggest supporter, and my proudest fan, Ömer, for his love, kindness, and especially his patience during the final, slightly sleepless nights of writing this thesis when I was equal parts researcher and emotional wreck.

Finally, I hold a special place in my heart for my dad and my favorite person in the world, my aunt. Though they are no longer with us, I know they would have been incredibly proud and overjoyed to see this PhD completed. This one is for you both.

ABSTRACT

STUDYING THE EVOLUTIONARY HISTORY AND CONSERVATION OF THE COMMON PIPISTRELLE IN TÜRKİYE BY USING ACOUSTIC AND PHYLOGENETIC ANALYSES, AND ECOLOGICAL NICHE MODELING

Bats face escalating pressures from habitat fragmentation, climate change, and renewable energy expansion. This thesis provides a comprehensive threat assessment of the common pipistrelle (*Pipistrellus pipistrellus*), focusing on Türkiye, a critical biogeographic region between Europe, Asia, and the Middle East. By integrating population genetics, field-based acoustic monitoring, and habitat suitability modeling, this research addresses key knowledge gaps in a complex landscape. Genetic analyses building on previous phylogeographic work revealed strong mitochondrial structure consistent with a Mediterranean-centered phylogeographic history, with low divergence across western and northern Europe suggesting recent postglacial expansion. Nuclear markers showed weaker, heterogeneous spatial structure, suggesting male-biased gene flow, though expanded sampling is needed to fully resolve connectivity patterns. Field monitoring at a northwestern Turkish wind farm identified *Pipistrellus nathusii* as the primary victim of turbine collisions. Mortality peaked during autumn migration and was driven by a complex interplay of environmental variables. Notably, higher activity levels were detected near turbines when compared to a control site suggest an attractive effect, heightening collision risk. Finally, species distribution models for *P. pipistrellus* project a northward range shift and net habitat loss under future climate scenarios. Collectively, these findings underscore Türkiye's role as a conservation corridor. This multi-disciplinary framework provides evidence-based strategies for mitigating wind energy impacts and prioritizing habitat protection for migratory bats amidst global environmental shifts.

ÖZET

AKUSTİK VE FİLOGENETİK ANALİZLER İLE EKOLOJİK NİŞ MODELLEMESİ KULLANILARAK TÜRKİYE'DE CÜCE YARASANIN EVRİMSEL TARİHİNİN VE KORUNMASININ ARAŞTIRILMASI

Yarasalar, habitat parçalanması, iklim değişikliği ve yenilenebilir enerji yaygınlaşmasından kaynaklanan artan baskılarla karşı karşıyadır. Bu tez, Avrupa, Asya ve Orta Doğu arasında kritik bir biyocoğrafik bölge olan Türkiye'ye odaklanarak, cüce yarasa (*Pipistrellus pipistrellus*) türünün kapsamlı bir koruma değerlendirmesini sunmaktadır. Popülasyon genetiği, saha tabanlı akustik izleme ve habitat modellemesini entegre eden bu araştırma temel bilgi boşluklarını ele almaktadır. Önceki filocoğrafik çalışmalara dayanan genetik analizler, Akdeniz merkezli bir filocoğrafik tarihle tutarlı güçlü bir mitokondriyal yapı ortaya koymuş ve batı ve kuzey Avrupa'da düşük farklılaşmaya ve yakın zamandaki buzul sonrası genişlemeye işaret etmiştir. Çekirdek DNA belirteçleri, daha zayıf, heterojen bir mekansal yapı göstermiş ve erkek ağırlıklı gen akışının varlığını düşündürmüştür; ancak bağlantı modellerini tam olarak çözmek için daha genişletilmiş örneklemeye ihtiyaç duyulmaktadır. Kuzeybatı Türkiye'deki bir rüzgar çiftliğinde yapılan saha izlemesi, türbin çarpışmalarından birincil etkilenen türün *Pipistrellus nathusii* olduğunu göstermiştir. Ölüm oranları sonbahar göçü sırasında zirveye ulaşmış ve çevresel değişkenlerin karmaşık etkileşim göstermiştir. Özellikle, kontrol alanlarına kıyasla türbinlerin yakınında daha yüksek aktivite seviyeleri tespit edilmiştir, bu da çarpışma riskini artıran çekici bir etkiyi düşündürmektedir. Son olarak, *P. pipistrellus* türü için tür dağılım modelleri, gelecekteki iklim senaryoları altında kuzeye doğru bir dağılım kayması ve net habitat kaybı öngörmektedir. Toplu olarak, bu bulgular Türkiye'nin bir koruma koridoru olarak rolünün altını çizmektedir. Bu çok disiplinli çerçeve, küresel çevresel değişimler arasında göçmen yarasalar için habitat korumasını önceliklendirmek ve rüzgar enerjisi etkilerini azaltmak için kanıta dayalı stratejiler sunmaktadır.

TABLE OF CONTENTS

ACKNOWLEDGEMENTS..... iii
ABSTRACT..... v
ÖZET..... vi
TABLE OF CONTENTS..... vii
LIST OF FIGURES..... ix
LIST OF TABLES..... xiii
LIST OF SYMBOLS/ABBREVIATIONS..... xv
1. INTRODUCTION.....1
2. LITERATURE REVIEW..... 3
2.1. Climate Change and Constraints on Population Persistence.....3
2.2. Bat Ecology and Conservation Importance.....3
2.3. Bats as Phylogeographic Models..... 4
2.4. Phylogeography of the *Pipistrellus* Species Complex.....5
2.5. Anatolia as a Refugium, Corridor, and Contact Zone.....5
2.6. Limitations of Mitochondrial DNA.....6
2.7. Nuclear Introns as Complementary Markers.....6
2.8. Current and Future Threats.....7
2.9. Implications for Climate-Driven Range Shifts.....9
3. CHAPTER 1: EVOLUTIONARY HISTORY AND GENETIC STRUCTURE OF *Pipistrellus pipistrellus*.....11
3.1. Introduction.....11
3.2. Materials and Methods.....14
3.2.1. Sample Collection.....14
3.2.2. Genomic DNA Extraction.....16
3.2.3. Mitochondrial DNA.....16
3.2.3.1. Phylogenetic Reconstruction and Demographic History.....19
3.2.4. Nuclear DNA.....20
3.2.4.1. Designing Primers.....20
3.2.4.2. Phylogenetic Reconstruction and Demographic History.....22
3.3. Results.....23
3.3.1. Mitochondrial DNA Analyses.....23
3.3.2. Nuclear DNA Analyses.....36

3.3.2.1. The intron 4 of the *COPS7A* gene....36
3.3.2.2. The intron 5 of the *ABHD11* gene....40
3.4. Discussion.... 46
4. CHAPTER 2: UNDERSTANDING BAT ACTIVITY AND MORTALITY PATTERNS IN A WIND FARM IN TÜRKİYE....50
4.1. Introduction....50
4.2. Materials and Methods....54
4.2.1. Site Description....54
4.2.2. Acoustic Surveys....54
4.2.3. Bat Carcasses....55
4.3. Results....56
4.3.1. Carcass Collection Analyses....60
4.3.2. Field Survey Conditions....65
4.4. Discussion....71
5. CHAPTER 3: ECOLOGICAL NICHE MODELING OF THE COMMON PIPISTRELLE....75
5.1. Introduction....75
5.2. Materials and Methods....77
5.2.1. Study Area and Presence Records....77
5.2.2. Preparation of the Occurrence Data....78
5.2.3. Preparation of the Environmental Layers for the Current Prediction Model....79
5.2.4. Operations on the Presence Records....80
5.2.5. Operations on the Environmental Variables....81
5.2.6. Selecting Ecologically Relevant Environmental Variables....82
5.2.7. Standardizing the Variables....85
5.2.8. Ecological Interactions for the Species Distribution Model....85
5.3. Results....86
5.3.1. Correlation Matrix....86
5.3.2. MaxEnt Operations....88
5.3.3. Future Projections....92
5.4. Discussion....94
6. CONCLUSION, LIMITATIONS AND FUTURE RECOMMENDATIONS....97
REFERENCES....101
APPENDIX A: INFORMATION ON THE SAMPLES OF THE STUDY....123

LIST OF FIGURES

Figure 3.1. Geographic distribution of sampling localities of collected specimens for the mitochondrial DNA (mtDNA) component of the study.....15

Figure 3.2. Schematic representation of primer placement for intron amplification.....21

Figure 3.3. Map representing the geographic distribution of the selected samples for nuclear DNA analyses…….22

Figure 3.4. Haplotype network generated by PopART to visualize the relationships between the mitochondrial DNA sequences from different geographic regions.……..26

Figure 3.5. Neighbor-Joining Bootstrap consensus tree.……...29

Figure 3.6. Maximum Likelihood Bootstrap consensus tree…..……30

Figure 3.7. Heatmap of pairwise FST values among geographic regions based on mitochondrial DNA sequences…….....31

Figure 3.8. Bayesian Skyline Plots showing historical changes in effective population size (Ne) for five geographic regions: (a) Anatolia, (b) British Isles, (c) Eastern Europe, (d) Middle East, and (e) Western Europe.…….35

Figure 3.9. Bayesian Skyline Plot for all populations combined, showing overall demographic history of *Pipistrellus pipistrellus* across its range based on mtDNA HVII sequences.…….….35

Figure 3.10. Haplotype network of the nuclear intron *COPS7A* constructed in PopART..……...38

Figure 3.11. Neighbor-Joining Bootstrap consensus tree……..38

Figure 3.12. Maximum Likelihood Bootstrap consensus tree……...39

Figure 3.13. Pairwise FST estimates among geographic regions based on the *COPS7A* nuclear marker.……....……....40

Figure 3.14. Haplotype network of the nuclear intron *ABHD11* constructed in PopART…….....43

Figure 3.15. Neighbor-Joining bootstrap consensus tree.……..43

Figure 3.16. Maximum Likelihood bootstrap consensus tree. ……..44

Figure 3.17. Pairwise FST estimates among geographic regions based on the *COPS7A* nuclear marker.……....……....45

Figure 4.1. A map showing the location of the turbines in the Wind Farm..……..54

Figure 4.2. A graph showing bat passes per Month by Condition..……57

Figure 4.3. Pearson correlation and significance between bat count and noise count across all recording conditions……58

Figure 4.4. Bat species composition recorded during survey nights under different conditions...60

Figure 4.5. Total number of carcasses per month.……60

Figure 4.6. Map showing the number of carcasses found under each turbine.……..61

Figure 4.7. Photographs taken by Emre Çetin (Bird surveyor in the wind farm) of dead bats getting attacked by insects.……61

Figure 4.8. Bat carcass species composition by turbine.……62

Figure 4.9. Monthly bat activity and carcass observations at turbines (July–November 2024)….62

Figure 4.10. Monthly trends of bat count and carcass count. Solid lines: bat counts, dashed lines: carcass counts (scaled).……63

Figure 4.11. A graph showing bat activity vs carcass count by turbine condition.……64

Figure 4.12. Pearson correlation coefficients (r) between monthly weather variables (rows) and bat activity (Bat counts) recorded during two sampling nights per month.……66

Figure 4.13. Photos showing wood storage by local workers in the area under a turbine.…..…..69

Figure 4.14. A box plot of bat count by wood storage presence..……..70

Figure 4.15. A box plot of bat count by turbine brand.……..……70

Figure 5.1. Map of all the *Pipistrellus pipistrellus* records (blue circles) obtained for this study, shown in the WGS 84 geographic coordinate reference system(EPSG:4326)……78

Figure 5.2: Spatial Distribution Map covering Europe to Western Asia……70

Figure 5.3. Plot showing the thinning results of the presence records from Europe...…….……..81

Figure 5.4. Correlation matrix of all the environmental variables..…….... 87

Figure 5.5. Variance inflation factor (VIF) scores for selected variables……88

Figure 5.6. MaxEnt model performance evaluation showing (a) ROC curve with AUC = 0.895, (b) True Skill Statistic optimization, (c) sensitivity and specificity trade-offs.…..….90

Figure 5.7. Variables contributions to Maxent (%).……90

Figure 5.8. Binary Habitat Suitability map.……91

Figure 5.9. Continuous Habitat Suitability map.……91

Figure 5.10. Habitat suitability projections for 2041-2060 across five global climate model……93

Figure 5.11. Ensemble mean habitat suitability projection (2041-2060).……..93

Figure 5.12. Projected habitat change categories from current to future conditions..……94

Figure A.1. Geographic distribution of mtDNA haplotypes of the Mixed cluster. Sampling localities are color-coded by geographic region…….136

Figure A.2. Geographic distribution of mtDNA haplotypes of the Western Europe cluster. Samples originate from France, Spain, Portugal, and England…….137

Figure A.3. Geographic distribution of mtDNA haplotypes of the British Isles cluster, including samples from France, Italy, Northern Ireland, Ireland and England. …….137

Figure A.4. Geographic distribution of mtDNA haplotypes of the Southern Europe cluster. Samples originate from Sicily, Corsica, and Malta. Star-shaped symbols indicate samples that did not cluster and originate from Greece, Northern Ireland, and Spain.……138

Figure A.5. Geographic distribution of mtDNA haplotypes of the Eastern Europe cluster. Samples originate from Ukraine, Russia and Iran.……138

Figure A.6. Geographic distribution of mtDNA haplotypes of the Central Asia and Middle East clusters. The Central Asia cluster (green) includes samples from northeastern Iran, Turkmenistan, and Tajikistan. The Middle East cluster (dark blue) comprises samples from Anatolia, Russia, Cyprus, Lebanon, Syria, Jordan, and one sample from central Iran.……139

Figure A.7. Geographic distribution of mtDNA haplotypes of the Anatolia cluster..……139

Figure A.8. Geographic distribution of mtDNA haplotypes within the North African clusters. Cluster 1 includes samples from Tunisia, Algeria, and Morocco, whereas Cluster 2 comprises two closely located samples from Morocco...……140

LIST OF TABLES

Table 3.1. Sampling locations and sample sizes. N(HVII) indicates the number of samples sequenced for the HVII region…….…….…….……17

Table 3.2. Genetic diversity metrics across regions, based on mitochondrial DNA sequences….24

Table 3.3. Summary of neutrality tests: Tajima's D, Fu's Fs metrics across regions, based on mitochondrial DNA sequences……..……..…….25

Table 3.4. Genetic diversity metrics across regions, based on nuclear DNA sequences of the intron 4 of the *COPS7A* gene. ……..37

Table 3.5. Genetic diversity metrics across regions, based on nuclear DNA sequences of the intron 5 of the *ABHD11* gene……41

Table 3.6. Summary of neutrality tests: Tajima's D, Fu's Fs metrics across regions, based on nuDNA sequences of the intron 5 of the *ABHD11* gene...……..53

Table 4.1. Summary of the various attraction hypotheses.……..53

Table 4.2.a. Monthly bat detections by condition….……...56

Table 4.2.b Monthly noise counts by condition.……..56

Table 4.3. Recorded bat species, their IUCN status and their number of passes for each condition in all the visits in this study. ……..58

Table 4.4. Correlations by Condition. ……65

Table 4.5. Monthly averages of weather conditions on recording nights..……..65

Table 4.6. Mean weather conditions averaged over the three days preceding bat carcass detection events……..67

Table 4.7. Pearson correlations between weather variables and bat carcass counts..……..60

Table 5.1. Environmental variables chosen to be used in MaxEnt..……83

Table A.1. Summary of sample origin, geographic information (country and/or city), sample type, and ownership information for specimens used in Chapter 1.……...…123

Table A.2. Geographic and clade-based summary of mtDNA haplotypes identified in the haplotype Network..……..….125

Table A.3. Classification of the countries of each sample according to global regions...……...….135

Table A.4. Nuclear DNA haplotypes (*COPS7A* and *ABHD11*) and sampling coordinates of analyzed individuals.……...…140

Table A.5. Neutrality test results (Tajima's D and Fu's Fs) based on nuDNA sequences of the intron 4 of the *COPS7A* gene by region……..….141

Table A.6. Summary of the species of bat carcasses collected from under different Turbines between March and November (Chapter 2). ..……..….142

LIST OF SYMBOLS/ABBREVIATIONS

Symbol	Explanation
%	Percent
°C	Degree Celsius
~	Approximately
Hz	Hertz
KHz	Kilo Hertz
m	Meters
Ma	Megaannum (Million years)
MW	Megawatt
U	Units
U/µl	Units per microliter
bp	Base pair
km	kilometer
km²	Square kilometer
min	Minutes
mm	Millimeter
mM	Millimole
m/s	Meters per second
µl	Microlitre
µM	Micromole
s	Seconds

Abbreviation	Explanation
A	Adenine
ACCESS-CM2	Australian Community Climate and Earth-System Simulator Coupled Model version 2
AUC	Area Under the Curve
Aug	August
BED	Browser Extensible Data
Bio1	Annual Mean Temperature
Bio4	Temperature Seasonality
Bio15	Precipitation Seasonality

C	Cytosine
CCI	Climate Change Initiative
CMIP6	Coupled Model Intercomparison Project Phase 6
CO_2	Carbon dioxide
DEM	Digital Elevation Models
dNTP	Deoxyribonucleotide triphosphate
DNA	Deoxyribonucleic Acid
E	East (longitude)
EC-Earth3-Veg	European Consortium Earth System Model version 3 with Vegetation module
Edge_Heter Int	Edge Habitat x Landscape Heterogeneity
EEC	European Economic Community
ENM	Ecological Niche Models
EOG	Earth Observation Group
ESA	European Space Agency
G	Guanine
GBIF	Global Biodiversity Information Facility
GCM	Global Climate Models
GMTED	Global Multi-resolution Terrain Elevation data
GWEC	Global Wind Energy Council
h	Number of Haplotypes
HadGEM3-GC31-LL	Hadley Centre Global Environment Model version 3 – Global Coupled 3.1 – Low Resolution
Hd	Haplotype Diversity
HVII	Hypervariable Domain II
IUCN	International Union for Conservation of Nature
Jul	July
LC	Least Concern
MgCl2	Magnesium Chloride
MIROC6	Model for Interdisciplinary Research on Climate version 6 (Japan)
mRNA	Messenger RNA
ML	Maximum Likelihood
MCMC	Markov Chain Monte Carlo
MPI-ESM1-2-HR	Max Planck Institute Earth System Model version 1.2 – High Resolution

mtDNA	Mitochondrial Deoxyribonucleic Acid
N	North (latitude)
NJ	Neighbor-Joining
N. leislerii	*Nyctalus leislerii*
N. noctula	*Nyctalus Noctula*
NOAA	National Oceanic and Atmospheric Administration
Nov	November
ns	non-significant
NT	Nearly Threatened
Oct	October
p	p-value
PCR	Polymerase Chain Reaction
P. nathusii	*Pipistrellus nathusii*
P. pipistrellus	*Pipistrellus pipistrellus*
P. pipistrellus SW	*P. pipistrellus* from Maghreb and central Mediterranean
π / Pi	Nucleotide diversity
r	Pearson correlation coefficient
ROC	Receiver Operating Characteristic
S	South (latitude)
s.str.	sensu stricto
SDM	Species distribution models
Sd	Standard Deviation
Sep	September
sp.	species
SRTM	Shuttle Radar Topography Mission
SSP2-4.5	Shared Socioeconomic Pathway 2
summer_wind_avg	Average of Summer wind speed
T	Thymine
Tn (e.g., T20)	Turbine number
TSS	True Skill Statistic
Urban_Water Int	Urban Proportion x Water Proximity
v	Version
VIF	Variance Inflation Factor
VIIRS	Visible Infrared Imaging Radiometer Suite
VU	Vulnerable

w	Wilcoxon rank-sum test
W	West (longitude)

1. INTRODUCTION

Climate change provides a severe and growing threat to biodiversity when combined with habitat loss and other causes of environmental degradation. Evidence gathered over the last 30 years suggests that communities' composition and dynamics, species biogeography, and organisms' phenology are altering in response to a changing climate (Walther et al., 2002). Although in the past 420,000 years, at least four significant events have been associated with climate change (Petit et al., 1999), according to IUCN assessments its current rate is seriously threatening many species (Bradshaw and Holzapfel, 2006). The impact of global climate change may vary greatly as a result of the unequal scale of change across the globe and the variety in reactions of individuals, groups, or species (Hunter et al., 2010). According to estimates, current extinction rates are much higher than what is expected under natural conditions, and climate change played a significant role in earlier major extinction events (Barnosky et al., 2011). The International Union for the Conservation of Nature estimates that 52 species of mammals, birds, and amphibians get one step closer to extinction every year due to climate change (Hoffmann et al., 2010).

The Red List Index also indicates that mammals are in decline, and more species are entering categories with increasing extinction risks every year. These negative trends are expected to last into the twenty-first century (Pereira et al., 2010). Due to their sensitivity to environmental stress and poor reproduction rates, bats, along with other mammals, are frequently in decline (Jones et al., 2009). They are among the most diversified and widely dispersed groups of mammals (Yalden & Morris 1975) and their role in the environment is extremely important. By performing their role as pollinators, they considerably improve ecosystem services by managing insect populations, and dispersing nutrients across the environment (Pierson 1998; Boyles et al., 2011). Hence their conservation is critical from an ecosystem perspective as well.

The identification of distinct evolutionary lineages with little morphological differentiation has been made possible by phylogeographical analyses, which have had a significant impact on the field of animal conservation (Bermingham et al., 1998; Hammond et al., 2001; Roman et al., 1999). *Pipistrellus pipistrellus* is an interesting species to be studied in this phylogeographic conservation perspective, since although it is one of the most common bats in the Mediterranean region and Europe, there is a significant gap in our understanding of its phylogeographic history in the Middle East, Anatolia, and Asia. In the first chapter, we used *P. pipistrellus* samples representatively covering the ranges of this species in detail to study the genetic differences between its different groups, enabling

a combination of phylogeographic and comparative population genetic approaches Our sampling extensively represented the previously understudied Middle East and Anatolia, with samples extending into Central Asia and across Europe. In the second chapter, bats activity and mortality in a wind farm in Türkiye was evaluated. Generating electricity from renewable sources, such as wind power, is one strategy to lessen the consequences of climate change (Kiesecker et al., 2011). Nevertheless, one of the unintended outcomes that, regrettably, may endanger the persistence of bat species is bat mortality at wind farms (Frick et al., 2017). However, the factors contributing to fatalities caused by wind turbines are complex. They include physiological and behavioural factors, habitat and weather-related factors like wind and temperature (Guest et al., 2022). To create effective mitigation measures, understanding bat interactions with wind turbines is essential. Chapter 2 provides a descriptive analysis of bat activity and mortality patterns at a Turkish wind farm, exploring relationships with environmental conditions and turbine operational status. As one of the first studies of its kind in Turkey, this chapter establishes baseline data for a previously understudied region while acknowledging limited generalizability due to the single-site design.

Changes in land use, driven by increased agriculture and urbanization, have eliminated valuable bat habitats while also accelerating the effects of climate change, which threaten both bats and their ecosystem services (Williams et al., 2008). Even though there is a variety of knowledge on the usage of bat habitat in many regions (Furlonger et al., 1987; Walsh and Harris 1996a, b; Vaughan et al., 1997a, b), little to nothing is known about the preferred habitats of bats in the Mediterranean region. The common pipistrelle, one of the most common bats in this biodiversity hotspot (Blondel et al., 2010), is known for its highly opportunistic selection of foraging locations (Vaughan et al., 1997a). Understanding habitat suitability is particularly important for this species given its wide distribution and potential genetic structure. Ecological niche modelling (ENM) uses species occurrence data and environmental variables to assess habitat suitability across geographic space and predict distributional shifts under environmental change (Graham et al., 2004; Hosseinian et al., 2016). In the third chapter, we developed ENMs for *P. pipistrellus* under current and future climate change scenarios to evaluate potential range shifts in response to climate change.

2. LITERATURE REVIEW

2.1. Climate Change and Constraints on Population Persistence

At the beginning of the 21st century, climate change emerged as a significant issue, receiving attention from both mainstream media and specialized scientific journals. It is considered one of the most significant threats to biodiversity in the Anthropocene and is expected to significantly alter species distributions over the next few years (Parmesan & Yohe, 2003; Chen et al., 2011). Several species have already been impacted, including proven effects on phenology, global distribution, and local survival (McMahon & Burton, 2005). Temperature-related changes are impacting over 100 species (Root et al., 2003). Recent research indicates that the effects of global climate change are expected to be far more severe, with global temperatures projected to rise by up to 6°C (Hegerl et al., 2007). Moreover, due to rapid climate shifts, populations tend to migrate to more suitable habitats outside their historical ranges, which can cause population fragmentation and lead to local extinctions (Thomas et al., 2004; Bellard et al., 2012). However, if these circumstances persist for extended durations, it is probable that other conservation challenges may emerge, such as reduction in genetic diversity and elevated inbreeding levels between species persisting in isolated populations (Ezard & Travis, 2006), hence threatening the survival of the remaining populations. Human activities, especially land conversion and habitat degradation, are significant drivers of species extinctions (Dirzo et al., 2014; Newbold et al., 2015). The ability of species to survive under these circumstances depends primarily on their capacity to follow suitable habitats via dispersal, to sustain genetic connectivity across gradually fragmented landscapes, and to have necessary evolutionary potential for adaptation to new environmental conditions (Hoffmann & Sgrò, 2011; Alsos et al., 2012).

2.2. Bat Ecology and Conservation Importance

Bats represent more than twenty per cent of mammalian biodiversity worldwide (Burgin et al., 2018, Frick et al., 2020, Mammal Diversity Database 2025). Over one third of bat species evaluated by the International Union for the Conservation of Nature (IUCN) are classified as either threatened (15%) or data deficient (18%) (Frick et al., 2020). Bat populations globally face increasing threats from habitat destruction, disease, and climate change, despite their adaptive radiation into various food and roosting niches (Jones et al., 2009; Frick et al., 2020). The physiological limitations related to flight, such as elevated metabolic rates and restricted thermoregulatory abilities in numerous species, make bats especially vulnerable to temperature and precipitation patterns (Speakman &

Thomas, 2003; Sherwin et al., 2013). Moreover, their dependence on specific roost microclimates, seasonal insect availability, and geographically distinct foraging zones establishes intricate habitat necessities that may be compromised by changing climate conditions (Adams & Hayes, 2008; Rebelo et al., 2010). The decline of bat populations will result in a reduction or loss of the ecosystem services they provide. Humans worldwide obtain direct and indirect advantages from the ecological services provided by bats, including the control of arthropods, such as agricultural and forest pests, seed dissemination, pollination, and nutrient redistribution through feces (guano) (Kunz et al., 2011; Ghanem & Voigt, 2012). Therefore, effective conservation requires an understanding of habitat requirements and population dynamics. However, the conservation of bat habitats is challenging due to the species' cryptic behavior, their requirement for roosts with specific microclimatic conditions that change throughout their annual cycle necessitating frequent roost changes, the lack of data regarding the hibernation sites of most bat species, and the absence of visible signs of their roosting, making the identification of roosts exceedingly challenging (Lausen et al., 2022). These challenges are compounded by climate change, which is altering the environmental conditions that determine habitat suitability across species' ranges. Understanding species' responses to historical climatic variations is crucial for forecasting their resilience to current and future environmental changes (Hewitt, 2000; Nogués-Bravo et al., 2018). Multiple complementary approaches are therefore necessary to assess bat populations and inform conservation strategies.

2.3. Bats as Phylogeographic Models

Understanding how historical processes have shaped modern genetic diversity is essential for predicting how species will respond to current environmental changes. Phylogeography combines elements of population genetics, phylogenetics, and biogeography to map out the spatial and temporal distribution of genetic lineages, offering valuable insights into species' responses to historical climatic and geological changes (Avise, 2000). Bats represent a particularly informative group for phylogeographic and population genetic studies. Considering their ability to fly, numerous bat species display significant genetic structure, influenced by factors such as extended longevity, low reproduction rates, complex social structures, and sex-biased dispersal (Burland & Worthington-Wilmer, 2001). In numerous temperate bat species, females exhibit pronounced philopatry to their natal roosts, while males disperse more extensively, resulting in distinct patterns of genetic structure between maternally inherited mitochondrial DNA (mtDNA) and biparentally inherited nuclear markers (Castella et al., 2001; Kerth et al., 2002). Phylogeographic research across Europe has revealed that Pleistocene variations in climate significantly influenced the gene pool of various bat species, with southern locations, including the Iberian Peninsula, Italy, the Balkans, and Anatolia,

serving as key refugia during glacial maxima (Ruedi & Castella, 2003; Rossiter et al., 2007). Unlike highly migratory bat species that frequently exhibit minimal genetic structure over broad geographic areas, stationary species generally demonstrate pronounced phylogeographic separations and isolation-by-distance patterns (Burland et al., 1999; Rivers et al., 2005). These characteristics make bats especially suitable for investigating the interplay between historical climatic processes, dispersal, and population connectivity.

2.4. Phylogeography of the *Pipistrellus* Species Complex

The genus *Pipistrellus* includes one of the most widely distributed bat groups in the Palearctic. It serves as a model system for studying cryptic diversity and the initial stages of speciation. The identification of cryptic species within the common pipistrelle (*Pipistrellus pipistrellus* sensu lato) has shown the limitations of morphology-based taxonomy and highlighted the efficacy of molecular and acoustic methodologies (Barratt et al., 1997; Mayer & von Helversen, 2001). Further studies have revealed that the *Pipistrellus pipistrellus* species complex comprises several divergent mitochondrial lineages, with centers of variation located in the Mediterranean Basin (Hulva et al., 2004, 2007).

These findings suggest that the Mediterranean region facilitated lineage diversification through numerous periods of isolation and secondary contact, acting as both a center of radiation and a refugial zone. The complex geomorphology and paleoclimatic history of the region enabled the creation and breakdown of barriers to gene flow, resulting in a mosaic of lineages at various stages of divergence. Although mitochondrial data have been essential in revealing this diversity, the degree to which these mtDNA lineages align with genome-wide differentiation and long-term population isolation remains an unresolved issue.

2.5. Anatolia as a Refugium, Corridor, and Contact Zone

As a key center of genetic diversity for the western Palearctic biota, Anatolia occupies an essential biogeographic location at the intersection of Europe, Asia, and the Middle East (Hewitt, 1999; Médail & Diadema, 2009). Its complicated geography, numerous geographic obstacles, and comparatively moderate climate during glacial periods likely allowed populations to persist when conditions in central and northern Europe became unfavorable. Anatolia has been identified as a refugium and a source of post-glacial recolonization, as well as a region with endemic lineages and cryptic diversity, according to phylogeographic studies conducted across a broad range of species (Bilgin et al., 2006, 2009; Bilgin, 2012).

Multiple studies have revealed genetically distinct Anatolian lineages in bats, suggesting that eastern populations may represent cryptic species or independent evolutionary units (Furman et al., 2010). However, compared to European refugial locations, Anatolia is still relatively understudied, and many taxa still lack extensive, regionally targeted sampling. Understanding whether Anatolian populations of widespread species, such as *Pipistrellus*, are extensions of European populations, distinct lineages, or admixture zones is essential for reconstructing the evolutionary history and setting conservation priorities in a region under increasing anthropogenic pressure.

2.6. Limitations of Mitochondrial DNA

Mitochondrial DNA is extensively utilized in phylogeographic research because of its rapid evolutionary rate, absence of recombination, and straightforward amplification with universal primers (Avise, 2000). These characteristics made mtDNA very valuable for understanding past population structure and identifying divergent lineages. However, mtDNA constitutes a singular, maternally inherited locus and hence embodies merely one genealogical lineage, thus failing to depict species-level evolutionary events adequately. Numerous factors can bias mtDNA-based findings, such as poor lineage sorting, introgression, selective sweeps, heteroplasmy, and the existence of nuclear mitochondrial pseudogenes (Balloux, 2010; Galtier et al., 2009). Consequently, dependence solely on mtDNA may exaggerate population differentiation or inaccurately represent the timing and extent of lineage divergence. According to coalescent theory, stochastic variation in lineage sorting, especially in recently separated or large populations, will cause distinct loci to have distinct genealogical histories (Hudson, 1990; Wakeley, 2009). Therefore, a multilocus strategy incorporating distinct genetic markers is necessary for robust inference of phylogeographic structure and demographic history.

2.7. Nuclear Introns as Complementary Markers

The evaluation of both male- and female-mediated gene flow is made possible by nuclear loci, which offer a genome-wide perspective on genetic variation. In addition, the larger adequate population size of nuclear genes increases the influence of coalescent stochasticity, reinforcing the need to sample multiple unlinked loci (Knowles & Maddison, 2002). However, nuclear genes typically evolve more slowly than mitochondrial genes and, when used individually, may lack sufficient variability for intraspecific analyses. Among nuclear markers, introns represent particularly suitable candidates for phylogeographic and population genetic studies at shallow evolutionary timescales. Introns, as non-coding areas, have weaker selective pressures compared to exons and can

accumulate high levels of neutral variation. Simultaneously, they might be easily amplified utilizing primers crafted in adjacent exons, avoiding many of the technical challenges associated with intergenic regions (Chojnowski et al., 2008; Salicini et al., 2011). Although introns vary widely in evolutionary rate and not all are equally informative, careful selection of single-copy introns of appropriate length has been shown to provide robust resolution of recent phylogenetic relationships and population structure (Foley et al., 2015; Jarvis et al., 2014).

Comparative studies have shown that nuclear introns can complement the signals from mitochondrial DNA (mtDNA) by identifying patterns of gene flow and lineage divergence that are not evident from mitochondrial data alone, thus refining the understanding of species history and population connectivity (Puechmaille et al., 2011).Incorporating mitochondrial and nuclear data into a multilocus framework offers an effective method for identifying genetically different populations and evaluating their connection. This knowledge is crucial for conservation planning, especially for bat species confronting escalating threats from habitat alteration, climate change, and wind energy development. In locations like Anatolia, characterized by high biodiversity and increasing conservation demands, comprehensive phylogeographic and population genetic analyses are essential for assessing the evolutionary importance of local populations and for prioritizing conservation initiatives. A multilocus strategy that integrates mitochondrial DNA (mtDNA) and nuclear introns provides the clarity needed to connect historical events with current conservation issues for widely distributed yet genetically organized taxa such as *Pipistrellus pipistrellus*.

2.8. Current and Future Threats

Although phylogeographic studies provide valuable insight into how *Pipistrellus pipistrellus* responded to past climatic changes, these historical patterns do not necessarily predict how populations will respond under present and future conditions. While renewable energy infrastructure has become essential for mitigating greenhouse gas emissions, one of the main drivers of anthropogenic climate change, multiple studies revealed that wind turbines significantly contribute to bat mortality, particularly in late summer and early fall, coinciding with migratory, dispersal, and mating periods (Arnett et al., 2008; Cryan et al., 2012). Consequently, there is concern that turbine-related fatalities disproportionately decrease the dispersing individuals, a part of the population essential to sustaining gene flow (Burland & Worthington-Wilmer, 2001), resulting in patterns that resemble those generated by historical barriers and observed in phylogeographic studies (Avise, 2000; Slatkin, 1987; Holderegger & Wagner, 2008). Consequently, understanding patterns of genetic connectivity is essential for evaluating whether wind farm mortality represents a reversible

demographic impact or a longer-term evolutionary threat with implications for population persistence and adaptive potential (Latch et al., 2006; Frick et al., 2017).

Ultrasonic acoustic monitoring is widely used to assess bat activity and estimate collision risk at operating wind energy facilities. By automatically recording echolocation calls and storing them for subsequent species identification and activity quantification, acoustic detectors provide a non-invasive method for evaluating the presence of bats and temporal patterns of activity around turbines (Korner-Nievergelt et al., 2013). This data allows researchers to correlate bat activity with environmental variables that can influence bat flight behavior and collision risk. Knowledge of these environmental drivers has been instrumental in the development of mitigation strategies aimed at reducing turbine-related bat mortality. Among operational measures tested to date, increasing turbine cut-in speed has consistently proven to be the most effective means of reducing fatalities. Because bat activity typically declines at higher wind speeds, curtailing turbine operation during low-wind periods, particularly during seasons of high bat activity, can substantially reduce mortality (Arnett et al., 2011; Baerwald et al., 2009; Mantoiu et al., 2020). More targeted mitigation approaches have been developed, including adaptive curtailment strategies that use real-time bat activity thresholds rather than fixed wind-speed limits to regulate turbine operation (Behr et al., 2011; Lagrange et al., 2013). While these approaches show promise, their effectiveness ultimately depends on understanding the ecological mechanisms driving bat interactions with wind turbines.

Although research on bat mortality at wind energy sites has increased substantially, the ecological factors driving bats' interactions with wind turbines remain poorly understood. In particular, it is critical to distinguish between incidental encounters driven by local bat activity and interactions resulting from active attraction. These mechanisms imply fundamentally different approaches to turbine placement, operational mitigation, and landscape-level planning. The issue of bat mortality at wind energy facilities is of particular relevance in Türkiye, where renewable energy development has accelerated following the adoption of the National Energy Policy in 2017. Türkiye has an estimated wind energy potential of approximately 48,000 MW, and the number of installed turbines has increased rapidly over the past decade. This expansion is expected to continue, raising concerns about cumulative impacts on bat populations. Monitoring data from multiple regions of Türkiye indicate that bat fatalities occur across a range of species, with *Pipistrellus pipistrellus*, and *Pipistrellus nathusii* often among the most frequently recorded taxa (KAB Ecology, unpublished). This pattern may reflect a combination of high local abundance, species-specific flight behavior, and detectability due to characteristic echolocation calls. Importantly, frequent occurrence in fatality datasets does not necessarily imply higher vulnerability at the population level, but it highlights the

need for species-specific assessments within a broader comparative framework. However, comprehensive, long-term datasets remain scarce, limiting the ability to assess population-level consequences. This knowledge gap is particularly concerning, given that wind turbine mortality acts in concert with other pressures, including climate change, insect population declines, and ongoing habitat loss (Hallmann et al., 2017; Frick et al., 2020).

Given the rapid expansion of wind energy infrastructure and the lack of robust population data for most bat species, prioritizing systematic and long-term monitoring is essential. Integrating acoustic monitoring with demographic and genetic data can improve estimates of population status, connectivity, and vulnerability, thereby strengthening the scientific basis for mitigation and management decisions (Jones et al., 2009; Hale et al., 2021). A clearer understanding of whether bat mortality at wind farms is driven primarily by habitat-related activity patterns or by turbine-specific attraction will be critical for designing effective and evidence-based conservation strategies.

2.9. Implications for Climate-Driven Range Shifts

Projections of species' responses to future climate change frequently assume that suitable habitat, once created, can be occupied. However, phylogeographic structure, dispersal behaviour, and anthropogenic mortality collectively challenge this assumption. Species distribution models (SDMs) have become the primary tools for forecasting range shifts under climate change, yet their outputs are highly sensitive to assumptions regarding dispersal capacity and landscape permeability (Araújo et al., 2006; Elith & Leathwick, 2009).

For bats, SDM projections suggest substantial redistribution of suitable habitat under warming scenarios, including northward shifts and contractions at southern range margins (Rebelo et al., 2010). However, the ability of populations to successfully navigate intervening environments determines how realistic these possible distributions are. When wind energy production is positioned along migratory corridors, it may act as a selective filter on migration, decreasing the likelihood that bats will follow quickly changing climate conditions. This raises the risk of extinction by making dispersal harder, in which populations continue to exist in declining habitats for a while without settling in newly appropriate locations.

When interpreting SDM outputs, phylogeographic data offer valuable baseline information. Even if climatic conditions improve elsewhere, populations with deep genetic divergence or historically low connectivity may be less able to contribute to range expansion. Conversely, if current

mortality pressures do not interfere with dispersal processes, genetically related populations might be better able to adapt to climate change.

These factors emphasize the need for integrative strategies that clearly connect evolutionary history, current threats, and climate projections for the future. Genetic information reveals current patterns of connectivity, identifies possible obstacles to gene flow, and indicates which populations represent long-standing evolutionary lineages. Where and when dispersal may be selectively restricted is made clear by empirical research on wind turbine mortality. Models of species distribution predict where favorable climate conditions will either appear or vanish over the next several decades. Combining these approaches can provide a framework for evaluating whether *Pipistrellus pipistrellus*'s historical resilience can be sufficient to withstand the combined pressures of growing renewable energy infrastructure and climate change.

3. CHAPTER 1: EVOLUTIONARY HISTORY AND GENETIC STRUCTURE OF *Pipistrellus pipistrellus*

3.1. Introduction

Habitats and ecosystems have undergone significant alteration as a result of human activity and climate change (Baker and Harris, 2007). Like other organisms, bat populations and species are also threatened (Tsang et al., 2016) by the same processes that resulted in the current biodiversity crisis. Due to their widespread distribution and significant biological diversity, bats make good models for studying evolutionary, ecological, and theoretical issues in ecology and evolutionary biology. Fundamental research that depends heavily on the understanding of the diversity and evolutionary relationships of bat species over time is also necessary to put conservation methods into perspective. Phylogenies are an essential starting point for understanding the patterns and processes involved in bats' diversification and speciation, which are also necessary for making conservation decisions. They are used to identify distinctive lineages that retain significant genetic diversity (evolutionarily significant units) (Moritz 1994), predict the location of biodiversity hotspots, and determine how distinct populations may be related at some genetic level, among others (Tsang et al., 2016).

With molecular tools, phylogenies and population networks can be better understood, opening new possibilities for defining species and other conservation-related units. For instance, The National Strategy for Biological Diversity of Germany (Federal Ministry for the Environment, Nature Conservation and Nuclear Safety [BMU], 2007)) acknowledges the need to consider the genetic makeup of organisms and their species boundaries when it comes to conservation concern. In addition, genetics can also help identify cryptic species and help detect previously unrecognized portions of a region's biota. The European pipistrelle (*Pipistrellus pipistrellus*) is a good example of a cryptic species complex, and it is one of the most common bats in its habitat. It was not until echolocation data revealed that several pipistrelle species were coexisting in sympatry across most of Europe that it was recognized as a cryptic species complex (Jones and van Parijs 1993; Barlow and Jones 1997). Since the first studies on echolocation, data on foraging (Davidson-Watts and Jones 2005), mitochondrial DNA (Hulva et al., 2004), micro-satellites (Hulva et al., 2010), and habitat selection (Davidson-Watts et al., 2006) have backed up the classification of the European pipistrelle as two separate species (*Pipistrellus pipistrellus* (Schreber, 1774) and *Pipistrellus pygmaeus* (Leach, 1825)).

Historical models comprise another approach that can be incorporated into research to help understand the influence of micro-evolutionary processes on species histories, by providing information on population genetics and phylogeography (Edwards and Beerli 2000). Although bats are the second most varied order of mammals, few phylogeographic studies have been conducted on them than on less diversified orders of mammals (Hulva et al., 2004). Traditionally, there are two subspecies of the P. pipistrellus: *P. p. pipistrellus*, which lives in continental Europe, and *P. p. aladdin* (Thomas, 1905), which is found from the Near East to Central Asia. Despite skepticism regarding the validity of *P. p. aladdin*, molecular research (Hulva et al., 2010) has supported the population's uniqueness. Following post-glacial range expansion from Mediterranean refugia, *P. pipistrellus* colonized extensive areas in continental Europe and Asia. This expansion brought historically isolated lineages into renewed geographic contact, resulting in a broad zone of secondary sympatry (Hulva et al., 2010).

The common pipistrelle (*Pipistrellus pipistrellus*) has emerged as one of the most intensively studied bat species in the Palearctic region, serving as an example of cryptic speciation and complex phylogeographic structuring. Jones and van Parijs (1993) demonstrated that *P.pipstrellus* and *P. pygmaeus* occurred sympatrically in Great Britain without sharing roosting sites, suggesting reproductive isolation despite spatial overlap. Subsequent investigations provided compelling evidence for species status through documentation of reproductive barriers (Park et al., 1996) and significant sequence divergence in mitochondrial cytochrome *b* gene fragments (Barratt et al., 1997). Extended surveys confirmed the sympatric occurrence of both species across southern Germany, Switzerland, Hungary, and Greece (Mayer and von Helversen, 2001; Benda et al., 2003), while morphological investigations revealed that these cryptic species remain essentially indistinguishable based on traditional morphometric characters (Barlow et al., 1997; Haussler et al., 1999).

The phylogeographic architecture of *P. pipistrellus* reflects a complex evolutionary history shaped by Quaternary climatic oscillations and Mediterranean Basin dynamics. Molecular evidence suggests a Mediterranean origin for the species complex, with *P. pipistrellus* colonizing Europe primarily via the Iberian route during the current glacial cycle, followed by secondary range overlap with *P. pygmaeus* and subsequent character displacement in echolocation frequencies (Hulva et al., 2004). Phylogenetic analyses have revealed substantial geographic structuring, including relatively isolated allopatric lineages distributed across Libya, Crete, Sicily, Corsica, and Morocco (Hulva et al., 2007). The Moroccan lineage represents a western dispersal center isolated from the Iberian Peninsula by the Strait of Gibraltar since approximately 5.33 Ma. The discovery of distinct Sicilian and Corsican lineages with phylogenetic affinities to Moroccan populations provided the first

evidence for a central Mediterranean refugium within the complex, with divergence times between Moroccan lineages and western Mediterranean *P. pipistrellus* populations estimated at 1.6-0.9 Ma (Hulva et al., 2007).

Demographic analyses have revealed contrasting evolutionary dynamics between Mediterranean and continental populations. Southern Mediterranean populations exhibit restricted gene flow and relatively stable population sizes, whereas northern continental populations show evidence of recent demographic expansion and higher genetic connectivity (Hulva et al., 2010). This pattern likely reflects the differential impact of Pleistocene glacial cycles, with genetic diversity patterns supporting a hypothesis of range expansion from western Mediterranean refugia, evidenced by a negative correlation between genetic diversity and longitude (Hulva et al., 2004). This longitudinal gradient, established during the Middle Pleistocene, was followed by northward expansion potentially associated with the Eemian interglacial period and the spread of warm, open habitats (Hulva et al., 2004; Horacek & Jahelkova, 2005). Population genetic data suggest that gene flow in *P. pipistrellus* may be limited across distances of approximately 1000 km even in landscapes lacking obvious geographic barriers (Hulva et al., 2010).

Understanding the evolutionary history of *P. pipistrellus* holds significance across multiple dimensions of biological research and conservation. As one of the most abundant and widespread bat species in Europe, *P. pipistrellus* plays crucial ecological roles in insectivorous predation and pest control. Its phylogeographic patterns provide critical insights into broader biogeographic processes that shaped Palearctic biodiversity, particularly regarding Mediterranean refugia during Quaternary glacial cycles and post-glacial colonization mechanisms. The contrasting demographic histories between Mediterranean and continental populations offer a natural experiment for understanding how different climatic regimes influence population genetic structure and evolutionary trajectories.

Despite substantial advances in western Europe and selected Mediterranean localities, vast portions of the species' range remain inadequately characterized. In Türkiye, where *P. pipistrellus* is widespread except in poorly documented central and southeastern Anatolia (Benda & Horáček, 1998; Krystufek & Vohralík, 2001), limited sampling has revealed considerable genetic differentiation even among geographically proximate populations. Analysis of samples from three Turkish localities (Hatay, Nevşehir, and Kırklareli) demonstrated substantial haplotype divergence with considerable mutational steps separating haplotypes (Hulva et al., 2010). The Levantine region remains poorly represented, with records limited to coastal areas of Lebanon (Lewis & Harrison, 1962) and Jordan, while genetic analysis of western Syrian specimens revealed geographic isolation from central

European populations, likely resulting from historical glaciation events (Benda et al., 2003). There is a substantial knowledge gap regarding the full evolutionary history and intraspecific diversification patterns of *P. pipistrellus* due to the lack of thorough sampling across these important biogeographic regions, which may contain additional cryptic lineages or serve as important corridors for historical gene flow. Addressing these knowledge gaps through systematic sampling across the species' full geographic range is essential for reconstructing a comprehensive picture of *P. pipistrellus* evolutionary history and for informing evidence-based conservation strategies.

Although *Pipistrellus pipistrellus* has been the subject of extensive phylogeographic research throughout Europe and the Mediterranean Basin (Hulva et al., 2004, 2007, 2010; Boston et al., 2014), significant geographic areas are still under-sampled, and our knowledge of gene flow and introgression dynamics is limited by the use of mitochondrial DNA alone. In order to fill in these gaps, the current study (1) uses nuclear intron markers together with mitochondrial DNA to analyze male-mediated gene flow and test for introgression, (2) expands coverage in Central Asia and the Middle East to better characterize the eastern extent of the species' diversity, (3) and intensively samples Türkiye (Anatolia + Thrace), regions Hulva identified as priority areas. This work attempts to improve our knowledge of refugial dynamics and offer insights into the evolutionary processes that have created genetic diversity in this common European bat species by combining multi-locus genetic data with increased geographic sampling.

3.2 Materials and Methods

3.2.1. Sample Collection

Samples for this part of the study were acquired in collaboration with our key contributors (details in Table A.1, Appendix A): 1- Petr Benda, the Curator of the mammal collection at the National Museum in Prague, Czech Republic, provided 77 samples spanning 14 distinct countries sourced from the Museum's collection (Albania, Bosnia and Herzegovina, Bulgaria, Czech Republic, Greece, Iran, Jordan, Lebanon, Morocco, Romania, Slovakia, Syria, Tajikistan, Ukraine). 2- KAB Ecology, an environmental consultancy company based in Istanbul, Türkiye, facilitated the acquisition of 143 samples from nine cities across Türkiye (Bursa, Mersin, Izmir, Balıkesir, Kıyıköy (Vize), Çanakkale, Tayakadın (İstanbul), Yalova, Kızılcaterzi (Tekirdağ)). 3- Doç. Dr. Tarkan Yorulmaz from Çankırı Karatekin University provided 33 samples representing 16 cities in Türkiye (Adana, Diyarbakır, Şanlıurfa, Manisa, İzmir, Yozgat, Kocaeli, Yalova, Bursa, Edirne, Antalya, Hamitköyü, Artvin, Van, Hakkâri, Kastamonu).

Sampling localities and the geographic origin of all individuals included in the mitochondrial DNA (mtDNA) analyses are illustrated in Figure 3.1. Not all collected specimens yielded PCR-positive mtDNA and therefore only a subset of samples from these localities was included in the mtDNA analyses. Figure 3.1.b shows sampling sites of specimens collected in the present study, represented by circles, from which DNA extractions were performed. Figure 3.1.a shows sampling localities of mtDNA control-region (HVII) sequences included later in this study, retrieved from GenBank and previous studies, represented by squares (accession numbers HM105963–HM106128

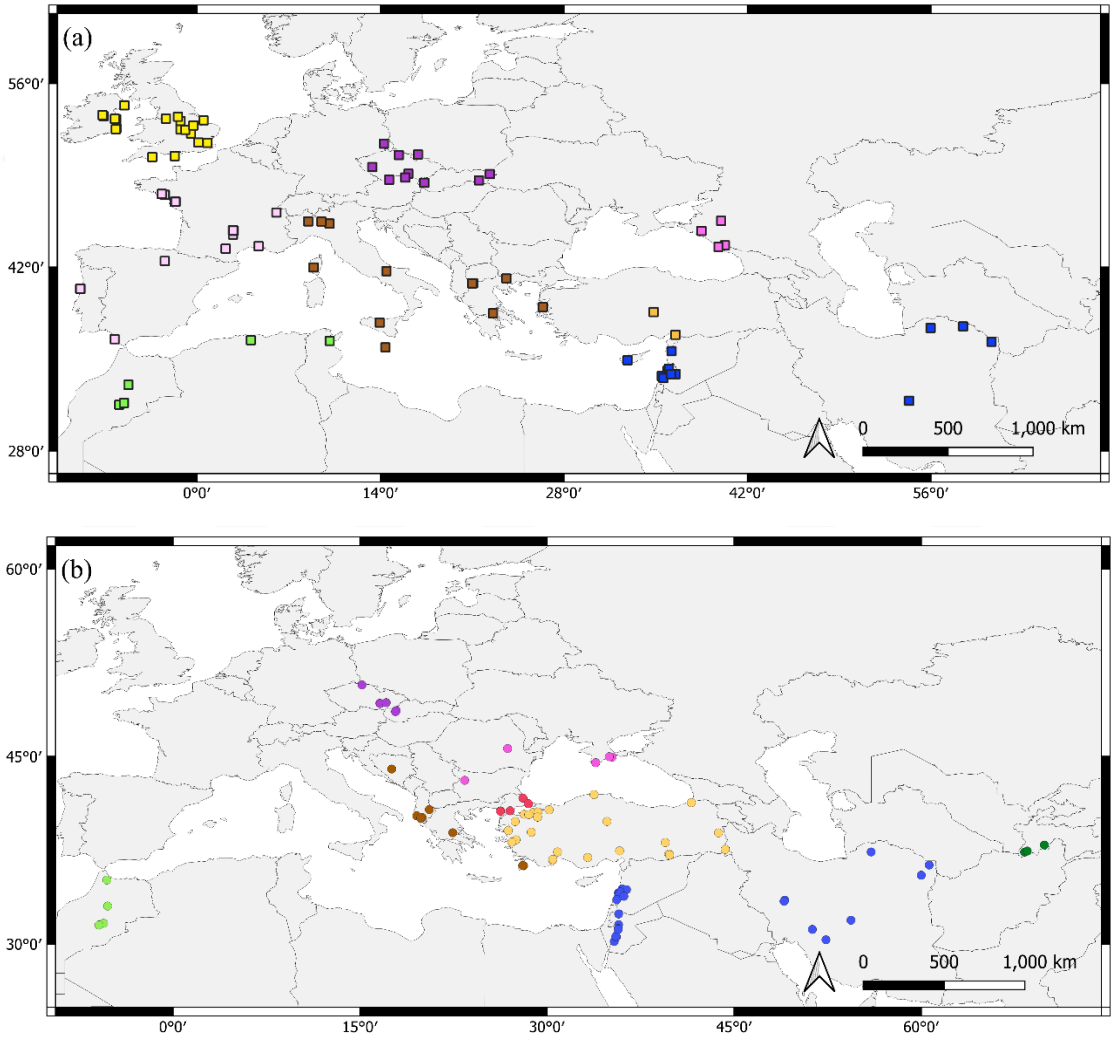


Figure 3.1. Geographic distribution of sampling localities of collected specimens for the mitochondrial DNA (mtDNA) component of the study.(a) Sampling sites corresponding to mtDNA control-region (HVII) sequences retrieved from GenBank and previous studies, shown as squares. (b) Sampling sites of specimens collected in the present study, shown as circles; not all collected specimens yielded successful PCR amplification and were therefore included in the mtDNA analyses. Colors indicate broad geographic regions based on country of origin.

from Hulva et al., 2010, and KP273505–KP273581 from Boston et al., 2014). Individuals were grouped according to their country of origin into broad geographic regions reflecting major biogeographic units, and each region is indicated by a distinct color in Figure 3.1.

3.2.2. Genomic DNA Extraction

The Genomic DNA from each sample provided by KAB Ecology was extracted using the AMBRD genomic DNA isolation kit (İstanbul, Türkiye) following the manufacturer's instructions. Some of the samples provided by KAB Ecology varied in quality. While certain bat carcasses collected from under wind turbines were relatively fresh, others had remained in the field for several days before sampling. Out of the 145 samples analyzed, only 36 yielded visible DNA bands following extraction with the AMBRD Genomic DNA Isolation Kit. Consequently, we decided to change the extraction kit. We next tested samples using the MagAttract HMW DNA Kit (Qiagen), but no positive results were obtained. Subsequently, we switched to the Qiagen DNeasy Blood & Tissue Kit, which successfully provided positive results for several samples that had previously tested negative with the other two kits. Therefore, this kit was used for the extraction of all remaining samples provided by KAB Ecology, as well as those collected from the National Museum of Prague. For the samples (buccal swab specimens) provided by Tarkan Yorulmaz, we used the Zymo Quick-DNA/RNA Microprep Plus Kit.

3.2.3. Mitochondrial DNA

In this study, we examined the second hypervariable domain (HVII), of the mitochondrial DNA control region, a noncoding segment that exhibits high sequence variability suitable for intraspecific phylogeographic analyses. After extracting DNA from the samples, we initiated the Polymerase Chain Reaction (PCR). The amplification of this segment was carried out using the primers we designed specifically for *Pipistrellus pipistrellus* L16517Pp (CATCTGGTTCTTTCTTCAGG) and H607Pp (TATACTCATCTAAGCATTTTCAGTG).

PCRs were conducted in 25 µL volumes consisting of 1x Taq buffer, 2.5 mM $MgCl_2$, 200 µM dNTPs, 0.5 µM of each primer, 1 U Taq polymerase, and 4 ul template DNA. The initial PCR protocol followed the method applied by Hulva et al. (2010), including pre-denaturation (94 °C, 3 min), ten cycles of denaturation (94 °C, 1 min), annealing (63 °C with a decrease of 0.5 °C in each cycle, 1 min), and extension (94 °C, 1 min), followed by 25 analogous cycles with an annealing temperature of 58 °C and a final extension (72 °C, 4 min). However, due to negative PCR results, the protocol was

modified to that of Korstian et al. (2015). The revised cycling parameters included an initial cycle at 95°C for 15 min, followed by 35 cycles of 30 s at 94°C, 90 s at 60°C, 90 s at 70°C, and a final extension at 60°C for 30 min. PCR products were stored at 4°C. The positive PCR products were sent to sequencing, which was performed commercially by Macrogen Europe (Netherlands). The summary of the locations of each sampling site, with the corresponding number of sequenced samples, is shown in Table 3.1.

Table 3.1. Sampling locations and sample sizes. N(HVII) indicates the number of samples sequenced for the HVII region.

Region	Country	Location	N(HVII)	Latitude	Longitude
Balkans	Albania	Zhulat,Kardhiqit river valley	2	40.116	19.983
	Albania	Selce, Selces river valley	1	40.750	20.550
	Albania	Borsh	1	40.0667	19.866
	Bosnia and Herzegovina	Izbisno	1	43.993	17.537
	Greece	Kombotades (Lamia)	1	38.899	22.435
	Greece	Rodos, Epta Piges	1	36.253	28.113
	Greece	Rodos, Eleoussa	1	36.274	28.037
	Romania	Motnau-Bai, Motau valley	1	45.633	26.833
	Türkiye	Vize, Kırklareli, Kıyıköy	4	41.672	28.058
	Türkiye	Tekirdag, Şarköy, Kızılcaterzi	6	40.657	27.037
	Türkiye	Istanbul, Tayakadın	13	41.222	28.503
	Türkiye	Edirne, Vakif Tabiat Park	5	40.618	26.262
	Iran	Shurlaq	1	36.316	60.630
	Iran	3 km E Tunel-e-Golestan (Golestan)	2	37.360	55.983
	Iran	10 km NW Eman Qoli (Khorasan Razni)	1	37.483	58.466
Jordan	Jordan	Jebel Masuda, Ain Amshit	2	30.200	35.383
	Jordan	Al Maqar'iyya	1	30.566	35.550
	Jordan	Wadi al walah	1	31.550	35.733
	Jordan	Arjan	1	32.400	35.733
Lebanon	Lebanon	Qadisha cave	1	34.248	36.029
	Lebanon	Majdal Tarchich	1	33.900	35.800
	Lebanon	Aaqura	1	34.122	35.904
	Lebanon	Adonis, Nahr Ibrahim	1	34.083	35.716
	Lebanon	Haqel el Azime	2	34.400	36.016

Table 3.1 continued

Region	Country	Location	N(HVII)	Latitude	Longitude
Lebanon	Lebanon	Afqa Cave	1	34.066	35.883
	Lebanon	Nahr es safa	1	33.745	35.708
	Lebanon	Ras al Assi	1	34.350	36.366
	Lebanon	Jenta	1	33.850	36.083
	Lebanon	Balaa	1	34.166	35.866
	Lebanon	Faraya el Mzar	1	34.000	35.816
	Morocco	Bekrite, 5km SE	1	33.033	-5.233
Slovakia	Slovakia	Tisovec (Rimavska Sobota)	1	48.671	17.906
	Slovakia	Erna	4	48.589	17.839
Syria	Syria	Sarghaya (Dimashq)	1	33.811	36.157
Turkmenistan	Turkmenistan	Germab, exit of Germab George	1	38.036	57.770
	Turkmenistan	Gokdere, Altiab river	3	38.009	58.007
Tajikistan	Tajikistan	Tygrovaja balka	3	37.350	68.280
	Tajikistan	Levap	2	37.433	68.500
	Tajikistan	Tuto	2	37.916	69.866
Anatolia	Türkiye	Çanakkale, Pazarköy	17	39.794	27.438
	Türkiye	Çanakkale, Saros	2	40.074	26.772
	Türkiye	Yalova	7	40.517	28.865
	Türkiye	İzmir, Fuat	8	38.335	27.501
	Türkiye	Balikesir, Bandirma	12	40.375	28.156
	Türkiye	Mersin, Mut	1	36.915	33.257
	Türkiye	Bursa, Har	4	40.347	28.532
	Türkiye	Manisa, Demirci, Çağıllar Köyü Yolu	2	38.940	28.730
	Türkiye	Izmir, Dikili	1	39.075	26.889
	Türkiye	Izmir, Menderes, Çileme Koyu	1	38.150	27.179
	Türkiye	Yozgat Çamlığı Milli Parkı	6	39.800	34.800
	Türkiye	Yalova, Güneyköy	1	40.555	29.270
	Türkiye	Bursa, Uludağ, Saitabat-AkÇay	1	40.150	29.236
	Türkiye	Antalya, Üçoluk	1	36.691	30.435
Ukraine	Ukraine	Crimea, Uzundza	1	33.900	44.500
	Ukraine	Crimea, Perevalovka	1	35.216	44.950
	Ukraine	Crimea, Perevalovka	1	34.983	44.983
	Ukraine	Crimea, Uzundza	1	33.900	44.500
	Czech Republic	Ivanovice na Hane	1	49.306	17.095

3.2.3.1. Phylogenetic reconstruction and demographic history. The mtDNA sequences were cleaned with Geneious prime 2024.0.7. (Biomatters Ltd.) and were aligned with Sequencher v. 5.2 (Gene Codes Corporation). Additional mtDNA control-region (HVII) sequences were retrieved from GenBank (accession no. HM105963–HM106128 (Hulva et al., 2010) and KP273505- KP273581 (Boston et al., 2014) and combined with newly generated sequences from our samples. The final alignment consisted of 272 unique HVII sequences (283 bp), representing all individuals included in the study. The countries from which each individual originated were grouped by regions (Appendix A, Table A.3).

The contig generated in Sequencher in nexus format was exported and used in DnaSP v6.12.03 (Rozas et al., 2017) to calculate genetic diversity measures and statistical tests of neutrality (Tajima's D and Fu's F). DnaSP was also used to generate a haplotype data file which was then used in PopART v1.7 (Leigh, Bryant, and Nakagawa, 2015) to create a haplotype network.

Phylogenetic relationships based on mitochondrial DNA were reconstructed in Mega v11.0.13 (Tamura, Stecher, and Kumar, 2021) using both Neighbor-Joining method (Saitou & Nei, 1987) (NJ) and Maximum Likelihood (ML) methods to assess the consistency of inferred patterns. Evolutionary distances were calculated using the Tamura three-parameter model for both trees. The Neighbor-Joining (NJ) tree provided a distance-based overview of mitochondrial haplotype clustering and was inferred from 1,000 bootstrap replicates to assess the robustness of the recovered relationships. The Maximum Likelihood (ML) tree was reconstructed to estimate mitochondrial DNA relationships under an explicit model of sequence evolution.

Historical demographic patterns were assessed using Bayesian Skyline Plots (BSPs) implemented in BEAST v2.7.7 (Bouckaert et al., 2019). Analyses were conducted using the Jukes-Cantor (JC69) substitution model (Jukes & Cantor, 1969) under a strict molecular clock with a substitution rate of 2.0×10^{-7} substitutions per site per year, corresponding to 20% divergence per million years for the mitochondrial control region hypervariable segment II (HVII) (Ho et al., 2007; Nabholz et al., 2008). Markov chain Monte Carlo (MCMC) simulations were run for 100,000,000 iterations, sampling every 1,000 iterations, with the first 10,000,000 iterations discarded as burn-in. Trace files were examined in Tracer v1.7.2 (Rambaut et al., 2018) to assess convergence and effective sample sizes (ESS > 200). Bayesian Skyline Plots were generated in Tracer to reconstruct changes in effective population size through time for individual geographic regions as well as for all regions combined. Additionally, pairwise FST values were calculated in DnaSP to assess genetic differentiation among geographic regions, with significance tested through 1,000 permutations.

3.2.4. Nuclear DNA

For the second part of this chapter, we used nuclear introns following the approach of previous studies (Salicini et al., 2011); Igea, Juste, and Castresana, 2010), where the following four markers were used: the intron 5 of *ABHD11* gene, the intron 3 of ACOX2 gene, the intron 4 of *COPS7A* gene, and the intron 7 of ROGDI gene, for several bat species. These primers contained degenerate bases indicating known sequence variability in the original primer binding sites. Despite multiple PCR optimization attempts, none of these primer sets produced successful amplification products. The failure was attributed to species-specific sequence divergence between *P. pipistrellus* and the taxa used in the original studies, highlighting the need for species-specific primer design based on actual target species genomic data.

3.2.4.1. Designing primers. We downloaded human mRNA sequences for all four target genes from NCBI GenBank: *ACOX2*: NM_148912.4 (acyl-CoA oxidase 2, 1,418 bp), *ABHD11*: NM_152804.4 (abhydrolase domain containing 11), *COPS7A*: NM_016258.3 (COP9 signalosome subunit 7A), *ROGDI*: NM_024589.4 (rogdi atypical leucine zipper). Human sequences were selected as references because they are well-annotated and enable reliable inference of exon–intron structure when aligned to genomic DNA, and because these genes are evolutionarily conserved and expected to exhibit similar genomic organization in bats. The complete *Pipistrellus pipistrellus* genome assembly (GCA_965203405.2_mPipPip2.hap1.2_genomic.fna) was downloaded from NCBI. This assembly represents a high-quality, chromosome-level reference suitable for precise genomic coordinate mapping. Bioinformatic analyses were conducted using the Galaxy web-based bioinformatics platform. Within Galaxy, a searchable nucleotide BLAST database was generated from the *P. pipistrellus* genome FASTA file using NCBI BLAST+ makeblastdb, with the database type specified as *nucl* (for nucleotide sequences). Human mRNA sequences were used as queries in BLASTN searches against the *P. pipistrellus* genome database. An E-value threshold of $< 1 \times 10^{-10}$ was applied to retain only highly significant alignments. BLAST output was generated in tabular format to enable systematic filtering and downstream interpretation.

For each gene, adjacent exon pairs flanking a target intron were selected for primer design as shown in Figure 3.2. Genomic coordinates corresponding to selected exon pairs were converted to Browser Extensible Data (BED) format, comprising chromosome or scaffold identifier, start coordinate (0-based, inclusive), end coordinate (0-based, exclusive), feature name, score, and strand orientation. To ensure adequate sequence space for primer binding within conserved exonic regions

and to avoid exon–intron junctions, exon coordinates were expanded by approximately 20–50 bp on each side.

Because Galaxy requires explicit genome build definitions for certain sequence extraction tools, bedtools getfasta, as implemented in Galaxy, was used to extract strand-specific genomic sequences from the genome assembly. Extraction parameters included BED-formatted input intervals, the *P. pipistrellus* reference genome loaded into the Galaxy history, strand-specific extraction enabled (–s), and feature-based FASTA header naming enabled (–name) to preserve coordinate and feature metadata. Primer design was carried out using Primer3 and NCBI Primer-BLAST, using extracted FASTA sequences containing both Forward and Reverse exonic regions flanking the target intron. Target regions were defined to ensure amplification across intronic sequence. For each gene, multiple primer pairs were designed. Expected amplicon lengths were calculated from extracted genomic sequence lengths and were optimized to fall primarily within the 300–1,000 bp range, balancing amplification efficiency with intronic sequence coverage.

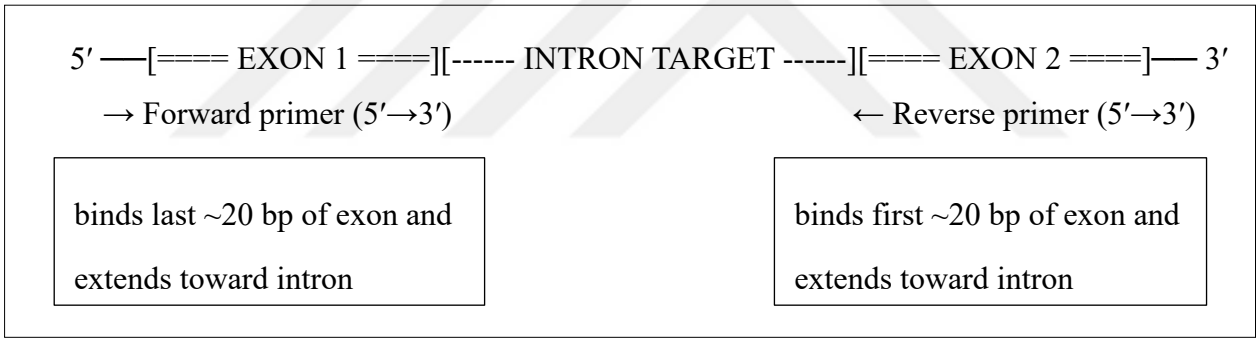


Figure 3.2**.** Schematic representation of primer placement for intron amplification. Forward and reverse primers designed within conserved exon regions flanking a target intron and are oriented toward the intronic sequence. Primers are shown in their 5′→3′ orientation.

Although primer pairs were designed for all four target genes, successful PCR amplification was obtained for only two genes. For the *COPS7A* gene, intron 4 was amplified using custom-designed primers: Forward_COPS_intron4 (5'-CCGAGCAACACCTGACTGAA-3') and Reverse_COPS_intron4 (5'-GGCACAGGAAGGCTCTTTGA-3'). For the *ABHD11* gene, intron 5 was amplified using custom-designed primers: Forward_ABHD11_intron5 (5'-AGCATGTGGACGAGATCATGG-3') and Reverse_ABHD11_intron5 (5'-TCCGGCACGGTCTGTATCT-3').

PCRs were conducted for each primer pair in 25 µl reaction volumes containing 4 µl DNA, 1 µl of each primer (0.5 µM), 2.5 µl Buffer, 0.5 µl dNTPs (200 µM), 1 µl $MgCl_2$ (2.5 mM), and 0.2 µl Taq DNA Polymerase Thermo Scientific (5U/µl). PCR amplification started with an initial denaturation at 94°C for 3 minutes, followed by 38 cycles of:: 1) a short denaturation at 94°C for 30 seconds; 2) annealing at 62°C for 40 seconds; 3) an extension at 72°C for 1 minute and 30 seconds. A final extension step was carried out at 72°C for 10 minutes. PCR products were stored at 4°C. The positive PCR products were sent to sequencing, which was performed commercially by Macrogen Europe (Netherlands). The locations of each sampling site, of sequenced samples, is shown in Figure 3.3.

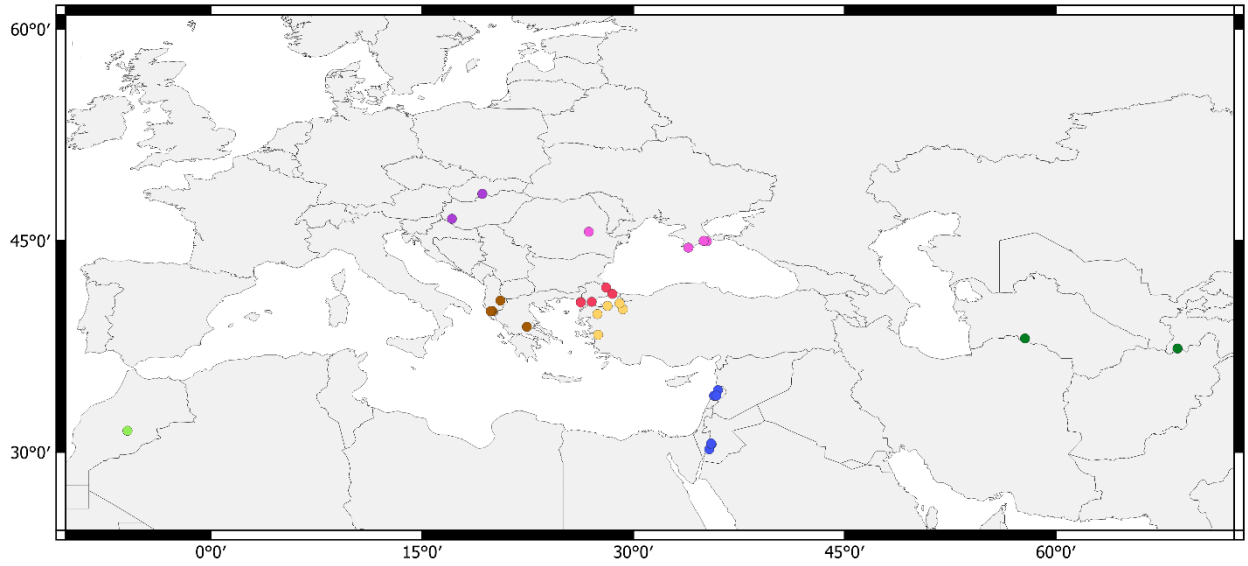


Figure 3.3. Map representing the geographic distribution of the selected samples for nuclear DNA analyses.

3.2.4.2. Phylogenetic reconstruction and demographic history. The nuclear DNA sequences for both introns a part were cleaned and aligned with Sequencher v. 5.2 (Gene Codes Corporation). The final alignment consisted of 33 sequences (253 bp and 324 bp) for the intron 4 of the *COPS7A* gene and the intron 5 of the *ABHD11* gene respectively, representing all individuals included in the study. The contigs generated in Sequencher were exported in nexus format. Because both markers are nuclear introns, sequences were treated as heterologous data in DnaSP v6.12.03 (Rozas et al., 2017), and both alleles per individual were included in the analyses, resulting in 66 sequences. In DnaSP statistical tests of neutrality Tajima's D and Fu's F and genetic diversity measures across global regions representing the countries of origin of our samples, including number of sequences, counts of invariable and variable sites, the number of singleton and parsimony-informative variable sites, total haplotypes, nucleotide diversity (π), and haplotype diversity (Hd), each with standard deviations were

generated for sequences of each gene. DnaSP was also used to generate haplotype data files, which were imported into PopART v1.7 (Leigh, Bryant, and Nakagawa, 2015) to construct median-joining haplotype networks. These networks visualized the phylogenetic relationships and geographic distribution of 6 haplotypes from intron 4 of the *COPS7A* gene and 16 haplotypes from intron 5 of the *ABHD11* gene.

Phylogenetic relationships based on nuclear DNA for each gene were reconstructed in Mega v11.0.13 (Tamura, Stecher, and Kumar, 2021) using both Neighbor-Joining (NJ) and Maximum Likelihood (ML) methods to assess the consistency of inferred patterns. Evolutionary distances were calculated using the Jukes-Cantor method for both trees. The Neighbor-Joining (NJ) trees provided a distance-based overview of nuclear haplotype clustering and were inferred from 1,000 bootstrap replicates to assess the robustness of the recovered relationships between haplotypes.

3.3. Results

3.3.1 Mitochondrial DNA Analyses

Genetic diversity measures for each geographic region are presented in Table 3.2, including the number of samples, invariable and variable sites, singleton and parsimony-informative variable sites, total haplotypes, nucleotide diversity (π), and haplotype diversity (Hd), each with standard deviations. Neutrality test results (Tajima's D and Fu's Fs) with their corresponding p-values are shown in Table 3.3.

Across all 272 samples, 175 haplotypes were identified from the mitochondrial DNA sequences, with high overall haplotype diversity (Hd = 0.992 ± 0.002) and nucleotide diversity (π = 0.054 ± 0.002). Among regions, nucleotide diversity was highest in North Africa (π = 0.058 ± 0.008) and Southern Europe (π = 0.059 ± 0.007), while Thrace Türkiye showed the lowest nucleotide diversity (π = 0.017 ± 0.005) and haplotype diversity (Hd = 0.809 ± 0.065). Anatolia and the Middle East exhibited relatively high nucleotide diversity (π = 0.042 ± 0.003 and π = 0.051 ± 0.003, respectively) and had high numbers of unique haplotypes (37 and 25, respectively). Central European populations showed low nucleotide diversity (π = 0.012 ± 0.001) despite high haplotype diversity (Hd = 0.981 ± 0.016).

Table 3.2. Genetic diversity metrics across regions, based on mitochondrial DNA sequences.

	Number of samples	Invariable Sites	Variable Sites	Singleton Variable sites	Parsimony informative sites	Number of Haplotype	Pi ± Sd	Hd ± Sd
Total	272	181	89	16	73	175	0.054 ± 0.002	0.992 ± 0.002
Anatolia	55	223	56	17	39	37	0.042 ±0.003	0.981 ±0.008
Middle East	34	218	55	11	44	25	0.051 ± 0.003	0.979 ± 0.013
North Africa	9	247	32	2	30	8	0.058 ± 0.008	0.972 ± 0.064
Southern Europe	24	220	59	11	48	19	0.059 ± 0.007	0.982 ± 0.016
Thrace Türkiye	27	154	25	7	18	11	0.017 ± 0.005	0.809 ±0.065
Central Europe	28	251	28	19	9	23	0.012 ± 0.001	0.981 ± 0.016
British Isles	31	232	46	29	17	17	0.022 ± 0.007	0.908 ± 0.042
Eastern Europe	17	241	36	20	16	14	0.023 ± 0.006	0.978 ± 0.027
Western Europe	41	242	37	8	29	33	0.021 ± 0.003	0.985 ± 0.010
Central Asia	6	253	25	23	2	5	0.032 ± 0.013	0.933 ± 0.122

Neutrality tests revealed significant values (Table 3.3). Central Europe showed significant negative values for both Tajima's D (-1.963, $p < 0.05$) and Fu's Fs (-22.745, $p < 0.05$), suggesting recent population expansion. The British Isles similarly showed significantly negative Tajima's D (-1.922, $p < 0.05$) and Fu's Fs (-3.709, $p < 0.05$) values. North Africa was the only region showing a significant positive Tajima's D (1.994, $p < 0.05$). Most other regions, including Anatolia, Middle East, Southern Europe, Thrace Türkiye, Eastern Europe, Western Europe, and Central Asia, showed non-significant neutrality test values ($p > 0.10$).

Table 3.3. Summary of neutrality tests: Tajima's D, Fu's Fs metrics across regions, based on mitochondrial DNA sequences.

Region	n	Tajima's D	P-value	Fu's Fs statistic:	P-value
Anatolia	54	-0.198	P > 0.10 (ns)	-13.738	P > 0.10 (ns)
Middle East	34	-0.067	P > 0.10 (ns)	-5.364	P > 0.10 (ns)
North Africa	9	1.994	P < 0.05	-0.066	ns
Southern Europe	19	-0.363	P > 0.10 (ns)	-2.742	P > 0.10 (ns)
Thrace Türkiye	27	-0.936	P > 0.10 (ns)	-0.585	P > 0.10 (ns)
Central Europe	28	-1.963	P < 0.05	-22.745	P < 0.05
British Isles	31	-1.922	P < 0.05	-3.709	P < 0.05
Eastern Europe	17	-1.580	P > 0.10 (ns)	-5.251	P > 0.10 (ns)
Western Europe	41	-1.153	P > 0.10 (ns)	-27.622	P > 0.10 (ns)
Central Asia	6	-1.198	P > 0.10 (ns)	0.618	ns

A median-joining haplotype network (Figure 3.4) was constructed to visualize the phylogenetic relationships and geographic distribution of the 175 mitochondrial haplotypes identified across all sampling regions. Haplotypes and their corresponding samples, together with their positions on the map, are shown in the clade-specific maps in the Appendix.

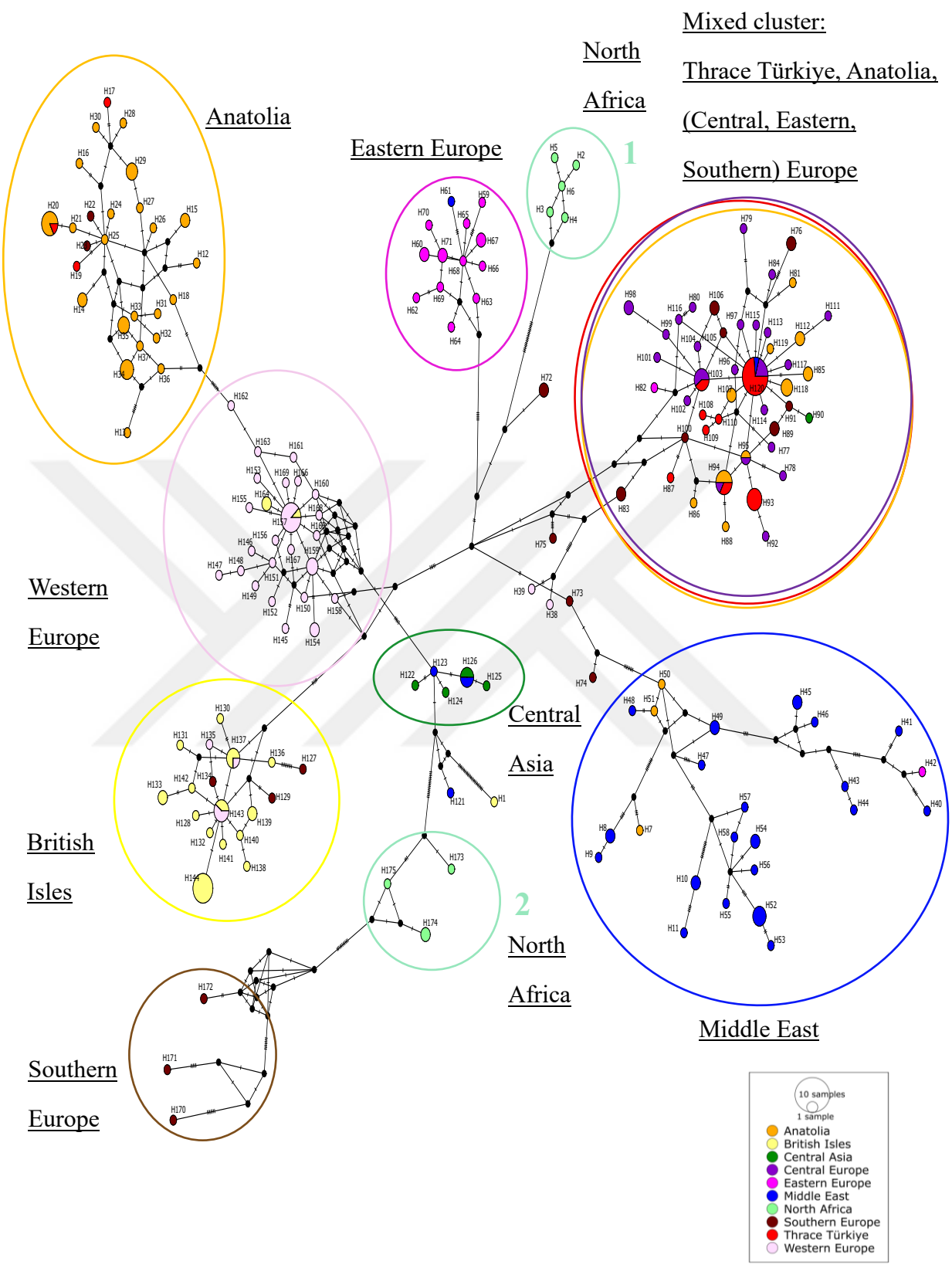


Figure 3.4. Haplotype network generated by PopART to visualize the relationships between the mitochondrial DNA sequences from different geographic regions.

A comprehensive description of each clade in Figure 3.4 is as follows:

-Right Upper Clades: A pink (Eastern Europe) clade with only one dark blue dot (Middle East).

Next to it, a small light green clade (North Africa 1). Both clades are connected to a large, highly diverse clade on the far right with red (Thrace Türkiye), orange (Anatolia) samples, along with some brown (Southern Europe), one pink (Eastern Europe) and one dark green (Central Asia) sample. All of these are extensively interconnected with purple (Central Europe) samples, creating a complex reticulated pattern.

-Right Lower Clade: Mainly blue representing the samples from the Middle east, with only one pink dot and several orange dots.

-Left Upper Clade: A moderately sized cluster with mixed colors including brown (Southern Europe), red (Thrace Türkiye), dominated by orange samples (Anatolia), showing connectivity to the network via a cluster primarily with powder pink dots (Western Europe) with scattered yellow dots (British Isles).

Middle Left Clade: A mixed clade mainly yellow (British Isles), with powder pink (Western Europe) and brown (Southern Europe) samples.

-Left Lower Clade: A small, isolated cluster dominated by brown dots (Southern Europe), connected to the main network via an extended branch. Along this branch, in the middle, there is a small light green cluster (North Africa 2). Closer to the center there is a mixed cluster with dark blue (Middle East) and dark green (Central Asia) samples.

The samples corresponding to the haplotypes shown in the haplotype network are provided in Appendix A, Table A.2, including their geographic coordinates and country of origin.

The mitochondrial DNA haplotype network generated in PopART V1.7 reveals the complex phylogeographic structure and lineage relationships across a broad geographic range spanning from Western Europe to Central Asia and North Africa (Figure 3.4). The median-joining haplotype network displays multiple clear geographic clustering patterns, with distinct mitochondrial lineages associated with specific regions. On the upper right side of the network, is a large mixed cluster, containing haplotypes from Thrace Türkiye and Anatolia combined with multiple European regions (Eastern, Central, and Southern Europe) as well as Middle East and Central Asia. This widespread sharing of mitochondrial lineages across the continental range suggests these regions maintained genetic connectivity throughout recent evolutionary history. The presence of both Turkish and European samples in this cluster indicates that Anatolia and the Balkans may have served as a bridge connecting Asian and European populations. The nearby pink group to its left includes the Eastern Europe haplotypes, with a single haplotype from the Middle East. The Middle Eastern cluster, positioned at the bottom right of the network and connected by a long branch indicating deep divergence, is highly diverse with 25 haplotypes from 34 individuals. This cluster with Middle East haplotypes with some

Anatolian haplotypes and a single Eastern European haplotype, is separated from others by multiple mutational steps and likely corresponds to the eastern 'aladdin' lineage described in earlier literature (Hulva et al., 2004, 2007), potentially representing a distinct refugial population that persisted in the Middle East through multiple glacial cycles. Adjacent to this cluster, Central Asian and Iranian samples group together.

Southern European and Anatolian samples show an interesting dual pattern: some haplotypes cluster within the mixed continental clade, while others form more isolated positions. The Anatolia-specific cluster on the top left stands out as a major diversity hotspot with 37 haplotypes from 54 individuals, with predominately Anatolian haplotypes in addition to some haplotypes from Thrace Türkiye and Southern Europe. The Southern Europe cluster on the bottom left is positioned near the second North African cluster. North Africa shows two distinct genetic clusters, Cluster 1 (closer to the mixed clade) contains samples from Tunisia, Algeria, and one Moroccan locality, while Cluster 2 (closer to Southern Europe) contains only Moroccan samples from geographically close but genetically distinct locations which suggests that even within the Maghreb, substantial population structure exists.

Moving up in the middle we see a haplogroup comprising western European haplotypes (powder-pink colored), which also includes haplotypes from the British Isles (yellow). Other peripheral clusters include the British Isles on the left, where samples form an isolated cluster with relatively long branches, consistent with island isolation and likely recent colonization after the Last Glacial Maximum.

The network supports a south-to-north diversity gradient, Southern regions including Anatolia, the Middle East, Southern Europe, and North Africa, retain much higher haplotype diversity, consistent with long-term persistence in Mediterranean and Near Eastern refugial areas. Northern regions including Central Europe, the British Isles, and Western Europe, show reduced diversity, consistent with post-glacial range expansion from southern refugia.

To complement the haplotype network analysis and assess the robustness of phylogenetic relationships, neighbor-joining tree (Figure 3.5) and maximum likelihood tree (Figure 3.5) were constructed. Bootstrap values represent the percentage of 1,000 replicate trees supporting each node, with values >70% indicating strong support for the branch.

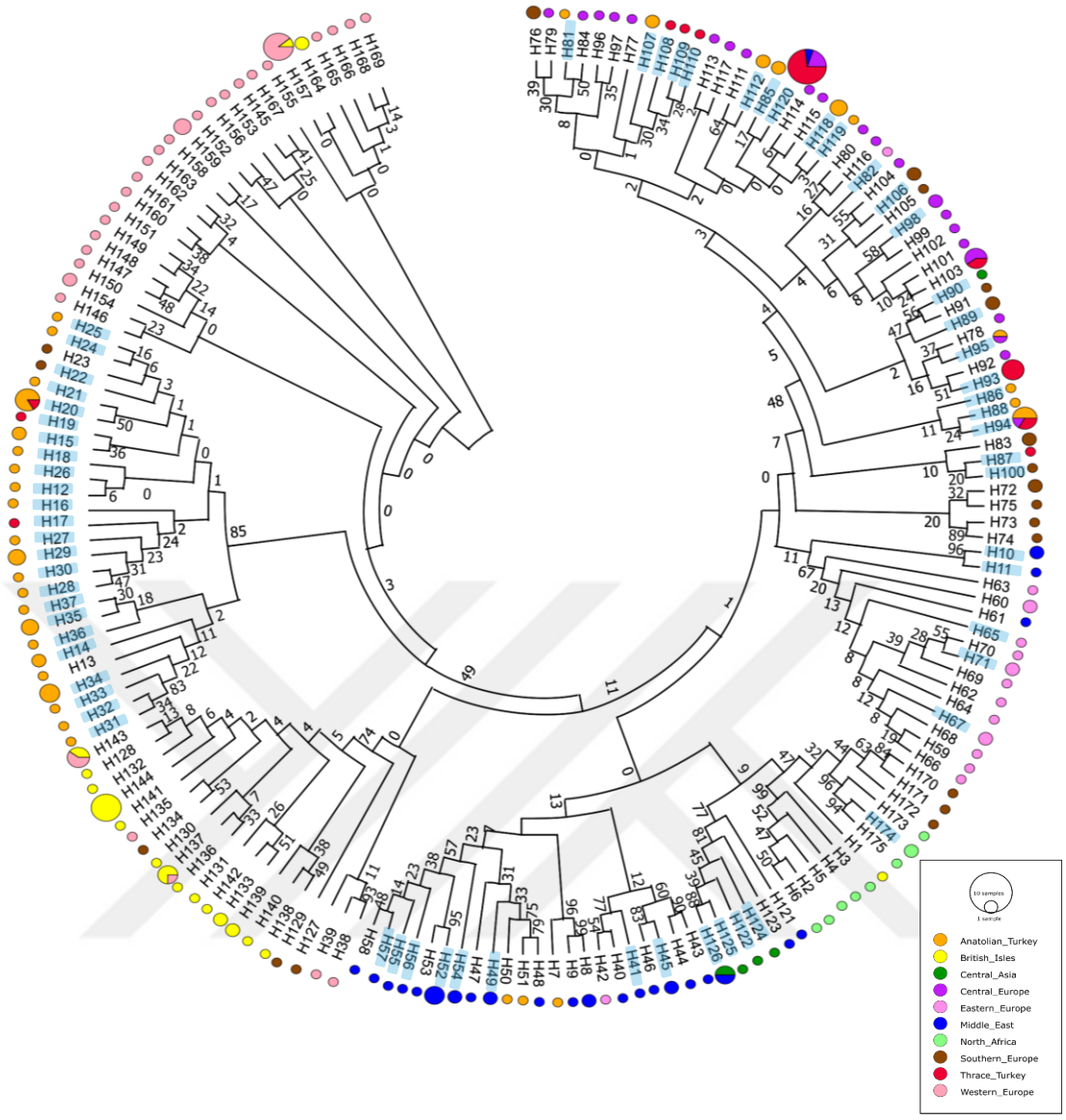


Figure 3.5. Neighbor-Joining Bootstrap consensus tree. Haplotypes are color-coded according to their geographic origin, with colors ranging from pink and red through yellow, green, blue, and purple, each representing a distinct regional group.

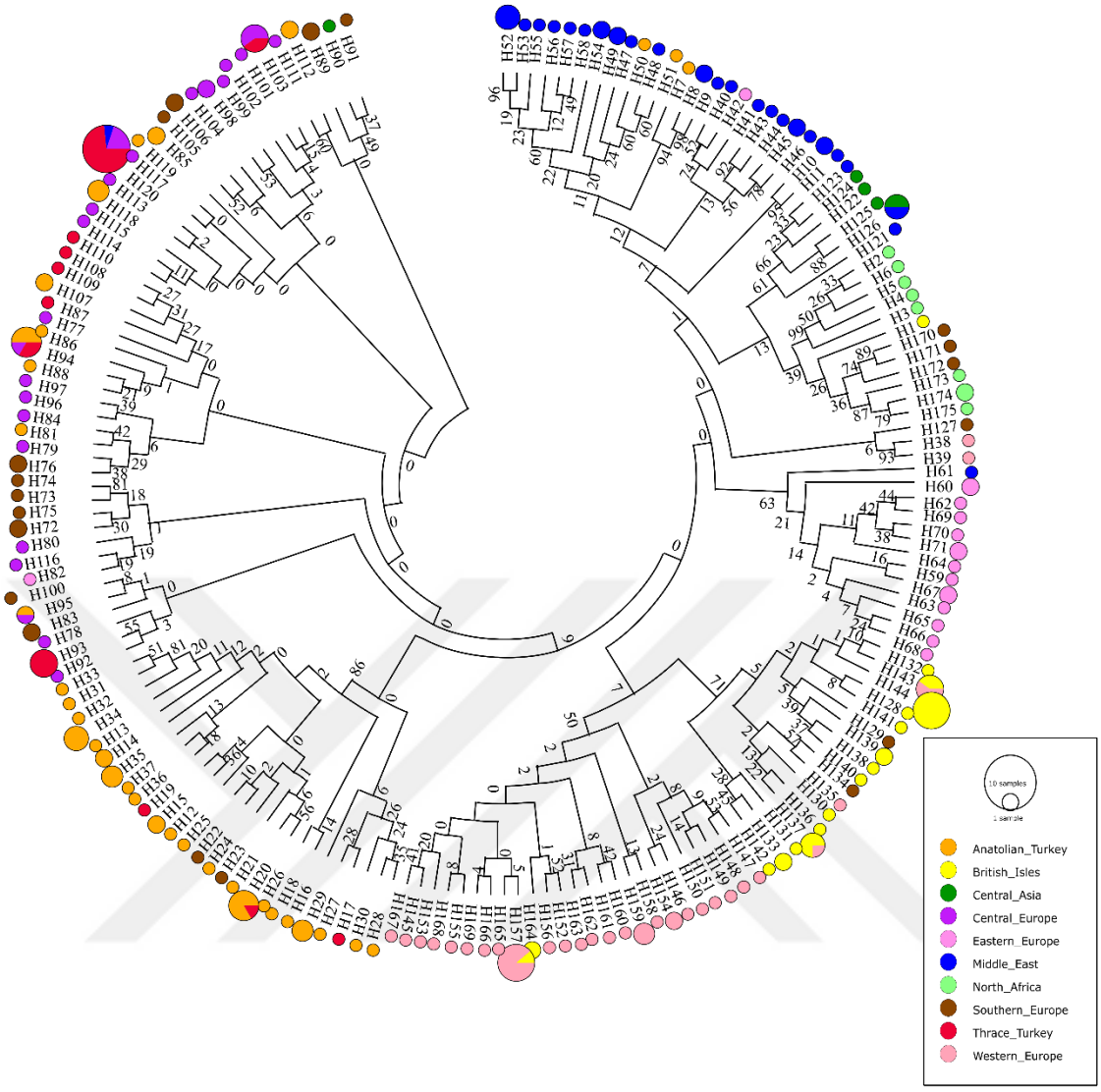


Figure 3.6. Maximum Likelihood Bootstrap consensus tree.

The generated NJ bootstrap phylogenetic tree (Figure 3.5) represents mitochondrial DNA relationships among the identified haplotypes and reveals clear clustering into several clades. These clades are concordant with the groupings observed in the haplotype network (Figure 3.4). The ML bootstrap phylogenetic tree (Figure 3.6) recovered well-supported clades that were mostly consistent with those identified in the Neighbor-Joining tree and the haplotype network. Major clustering patterns were consistent across methods, with haplotypes grouping according to their geographic origin.

The haplotypes selected for further nuclear analyses are marked in blue on the Neighbor-Joining Bootstrap consensus tree (Figure 3.5). Only samples that provided good geographic coverage of genetic diversity while being manageable for nuclear DNA sequencing were selected.

Pairwise FST values among geographic regions ranged from 0.052 to 0.698, indicating varying levels of genetic differentiation across *Pipistrellus pipistrellus*'s range.

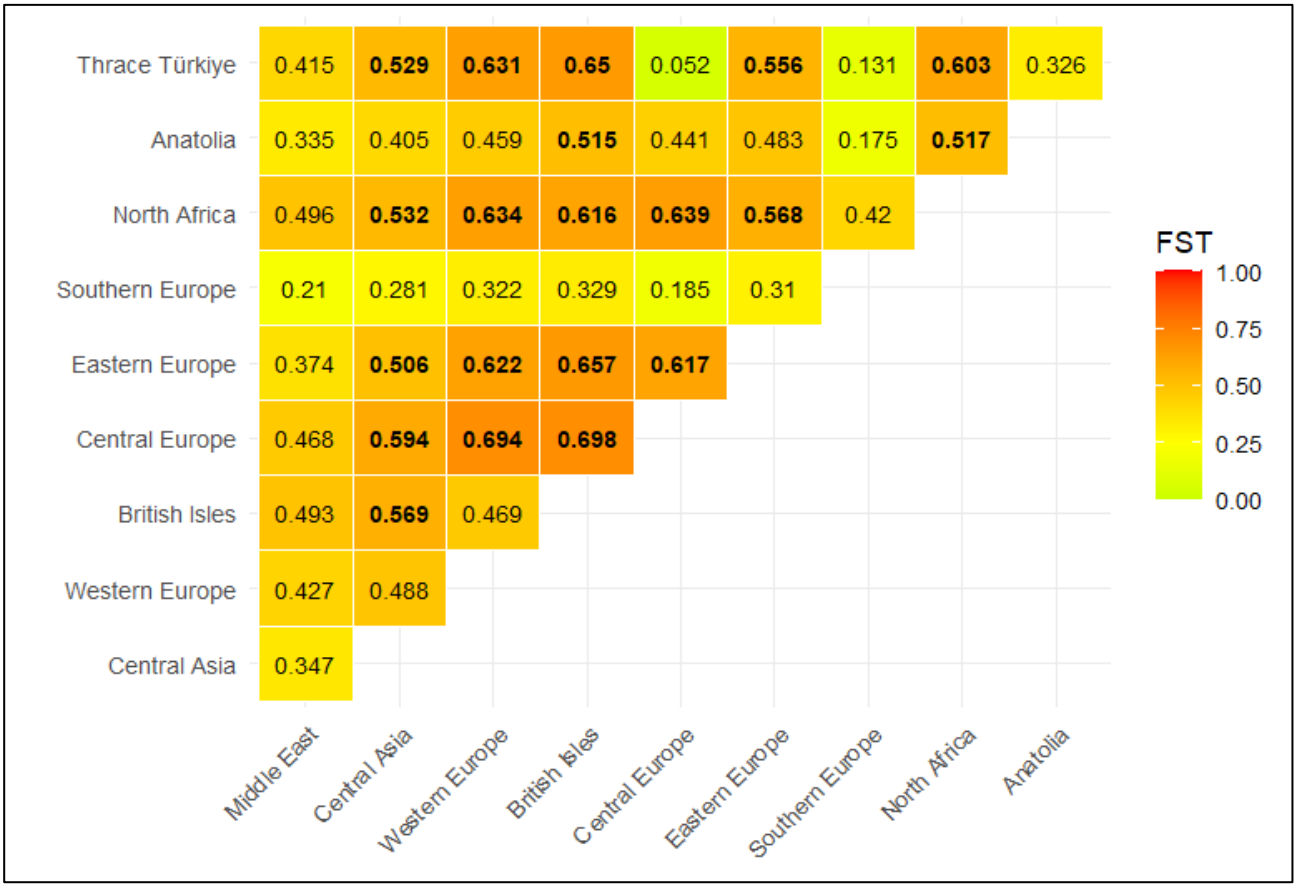


Figure 3.7. Heatmap of pairwise FST values among geographic regions based on mitochondrial DNA sequences. Values range from 0 (no differentiation) to 1 (complete differentiation). Color intensity indicates degree of genetic differentiation, with darker colors representing higher FST values.

The lowest FST value (0.052) was observed between Thrace Türkiye and Central Europe, suggesting recent connectivity or gene flow between these regions. Other notably low FST values were found between Southern Europe and Thrace Turkey (0.131), Southern Europe and Anatolia (0.175), Southern Europe and Central Europe (0.185), and Southern Europe and Middle East (0.210), indicating that Southern European populations maintain genetic similarity with multiple regions. Anatolia showed relatively low differentiation from Southern Europe (0.175) and Thrace Turkey (0.326), Anatolia also showed moderate differentiation from Middle East (0.335) and Central Asia (0.405), but higher values with Western Europe (0.459), Central Europe (0.441), Eastern Europe (0.483), and British Isles (0.515).

The highest FST value observed was 0.698 between Central Europe and British Isles, indicating substantial genetic isolation. Central Europe also showed very high differentiation from Western

Europe (0.694) and North Africa (0.639). The British Isles exhibited consistently high differentiation from most regions: 0.650 with Thrace Turkey, 0.616 with North Africa, 0.657 with Eastern Europe, 0.569 with Western Europe, and 0.617 with Central Europe, consistent with long-term island isolation.

North Africa displayed high levels of genetic differentiation from most regions, with FST values ranging from 0.420 (vs. Southern Europe) to 0.639 (vs. Central Europe and Eastern Europe). High differentiation was also observed between North Africa and Thrace Turkey (0.603), Western Europe (0.634), British Isles (0.616), and Central Asia (0.532). These high values suggest long-term isolation of North African populations.

Central Asia showed moderate differentiation from Middle East (0.347) and Anatolia (0.405), but higher values with European regions, ranging from 0.488 (Western Europe) to 0.594 (Central Europe). The Middle East exhibited moderate to high differentiation from most regions, with FST values ranging from 0.347 (Central Asia) to 0.631 (Thrace Turkey).

Eastern Europe showed intermediate to high FST values with most regions (0.374-0.657), while Western Europe displayed moderate differentiation from Southern Europe (0.322) and Middle East (0.427), but high values with Central Europe (0.694) and British Isles (0.694). The FST patterns are consistent with post-glacial expansion from southern refugia, with northern populations showing high genetic differentiation from southern regions (FST = 0.329-0.657) and from each other (FST = 0.569-0.698), indicating expansion from multiple refugial sources with limited subsequent gene flow.

To assess historical demographic patterns and test for signatures of population expansion or decline, Bayesian Skyline Plots (BSPs) were constructed for individual geographic regions (Figure 3.8) as well as for the combined dataset (Figure 3.9). The Y-axis in both of these figures shows effective population size expressed as the product of effective population size and generation time ($Ne \times \tau$) on a logarithmic scale. The X-axis represents time before present in years.

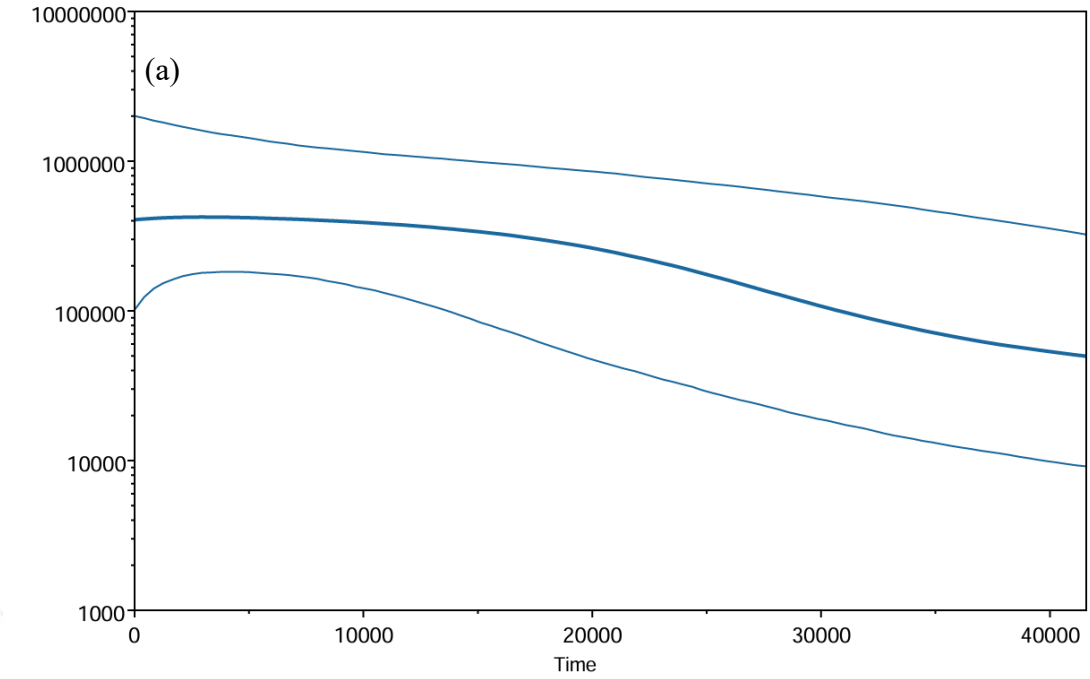


Figure 3.8.a. Bayesian Skyline Plot showing historical changes in effective population size (Ne) for Anatolia.

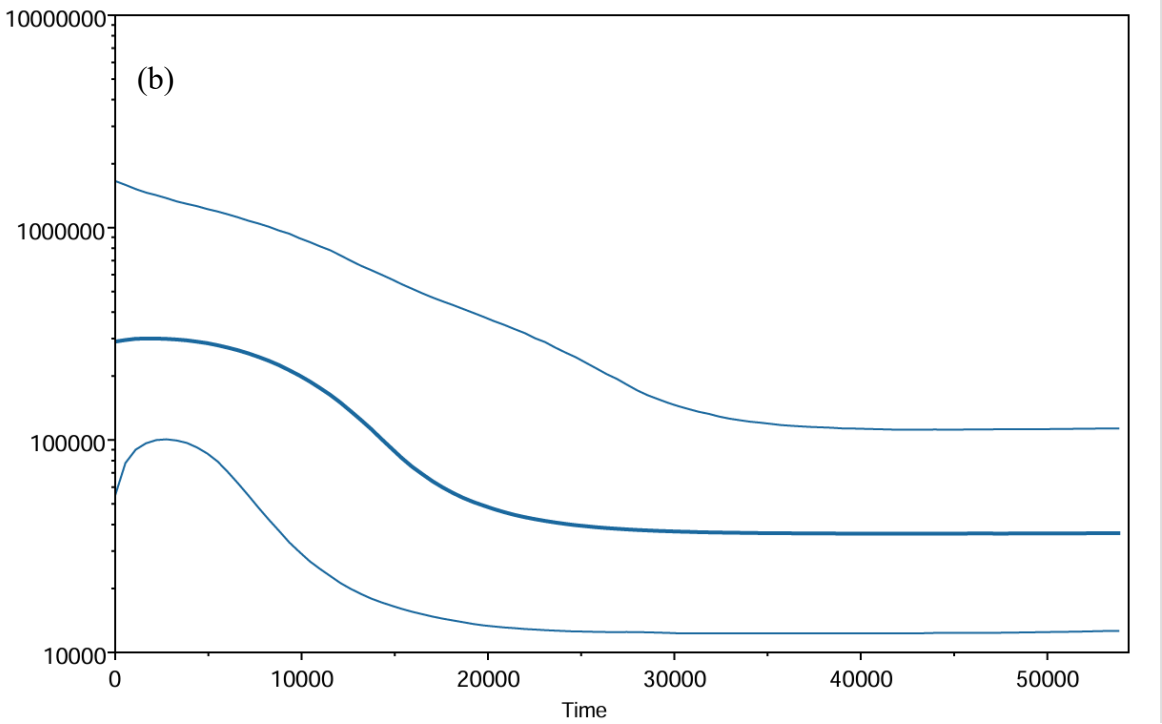


Figure 3.8.b Bayesian Skyline Plot showing historical changes in effective population size (Ne) for British Isles.

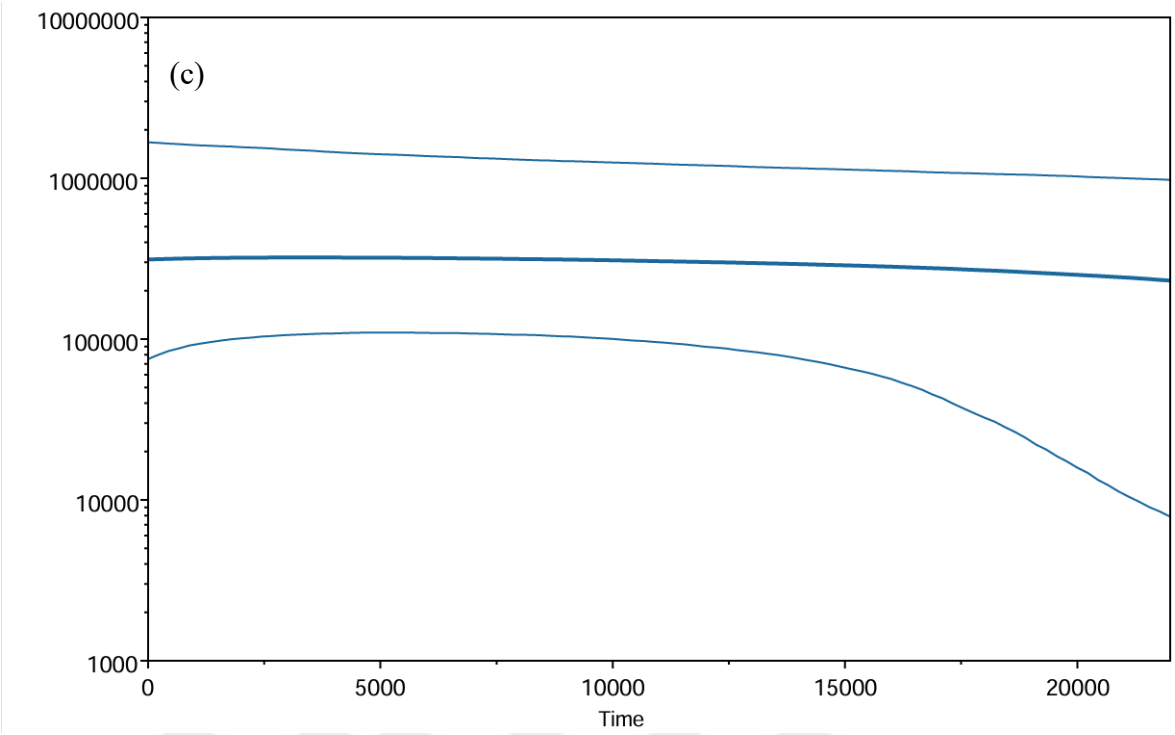


Figure 3.8.c Bayesian Skyline Plot showing historical changes in effective population size (Ne) for Eastern Europe.

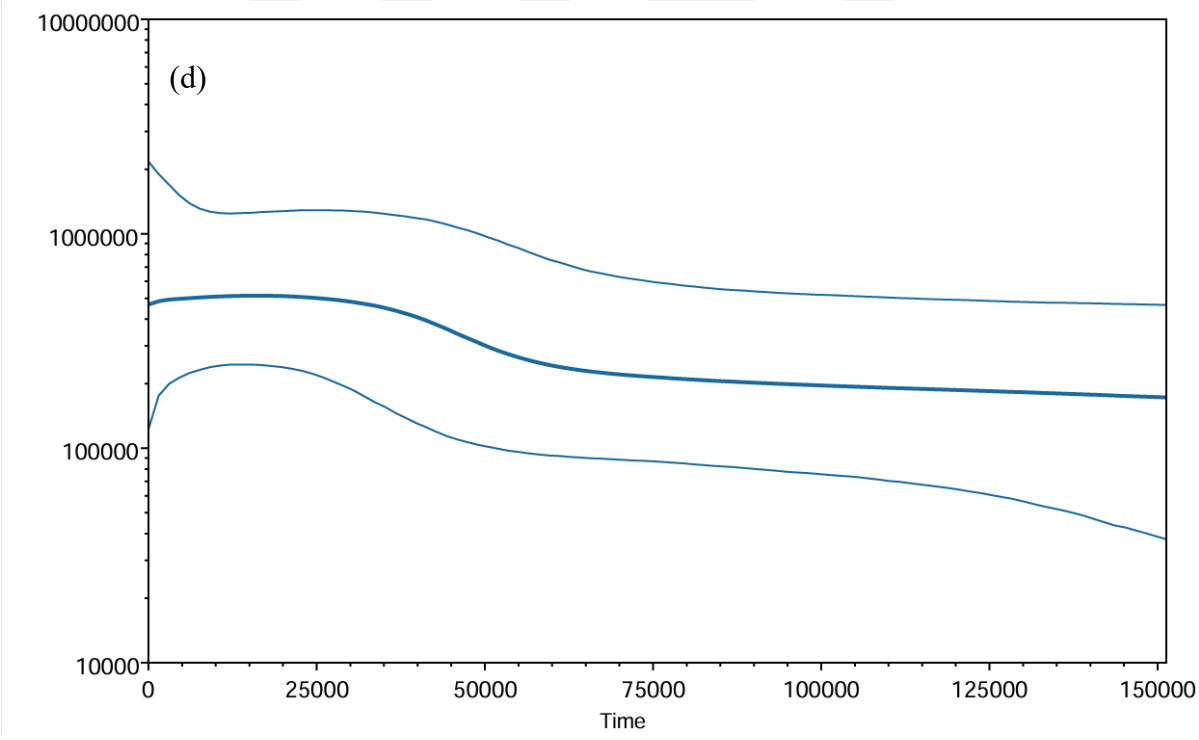


Figure 3.8.d Bayesian Skyline Plot showing historical changes in effective population size (Ne) for Middle East.

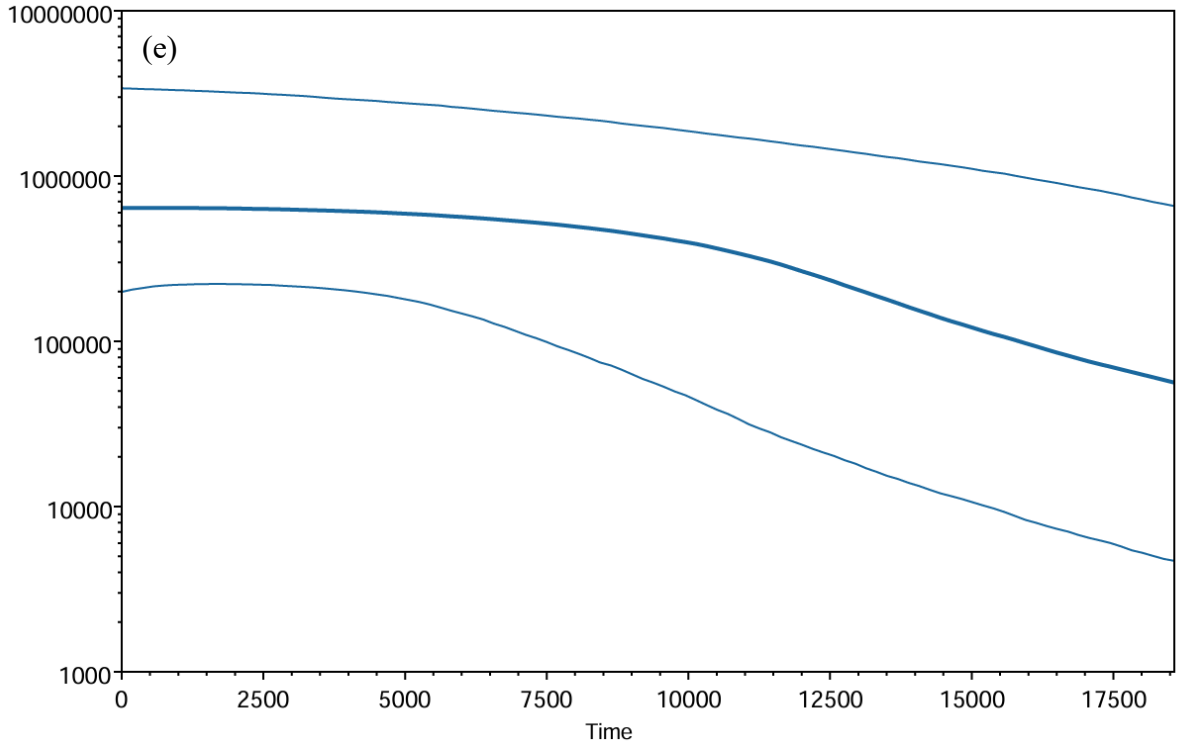


Figure 3.8. Bayesian Skyline Plot showing historical changes in effective population size (Ne) for Western Europe.

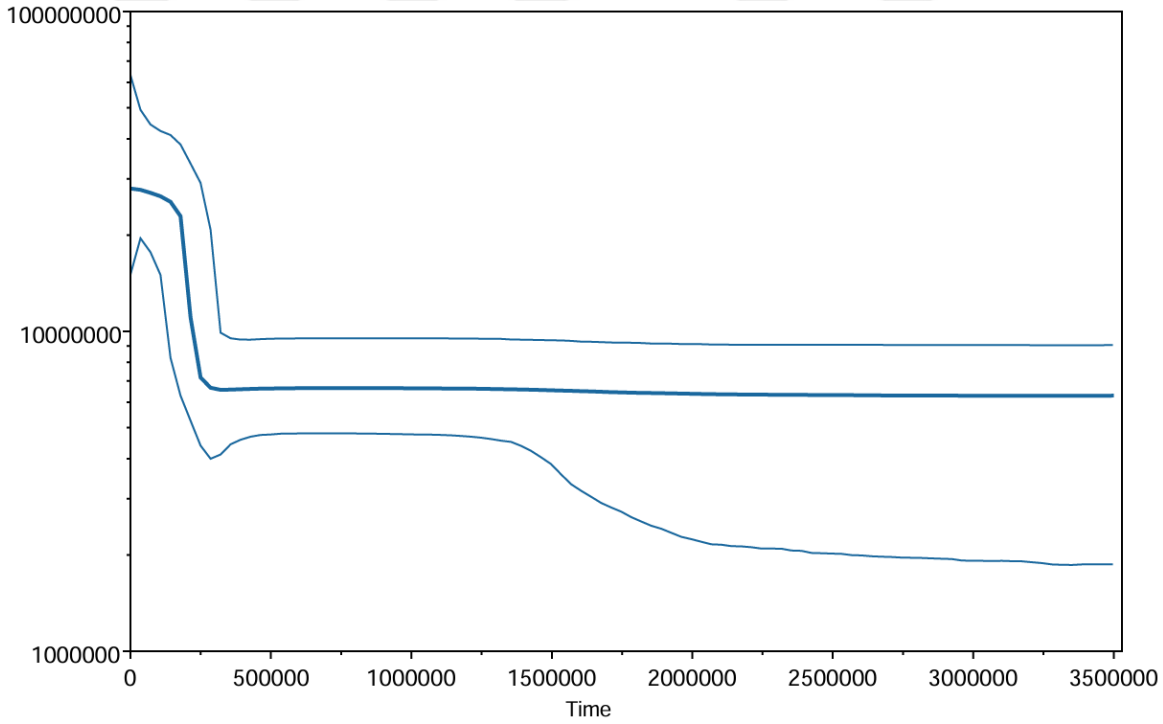


Figure 3.9. Bayesian Skyline Plot for all populations combined, showing overall demographic history of *Pipistrellus pipistrellus* across its range based on mtDNA HVII sequences.

Regional BSPs (Figure 3.8) reveal distinct demographic patterns across geographic areas. Anatolia shows relatively stable effective population sizes extending back approximately 40,000

years, the overall pattern suggests long-term population persistence rather than recent expansion, consistent with Anatolia serving as a glacial refugium. The British Isles exhibits the clearest signal of recent population expansion. The BSP shows low effective population sizes, followed by a pronounced expansion beginning around 10,000-15,000 years before present. This pattern is consistent with post-Last Glacial Maximum (LGM) colonization of the British Isles from southern refugia and aligns with the significant negative Tajima's D (-1.922, $p < 0.05$) and Fu's Fs (-3.709, $p < 0.05$) values observed for this region. Eastern Europe displays a relatively stable demographic pattern over approximately 25,000 years. Unlike the British Isles, there is no clear signal of recent dramatic expansion, suggesting that Eastern Europe was colonized earlier in the post-glacial period and has since maintained a stable population size. The Middle East shows evidence of long-term population stability extending back approximately 150,000 years. The overall pattern suggests demographic stability with some fluctuations, consistent with the Middle East serving as a long-term refugium. Western Europe shows evidence of population expansion over approximately the last 20,000 years. This expansion signal is consistent with post-glacial colonization, though the pattern appears more gradual compared to the sharp expansion observed in the British Isles. The expansion likely reflects northward colonization from southern refugia following the Last Glacial Maximum, with populations growing steadily as suitable habitat became available.

The combined BSP for all populations (Figure 3.9) extends back approximately 3.5 million years and indicates a stable population with an expansion beginning around ~300,000 years ago, with the rate of increase slowing around ~150,000 years ago, after which the population has remained relatively stable. The 95% HPD intervals were wider for older time periods, reflecting greater uncertainty in ancestral demographic estimates.

3.3.2. Nuclear DNA Analyses

3.3.2.1. The intron 4 of the COPS7A gene. The genetic diversity measures are shown in Table 3.4. The intronic *COPS7A* locus showed very low levels of polymorphism across the sampled range (5 variable sites in 253 bp). Most geographic regions were monomorphic, with genetic variation largely restricted to Turkish and Eastern European populations. Overall nucleotide diversity was low ($\pi = 0.001 \pm 0.001$), and haplotype diversity was also low ($Hd = 0.227 \pm 0.004$), indicating limited intraspecific variation at this locus. Neutrality tests based on the intron 4 of the *COPS7A* gene revealed no significant results across geographic regions (Tajima's D and Fu's F, Appendix A, Table A.5).

Table 3.4. Genetic diversity metrics across regions, based on nuclear DNA sequences of the intron 4 of the *COPS7A* gene.

	Number of sequences /alleles	Invariable Sites	Variable Sites	Singleton Variable sites	Parsimony informative sites	Number of Haplotype	Pi ± Sd	Hd ± Sd
Total	66	248	5	4	1	6	0.001 ± 0.001	0.227 ± 0.004
Anatolia	28	249	4	3	1	5	0.002 ±0.001	0.381 ±0.112
Thrace Türkiye	12	252	1	1	0	2	0.001 ± 0.001	0.167 ±0.134
Middle East	10	253	0	0	0	1	0 ±0	0 ±0
Southern Europe	6	253	0	0	0	1	0 ±0	0 ±0
Eastern Europe	2	252	1	1	0	2	0.004 ± 0.002	1 ±0.5
Central Asia	6	253	0	0	0	1	0 ±0	0 ±0
North Africa	2	253	0	0	0	1	0 ±0	0 ±0

The intronic *COPS7A* locus showed very low levels of polymorphism across the sampled range (5 variable sites in 253 bp). Most geographic regions were monomorphic, with genetic variation largely restricted to Turkish and Eastern European populations. Overall nucleotide diversity was low ($\pi = 0.001 \pm 0.001$), and haplotype diversity was also low (Hd = 0.227 ± 0.004), indicating limited intraspecific variation at this locus. Neutrality tests based on the intron 4 of the *COPS7A* gene revealed no significant results across geographic regions (Tajima's D and Fu's F, Appendix A, Table A.5).

The haplotype network analysis of the intron 4 of the *COPS7A* gene revealed low overall genetic variation across the sampled geographic regions as shown in Figure 3.10.

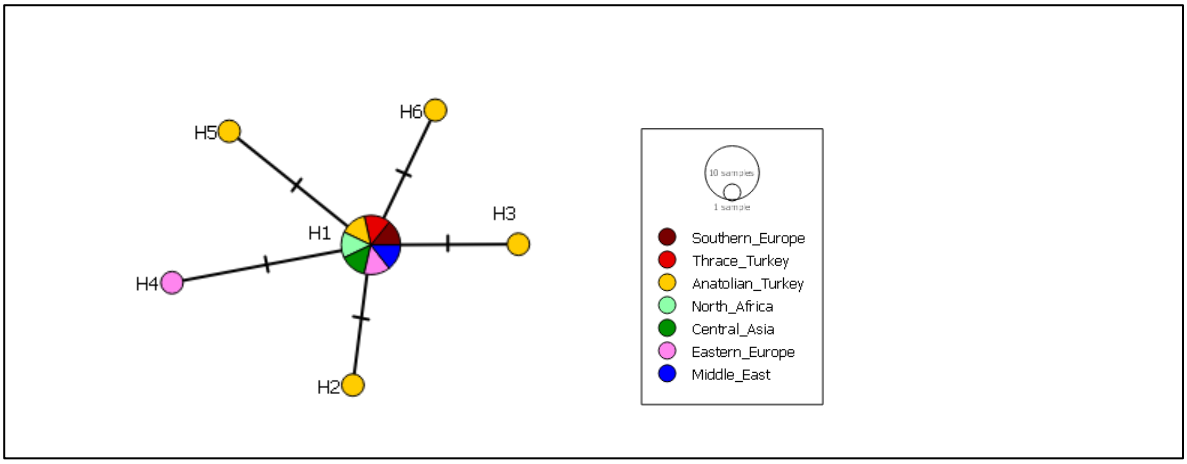


Figure 3.10. Haplotype network of the nuclear intron *COPS7A* constructed in PopART. Circles represent distinct haplotypes, with circle size proportional to haplotype frequency. Colors indicate the geographic origin of samples.

A total of six haplotypes were identified among 33 sequences, with one dominant haplotype occurring at high frequency and shared among all regions. This major haplotype comprised individuals from Southern Europe, Thrace Türkiye, Anatolia, North Africa, Central Asia, Eastern Europe, and the Middle East, indicating extensive haplotype sharing and little geographic structuring. The remaining haplotypes were rare, each differing from the dominant haplotype by a single mutational step and represented by one individual. These low-frequency haplotypes were largely restricted to Anatolia and Eastern Europe. Overall, the star-like topology of the network is consistent with limited nucleotide diversity and suggests recent common ancestry or ongoing gene flow among populations.

Phylogenetic relationships among samples were inferred using Neighbor-Joining and Maximum Likelihood methods, and the resulting trees are presented below.

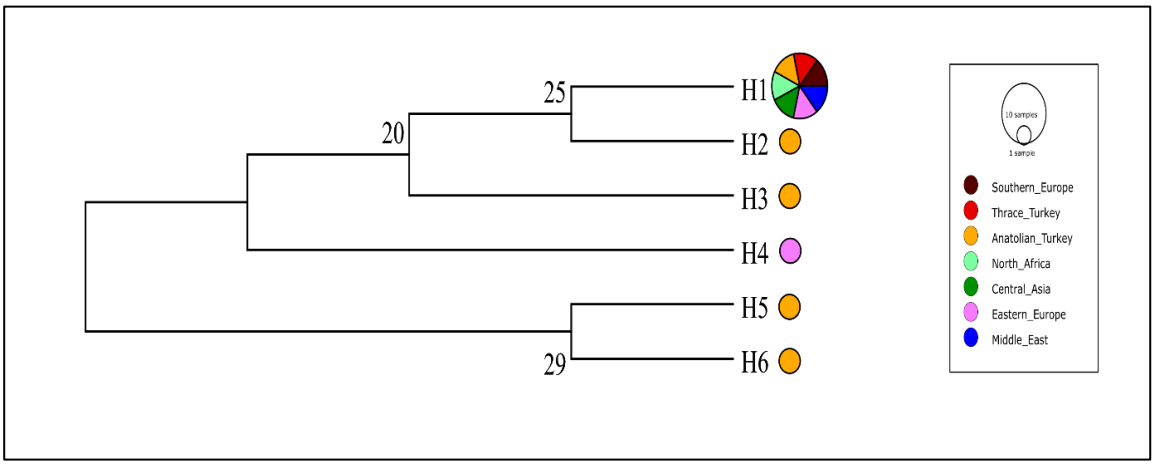


Figure 3.11. Neighbor-Joining Bootstrap consensus tree.

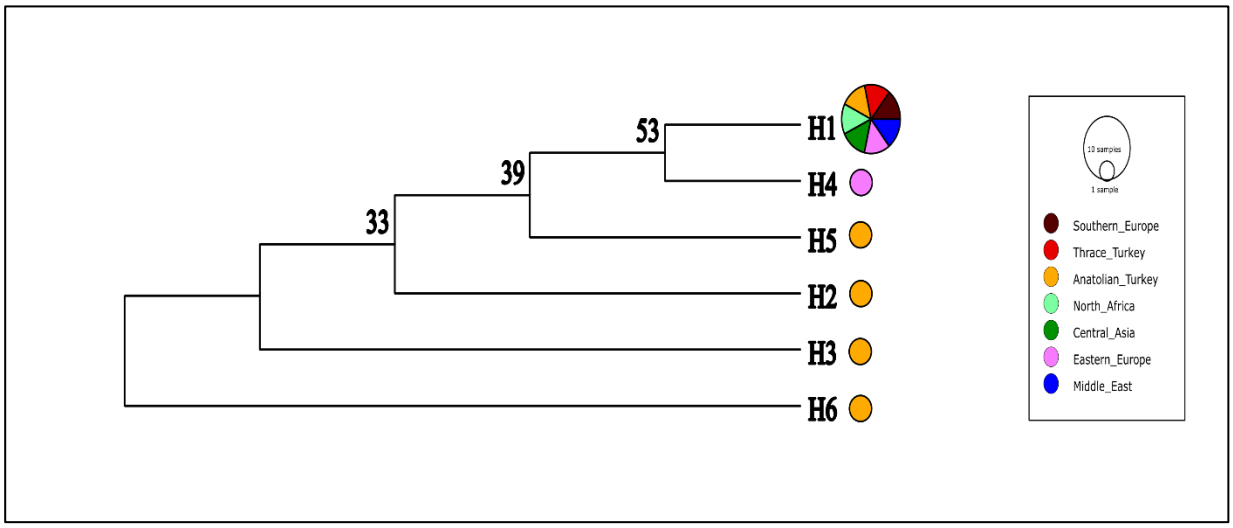


Figure 3.12. Maximum Likelihood Bootstrap consensus tree

The NJ tree (Figure 3.11) revealed a shallow phylogenetic structure characterized by a dominant, widely distributed haplotype surrounded by several low-frequency haplotypes separated by short branch lengths. Most haplotypes showed minimal sequence divergence, consistent with the low overall nucleotide diversity observed for this *COPS7A* locus. Haplotypes from different geographic regions were interspersed rather than forming strictly region-specific clades, indicating limited phylogeographic structuring. Several rare haplotypes formed terminal branches, suggesting recent mutational events rather than long-term regional isolation.

The ML tree (Figure 3.12) recovered a topology largely congruent with the NJ tree, supporting the same major clustering patterns and confirming the absence of deep genetic splits among haplotypes. As in the NJ tree, the ML tree was dominated by a central haplotype shared across multiple geographic regions, with other haplotypes differing by one or a few mutations. Bootstrap support values were generally higher for shallow groupings than for deeper nodes, reflecting limited sequence divergence within the dataset. The concordance between NJ, ML, and haplotype network analyses indicate a recent common ancestry of haplotypes and suggests ongoing or historical gene flow among regions rather than long-standing population subdivision.

Genetic differentiation among geographic regions was assessed using pairwise FST estimates (Figure 3.13).

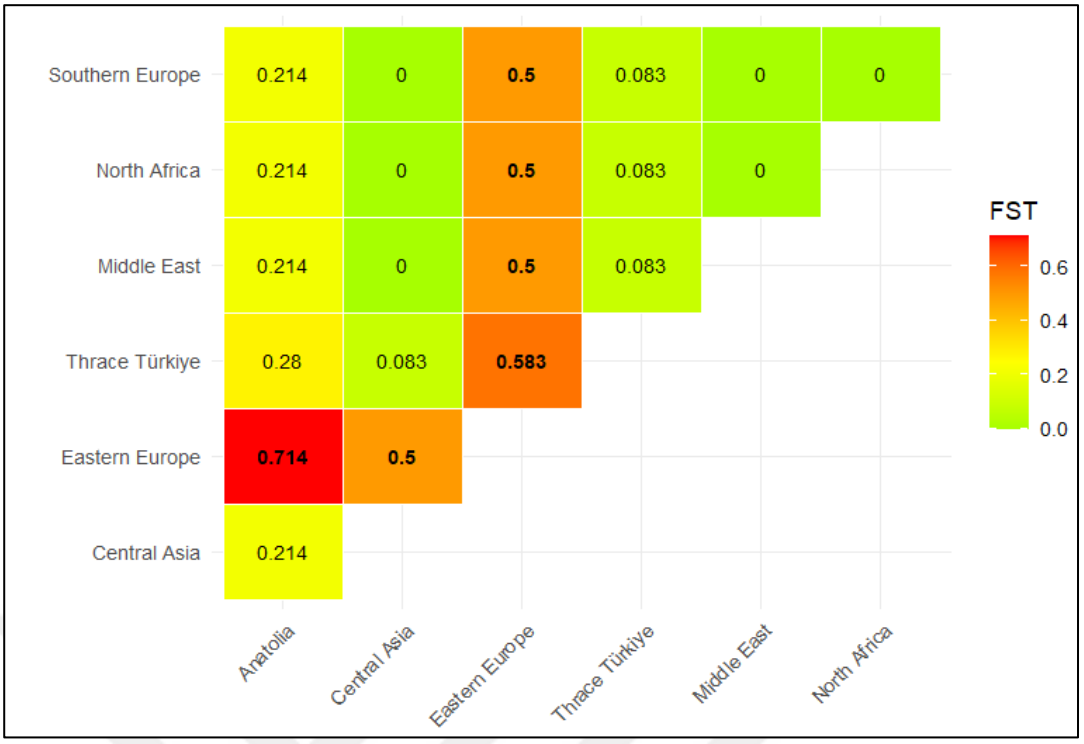


Figure 3.13. Pairwise FST estimates among geographic regions based on the *COPS7A* nuclear marker.

Pairwise FST estimates revealed overall low levels of genetic differentiation among the examined regions. Near-zero FST values were observed between Central Asia, Thrace Türkiye, the Middle East, and Southern Europe (FST = 0.000–0.083), indicating weak genetic structure and potential gene flow among these regions. Moderate levels of differentiation were detected between Anatolia and several regions (FST ≈ 0.21–0.28). In contrast, higher FST values were observed between Eastern Europe and multiple regions, particularly Central Asia and North Africa (FST = 0.50–0.71), suggesting stronger genetic differentiation. Overall, the results indicate limited genetic structuring across most Eurasian regions, with elevated differentiation involving Eastern Europe. These patterns should be interpreted with caution given the relatively small sample sizes in some regions.

3.3.2.2. The intron 5 of the ABHD11 gene. To characterize patterns of genetic variation across regions, genetic diversity and neutrality statistics were calculated**.** The generated genetic diversity measures are presented in Table 3.5, and the neutrality statistics are presented in Table 3.6.

Table 3.5. Genetic diversity metrics across regions, based on nuclear DNA sequences of the intron 5 of *ABHD11* gene.

	Number of sequences /alleles	Invariable Sites	Variable Sites	Singleton Variable sites	Parsimony informative sites	Number of Haplotype	Pi ± Sd	Hd ± Sd
Total	66	295	28	3	25	16	0.008 ± 0.001	0.800 ± 0.035
North Africa	2	323	1	1	0	2	0.003 ±0.001	1 ±0.5
Central Asia	6	321	3	2	1	3	0.004 ±0.001	0.733 ±0.155
Middle East	10	323	1	0	1	2	0.001 ±0.001	0.467± 0.132
Southern Europe	6	318	5	1	4	4	0.007 ±0.002	0.867 ±0.129
Eastern Europe	2	324	0	0	0	1	0 ±0	0 ±0
Anatolia	28	304	19	1	18	8	0.010 ±0.003	0.817 ± 0.050
Thrace Türkiye	12	316	8	4	4	6	0.006 ± 0.002	0.848 ±0.074

The Analysis revealed moderate overall genetic diversity across all populations ($\pi = 0.00856 \pm 0.00157$, $Hd = 0.800 \pm 0.035$), with 28 variable sites contributing to 16 distinct haplotypes. Regional comparisons demonstrated notable variation in genetic diversity patterns, with Anatolia displaying the highest nucleotide diversity ($\pi = 0.01003 \pm 0.00286$) and the greatest number of parsimony-informative sites, followed by Southern Europe and Thrace Türkiye, suggesting these regions have greater genetic variation and potentially serve as refugia or centers of diversification for this genomic region. In contrast, Eastern Europe showed complete monomorphism with no genetic variation detected, while Middle East, North Africa, and Central Asia displayed low diversity levels with minimal haplotype differentiation.

Neutrality tests based on this nuclear DNA marker revealed no significant results across all examined regions. Tajima's D values were negative in Anatolia, Thrace Türkiye, and Central Asia, and positive in the Middle East and Southern Europe; however, none of these values were statistically significant ($P > 0.10$). Similarly, Fu's Fs statistics varied among regions, with both positive and negative values observed, but none reached statistical significance.

Table 3.6. Summary of neutrality tests: Tajima's D, Fu's Fs metrics across regions, based on nuDNA sequences of the intron 5 of the *ABHD11* gene.

Region	**n**	**Tajima's D**	**P-value**	**Fu's Fs statistic:**	**P-value**
Anatolia	28	-1.18310	P > 0.10 (ns)	0.186	P > 0.10 (ns)
Middle Est	10	0.81980	P > 0.10 (ns)	0.818	P > 0.10 (ns)
Southern Europe	6	0.70767	P > 0.10 (ns)	-0.119	P > 0.10 (ns)
Thrace Turkey	12	-0.81861	P > 0.10 (ns)	-1.195	P > 0.10 (ns)
Central Asia	6	-0.18544	P > 0.10 (ns)	0.209	ns

The constructed haplotype network is shown in Figure 3.14 below. The haplotype network revealed a star-like topology with multiple haplotypes radiating from a central ancestral haplotype, indicating a relatively recent expansion from a common ancestor. The central node was shared predominantly by samples from Anatolia, Central Asia, and Southern Europe, suggesting these regions may harbor ancestral genetic diversity or serve as historical dispersal centers. Haplotypes from Anatolia showed the greatest divergence and formed multiple distinct branches, consistent with the high nucleotide and haplotype diversity observed in this region. Thrace Türkiye and Southern Europe haplotypes were distributed across different branches of the network, while Middle East haplotypes occupied peripheral positions with fewer mutational steps from the central haplotype. The presence of multiple mutational steps between certain haplotypes suggests accumulated genetic divergence over time, while the short branch lengths connecting most haplotypes reflect the overall low nucleotide diversity and recent common ancestry.

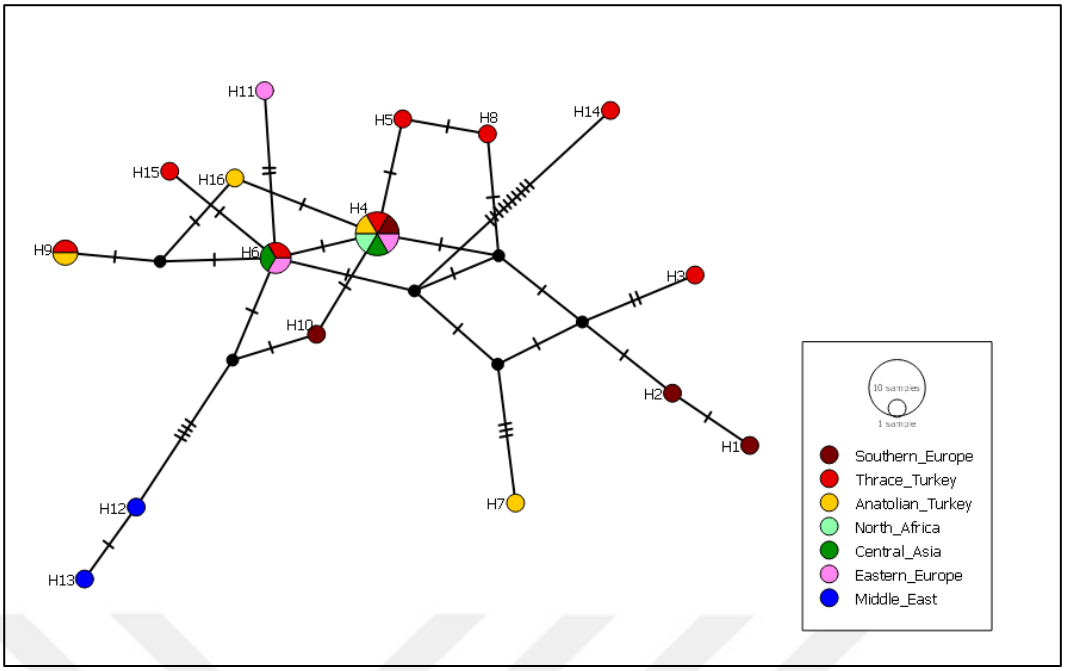


Figure 3.14. Haplotype network of the nuclear intron *ABHD11* constructed in PopART. Circles represent distinct haplotypes, with circle size proportional to haplotype frequency. Colors indicate the geographic origin of samples.

Then neighbor-joining (NJ) (Figure 3.15) and maximum likelihood (ML) (Figure 3.16) trees were constructed, they showed largely congruent structures with similar clustering patterns, though bootstrap support values varied across nodes.

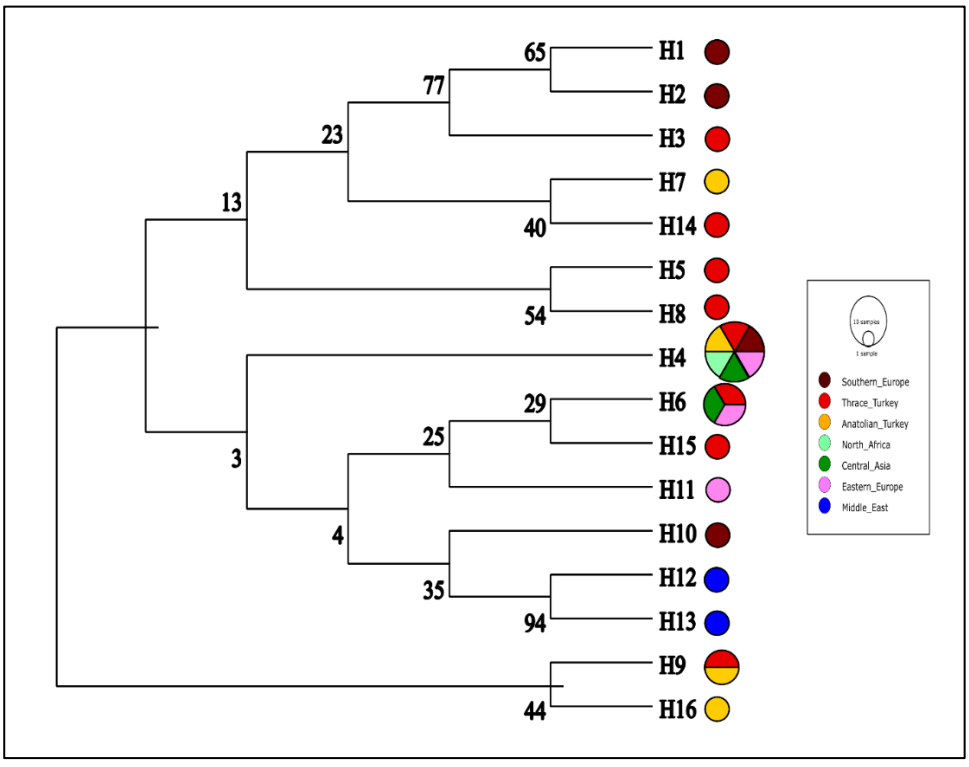


Figure 3.15. Neighbor-Joining bootstrap consensus tree.

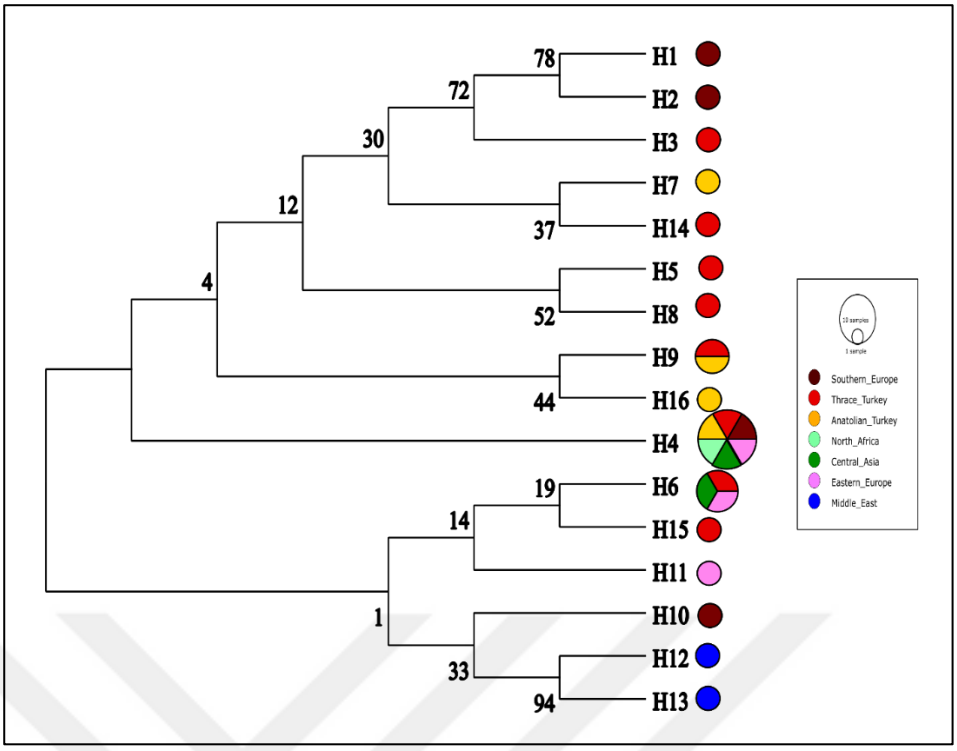


Figure 3.16. Maximum Likelihood bootstrap consensus tree.

The trees revealed the presence of several distinct clades with moderate to high bootstrap support, indicating phylogenetic structure among haplotypes. Thrace Türkiye haplotypes (H3, H5, H8, H14, H15) were distributed across multiple clades, reflecting the genetic diversity within this region. Middle East haplotypes (H12, H13) clustered together with strong bootstrap support (94% in both NJ and ML trees). Anatolia haplotypes (H7, H9, H16) showed phylogenetic divergence and were positioned in different parts of the tree, again consistent with the high genetic diversity observed in this region. The shared haplotype H4, which included samples from all regions, occupied a relatively basal position in the phylogeny, supporting its role as an ancestral and/or widely distributed haplotype. Overall, both phylogenetic analyses supported the presence of geographically structured genetic variation with some haplotypes showing regional specificity while others exhibited widespread distribution, suggesting complex historical patterns of dispersal and gene flow across the studied geographic range.

Genetic differentiation among geographic regions was assessed using pairwise FST estimates (Figure 3.17).

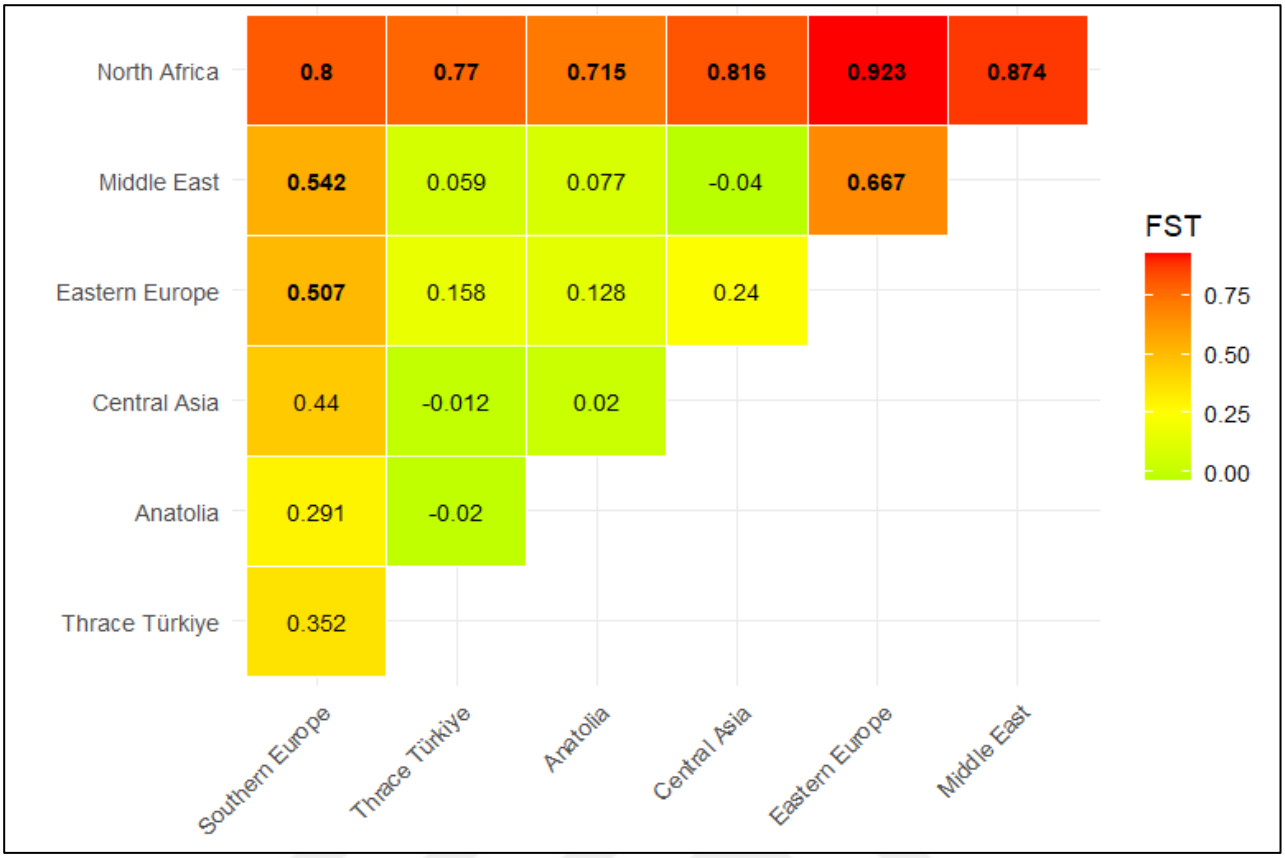


Figure 3.17. Pairwise FST estimates among geographic regions based on the *ABHD11* nuclear marker.

Pairwise FST values based on the nuclear marker *ABHD11* revealed variable levels of genetic differentiation among geographic regions. High levels of differentiation were observed between North Africa and all other regions (FST = 0.715–0.923), indicating strong genetic structuring involving this region. Moderate differentiation was detected between Southern Europe and several regions, including the Middle East, Eastern Europe, and Central Asia (FST ≈ 0.44–0.54). In contrast, low or near-zero FST values were observed among Anatolia, Thrace Türkiye, and Central Asia, as well as between Anatolia and the Middle East, suggesting weak genetic differentiation and potential gene flow among these regions. Overall, the *ABHD11* marker indicates pronounced differentiation of North Africa, while genetic structure among Eurasian regions appears comparatively weak.

Nuclear DNA haplotypes (*COPS7A* and *ABHD11*), together with the sampling coordinates of analyzed individuals, are presented in the Appendix A, Table A.4.

3.4. Discussion

The present study expands upon Hulva et al.'s comprehensive phylogeographic research (2004, 2007, 2010) on *Pipistrellus pipistrellus*, which established that this species represents a highly diversified complex with its radiation center in the Mediterranean Basin. Using mitochondrial markers (Cytochrome b and D-loop), Hulva identified deeply divergent clades: (1) P. pipistrellus s.str. (Continental Clade) with European and Asiatic sub-clades spanning Eurasia; (2) P. pipistrellus SW (Southwestern/Mediterranean Clade) split into Lineage A (Morocco, Sicily, Malta, Corsica) and Lineage B (Maghreb), with genetic distances (~10%) suggesting potential species-level divergence; and (3) isolated island lineages. Moreover, Hulva detected introgression among Mediterranean lineages despite deep divergence (splits dating 3.1–4.1 Ma), and explicitly identified Anatolia, Iran, Spain, Greece, and Southern Italy as containing divergent haplotypes requiring further investigation. We addressed some of the geographic gaps of Hulva et al. studies, by intensively sampling Anatolia and European/Thrace Türkiye, while expanding coverage in Central Asia (Tajikistan, Turkmenistan), North Africa, and the Middle East. Additionally, we employed nuclear intron markers due to the limitations of mtDNA-only approaches.

Our 175-haplotype mitochondrial network reveals phylogeographic complexity consistent with Hulva et al.'s "mosaic" model, while providing enhanced details of Anatolian and Middle Eastern populations. A distinct Southern European cluster, linked to North African haplotypes by comparatively long branches, is consistent with the *P. pipistrellus* SW Mediterranean clade (Lineages A and B) described by Hulva et al., (2007) and highlights the Mediterranean Basin as an important region in early diversification. The pronounced phylogenetic separation between Southern European and North African haplotypes, with their geographic proximity, supports long-term isolation across the southern Mediterranean, and is consistent with North Africa likely acting as an important extra-European refugial area during glacial periods (Husemann et al., 2014). In contrast, the cohesive British Isles and Western European cluster exhibit limited divergence, suggesting recent postglacial expansion from continental sources, again in agreement with Hulva et al.'s findings. This pattern is also consistent with Boston et al. (2014), who showed that *Pipistrellus pipistrellus*, with a broad ecological niche, survived in multiple refugia, including cryptic north-western European sites, unlike *P. pygmaeus*, which exhibits lower genetic differentiation indicative of expansion from a single eastern European source.

The pairwise FST analysis further supports this pattern of multiple refugia and differential post-glacial colonization routes. The extremely low FST between Thrace Turkey and Central Europe

(0.052) suggests an important eastern expansion corridor through the Balkans, while the very high FST between Central Europe and British Isles (0.698) indicates these northern populations expanded from different refugial sources with limited subsequent gene flow. North Africa showed consistently high FST values with all other regions (0.420-0.639), confirming long-term isolation across the Mediterranean barrier. The Bayesian Skyline Plot analyses provide temporal context for these patterns. Southern refugial populations, Anatolia and the Middle East, show stable, high effective population sizes through time, consistent with long-term persistence. In contrast, the British Isles exhibit a clear signature of recent population expansion beginning approximately 10,000-15,000 years ago, coinciding with post-Last Glacial Maximum warming and aligning with the significant negative neutrality test values (Tajima's D = -1.922, Fu's Fs = -3.709, both $p < 0.05$) observed for this region. Eastern Europe shows demographic stability without dramatic recent expansion, suggesting earlier colonization, while Western Europe displays gradual expansion over the last 20,000 years. These demographic patterns complement the genetic diversity gradient, with southern regions retaining high diversity (Anatolia: Hd = 0.981; Middle East: Hd = 0.979) and northern regions showing reduced diversity consistent with founder effects (British Isles: Hd = 0.908).

The highly connected cluster dominated by Anatolian and Thracian haplotypes with additional connections to Central European haplotypes, supports the interpretation of Anatolia as a significant genetic diversity hotspot within *Pipistrellus pipistrellus* and is in line with Hulva et al.'s conclusion that the region contains significant and possibly ancestral genetic diversity. Anatolia exhibits remarkably high genetic diversity (Hd = 0.981, 37 haplotypes from 54 individuals), which could reflect either (1) long-term persistence as a glacial refugium, or (2) secondary contact between divergent lineages from different refugia. While the elevated diversity, stable demographic profile in Bayesian Skyline Plots, and central position in the haplotype network are consistent with the refugium hypothesis, as suggested by Hulva et al. (2010), the presence of both Anatolia-specific haplotypes and haplotypes shared with European populations suggests Anatolia may have functioned both as a refugial area and as a contact zone connecting eastern and western lineages. The moderate FST values between Anatolia and neighboring regions (Southern Europe: 0.175; Thrace Turkey: 0.326) support gene flow and connectivity, reinforcing Anatolia's role as a genetic bridge.

This refugial role has been demonstrated across multiple bat taxa; for instance, phylogeographic analyses and ecological niche modelling of *Miniopterus schreibersii* revealed survival in eastern Mediterranean refugia during the Last Glacial Maximum, followed by postglacial expansion and regional diversification that included Anatolia as a key corridor and diversification area (Bilgin et al., 2016). As expected for long-term refugial populations, southern lineages have higher haplotype

diversity than rapidly expanding northern populations, which often show reduced genetic variation and star-like haplotype networks. Despite their geographic proximity, Anatolian and Thrace samples show genetic differentiation, indicating partial separation across the Marmara Sea, However, the presence of shared haplotypes confirms that gene flow has occurred, suggesting periodic connectivity across this marine barrier.

A distinct Middle Eastern cluster characterized by comparatively long branch lengths suggests the presence of another deeply structured population, potentially corresponding to the Asiatic sub-clade of *P. pipistrellus* suggested by Hulva et al. However, the degree of divergence observed, reflected by long branches separating the Middle Eastern cluster from adjacent European and Anatolian haplotypes, suggests that this group represents either major intraspecific differentiation within the Asiatic sub-clade or an unknown lineage comparable in depth to the SW Mediterranean clade. The relatively stable demographic pattern observed in Middle Eastern Bayesian Skyline Plots, extending back approximately 150,000 years, supports the hypothesis of long-term population persistence in this region through multiple glacial-interglacial cycles.

To complement mitochondrial DNA and assess nuclear gene flow patterns, we used nuclear intron markers that have been used for population-level phylogeographic studies in bats (Kerth et al., 2002; Rossiter et al., 2007). Of the targeted four nuclear introns, two yielded successful amplification results: *COPS7A* and *ABHD11*. The intron 5 of the *ABHD11* gene revealed moderate overall genetic diversity ($\pi = 0.00856 \pm 0.00157$, $Hd = 0.800 \pm 0.035$) with striking regional heterogeneity. Anatolia exhibited the highest nucleotide diversity ($\pi = 0.01003 \pm 0.00286$) with 18 parsimony-informative sites among eight haplotypes; Southern Europe and Thrace Türkiye showed moderate diversity, while Eastern Europe was completely monomorphic. This geographic gradient, characterized by higher genetic diversity in southern regions and reduced variation in northern populations, is consistent with expectations under postglacial expansion models and mirrors patterns documented using nuclear markers in numerous European mammal species (Jaarola & Searle, 2002; Tougard et al., 2008), as well as amphibians, arthropods, and plants (Schmitt, 2007). The monomorphism observed in Eastern Europe at the *ABHD11* locus, despite substantial variation elsewhere (16 total haplotypes), is consistent with strong founder effects associated with recent postglacial colonization, whereas the presence of eight Anatolian haplotypes supports long-term population persistence in this region.

In contrast, the intron 4 of the *COPS7A* gene exhibited extreme homogeneity ($\pi = 0.00094 \pm 0.00029$, $Hd = 0.227 \pm 0.00458$), with only five variable sites and a single widespread haplotype dominating across all sampled regions. Similar discordance among nuclear loci has been reported in

other bat species, underscoring that individual nuclear markers can differ markedly in their sensitivity to demographic history and selection (Kerth et al., 2002; Rossiter et al., 2007). The nuclear DNA results presented in this chapter are primarily descriptive due to the smaller sample sizes and variable amplification success for nuclear markers. Consequently, phylogeographic interpretations rely mostly on the mitochondrial DNA results, which provide comprehensive geographic coverage and higher confidence in the observed patterns.

The observed gradient of genetic structure, strong phylogeographic structuring in mtDNA, moderate structure in the intron 5 of the *ABHD11*, and minimal structure in the intron 4 of the *COPS7A* gene is also consistent with sex-biased dispersal, specifically female philopatry combined with male-mediated gene flow. Because mitochondrial DNA has a smaller effective population size and is maternally inherited, it is particularly sensitive to restricted female dispersal, whereas nuclear loci are homogenized by male movement, depending on locus-specific coalescent times and selective constraints (Prugnolle & de Meeus, 2002; Petit & Excoffier, 2009). This pattern accords closely with Hulva et al.'s (2010) microsatellite-based inference of female philopatry in *Pipistrellus pipistrellus* s.str. and parallels observations in other bat species, where fidelity to maternity colonies maintains mtDNA structure despite substantial male-driven nuclear gene flow (Kerth et al., 2002; Rossiter et al., 2007). Nevertheless, inference from only two nuclear loci remains limited, and broader nuclear or genomic datasets will be required to robustly assess gene flow and introgression.

4. CHAPTER 2: UNDERSTANDING BAT ACTIVITY AND MORTALITY PATTERNS IN A WIND FARM IN TÜRKİYE

4.1. Introduction

Generating electricity from renewable sources, such as wind power, is booming due to efforts to cut CO_2 emissions and slow down climate change (GWEC 2021). Despite having positive effects on the environment and the economy, wind energy production unintentionally affects wildlife, especially birds and bats that collide with the rotating blades (Northrup & Wittemyer, 2013; Voigt et al., 2015). The conflict between the environmental goals of preserving biodiversity and decarbonizing energy production, known as the "green-green dilemma," (Straka et al., 2020) has not yet been resolved (Voigt et al., 2016). Finding solutions to generate wind energy while minimizing negative impacts on biodiversity is critical, and it has long been an aim of collaboration between the wind industry and wildlife conservation organizations.

The growing documentation of bat mortality at wind energy facilities points to a potentially severe threat to many bat populations (Johnson et al., 2004; Arnett et al., 2005, 2008; Kunz et al., 2007). Although the Habitats Directive (92/43/EEC, Annex IV) and national laws in various countries provide strict protection for all European bat species, the influence of wind energy installations on bat populations is difficult to predict due to the lack of empirical data on bat population sizes and dynamics (Frick et al., 2017, 2020; Friedenberg & Frick, 2021) and due to the complexity of physiological and behavioural factors, and habitat and weather-related factors like wind speed, and temperature (Guest et al., 2022). Several attempts have produced cumulative estimates of the number of bat species impacted by wind turbines in a specific area for a specific year, each utilizing a different set of underlying assumptions and data. Some studies (Arnett et al., 2008; Kunz et al., 2007) found that some bat species are especially at risk to collision more than others, for instance in Europe, most bat casualties at wind farms are *Pipistrellus* species (EUROBATS, 2014). In general, bats observed flying at turbine rotor height are consistently categorized as "high-risk" species. In Europe, the species most at risk belong to the genera *Nyctalus*, *Pipistrellus*, *Vespertilio,* and *Eptesicus* (Brinkmann et al., 2006; Ahlén et al., 2007; Behr et al., 2007; Grünwald and Schäfer, 2007; Seiche, 2008; Bach and Niermann, 2010). Species classified as "low-risk," such as *Myotis*, *Plecotus*, and *Barbastella* species, tend to fly below the rotors, so generally avoiding danger (Behr et al., 2007; Grünwald and Schäfer, 2007; Seiche, 2008; Collins and Jones, 2009). The bat species most killed at wind farms are generally

common over parts of their European range, differing regionally and across habitats, and mortality occurs regardless of whether these species are resident or migrants (Rydell et al., 2010).

A four-year study (2003–2006, Dulac, 2008) at the seaside of Bouin, France, revealed most common mortality due to wind turbines comprised *P. pipistrellus*, *P. nathusii*, and a few *N. noctula*. The former among these species is thought to reside near the turbines, whereas the other two migrate significant distances (Dulac, 2008). In another 11-year period (2009–2019) study in the province of Cádiz, Spain, Salguero et al. (2023), analyzed bat fatalities at wind farms and they reported a total of 2,858 bat fatalities across 10 genera, with the majority (over 90%) belonging to the genera *Pipistrellus*, *Eptesicus*, and *Nyctalus*.

Despite the absence of published long-term studies on wind farms in Türkiye, available data from the Turkish Wind Energy Association (2021) indicates that the installed capacity of land-based wind energy in the country increased by more than 20 times between 2008 and 2020. Common Noctule (*Nyctalus noctule*), Lesser Noctule (*Nyctalus leisleri*), Nathusius' Pipistrelle (*Pipistrellus nathusii*), are the migratory tree-roosting bats in Türkiye that constitute most of the bat carcasses from wind turbine collisions, in addition to the common Pipistrelle (*Pipistrellus pipistrellus*); consequently, these are considered to be the most vulnerable to wind turbine-related deaths in Türkiye. Furthermore, collisions with wind turbines are known to cause the mortality of vulnerable species, including Schreiber's Bent-winged Bat (*Miniopterus schreibersii*), and Giant Noctule (*Nyctalus lasiopterus*) (Boyla K.A, 2024 Database (access restricted), KAB Ecology Consultancy.

The most accurate estimations for population-level consequences of wind energy belong to the hoary bats (*Lasiurus cinereus*) which in the early 2000s, constituted 38% of recorded bat fatalities at wind farms in the United States and Canada (Arnett & Baerwald, 2013). Frick et al. (2017) used models to estimate the hoary bat population size and growth rate in North America. They proposed that, if minimization strategies are not put in place, hoary bats could decline by 90% in the next 50 years from wind energy impacts alone. KAB Ecology, by using GenEst statistical modelling, estimated the number of bat fatalities for the year 2024 as 2402 bats per year in one wind farm in Türkiye. These estimates should be approached with caution, however. Piorkowski et al. (2012) recognized that it was impossible to obtain reliable estimates of fatality from the currently available data, and they identified the development of a standardized experimental design and generalized fatality estimator as a main challenge. Whether or not these estimates are entirely accurate, they show that a significant number of bat deaths are almost certainly occurring. This level of impact presumably

puts bat populations at risk because bats typically only have 1 or 2 pups per year and need high adult survival rates to prevent population declines (Barclay & Harder, 2003).

According to thermal video observations in wind farms, some bats may be actively approaching wind turbines and passing in and around the blades area (Horn et al., 2008; Goldenberg et al., 2021). In another study done by Richardson et al. (2021), they showed by using acoustic monitoring that *Pipistrellus* species is more active near the turbines compared to control sites with similar habitat. It is unclear, nevertheless, whether bat mortality and turbine height or size, are related; some research indicates a positive relationship (Barclay et al., 2007; Baerwald & Barclay 2009), while other research indicates a weak or nonexistent relationship (Thompson et al., 2017; Fiedler et al., 2007). According to a recent analysis (Huso et al., 2021), bat wind turbine-related mortality is better predicted by the relative quantity of energy produced rather than by turbine size measures.

While the aspect of bats' ecology that is bringing them into contact with wind turbines has not yet been conclusively established, we do know that they rely on echolocation for foraging and navigation (Altringham, 2011). Since all facets of their ecology depend on echolocation, and this system undoubtedly influences their interactions with wind turbines, by automatically recording echolocation calls in response to a trigger and storing the data for further analyses (identifying species and quantifying their activity), ecologists frequently use ultrasonic detectors to estimate the mortality risk of bats at the operating wind turbines (Korner-Nievergelt et al., 2013). Environmental factors, such as the season, time of day, ambient temperature, and wind speed, at which bats are most active, are also determined. Moreover, while bats are experiencing a relatively recent source of mortality linked to the development of wind energy, they are also dealing with other ongoing and new stressors, such as climate change (Frick et al., 2020), a global decline in the insects that serve as their primary food source (Hallmann et al., 2017), and continued habitat loss and degradation (Frick et al., 2020). It is therefore crucial to prioritize new data collection to better understand population status and trends, given the anticipated expansion of wind energy development in the near future.

Since most bat species have no population data, it is challenging to evaluate the damage of both natural and artificial stressors (Jones et al., 2009). Hence, our understanding of the viability of bat populations may be enhanced by the long-term, systematic collection of acoustic and genetic data (Hale et al., 2021), which eventually can help when it comes to taking mitigation decisions in order to protect populations. Fatalities due to wind farms have been documented for 27 bat species in Europe (EUROBATS, 2014). The only mitigation strategy that has significantly reduced bat fatalities at wind farms is raising the wind speed cut-off at which turbines turn on (Baerwald et al., 2009; Arnett

et al., 2010). At locations with solid and reliable winds, the estimated cost of increasing cut-in speeds to wind operators is negligible (1% reduction of total annual power output) (Huso et al., 2009). However, the percentage loss is higher and not commercially viable at more marginal wind farms, which are common in Europe (Richardson, 2016). As a result, more focused curtailment techniques have been researched, using predetermined bat activity thresholds to regulate the activation of the turbine (Behr, Niermann & Korner-Nievergelt, 2011; Lagrange, 2013). However, before determining the best mitigation measures, understanding the reason behind bat interactions with wind turbines is essential. Unfortunately, the underlying reasons for why bats approach wind turbines still remain unknown to us. To explain why bats are around wind turbines, two main hypotheses stand out. The first is that bat mortality is caused by coincidental occurrences that mainly reflect local bat activity, abundance, or behavior (Baerwald & Barclay 2009; Lehnert et al., 2014). The second hypothesis is that bats are attracted to wind turbines due to curiosity, misperception, or as possible locations for mating, roosting, eating, and flocking (Cryan & Barclay, 2009). The various attraction ideas that have been put up to date suggest that bats may be attracted to the motion of the blades, lights, sounds made by the moving blades and generators, or they intercept turbines as potential roost or mating sites (Cryan 2008; Cryan et al., 2014) or to feed on insect accumulations (Long, Flint & Lepper 2011; Cryan et al., 2014). Here in this study, a hypothesis of whether the environmental conditions (the habitat associated around the wind farms per se) or the turbines themselves are the reason behind bat mortality is tested. The hypotheses that are intended to be tested in this study are summarized in Table 4.1.

Table 4.1. Summary of the various attraction hypotheses

Hypotheses	Expectations
Turbine Effect Hypothesis	More activity around turbines compared to turbine-free areas but similar environmental characteristics and conditions
Attraction to Lights	More fatalities at turbines with aviation lights.
Attraction to Sound	More activity at moving blades than at nonmoving blades.
	Bats respond more to sound on low-wind nights.
Attraction to Blade Motion	More activity at moving blades than at nonmoving blades.
Attraction to Insect Aggregations	Insect abundance is greater around turbines.
Attraction to Turbines as Roosts	More fatalities on moonlight nights.
	More activity at the tallest, tree-like structures (different turbine types)
	Low activity among species that do not roost in trees.
	Equal activity at moving and nonmoving turbines.
Attraction to Turbines as Mating or Gathering Sites	Most activity at tallest tree-like structures in the landscape.
	Equal activity at moving and nonmoving turbines.

4.2. Materials and Methods

4.2.1. Site Description

The Wind Farm is located in the northwestern region of Türkiye, along the Black Sea coast. The facility covers an area extending several kilometers in the east–west and north–south directions and comprises 34 turbines distributed across the area, with elevations ranging from 50 to 120 meters above sea level (Figure 4.1). The surrounding landscape is characterized by coppiced oak forests (*Quercus spp*.), with trees reaching heights of 7 to 12 meters.

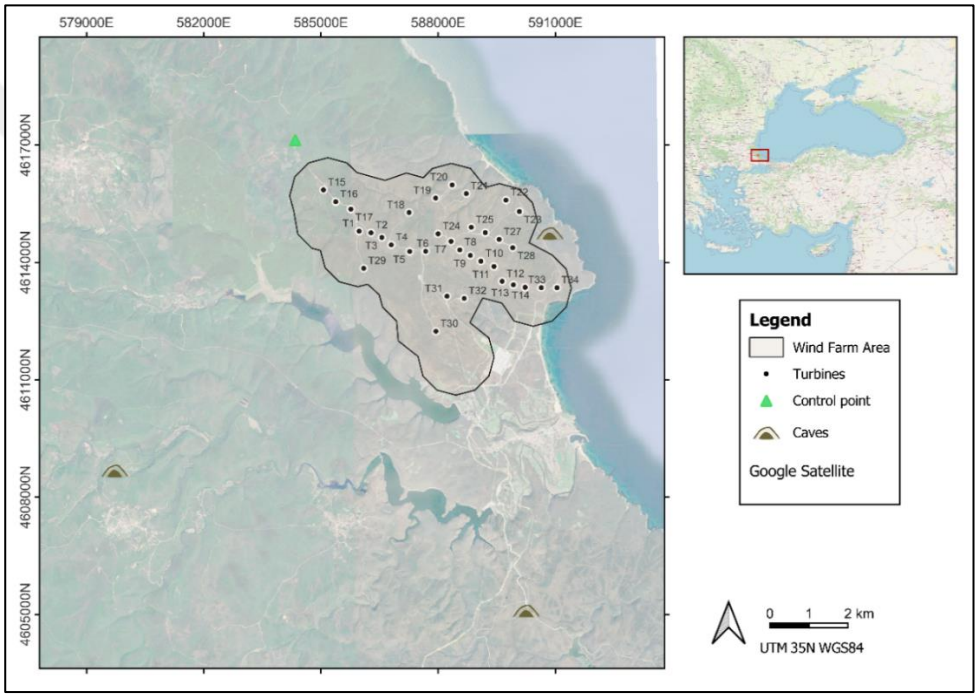


Figure 4.1. A map showing the location of the turbines in the Wind Farm.

4.2.2. Acoustic Surveys

The fieldwork was conducted from the last week of June and till mid-November 2024 to cover the summer and autumn seasons in which bats are most active; in total five visits were undertaken. During each visit, weather conditions were recorded one hour before sunset, coinciding with the initial setup of the recording devices on the first day. Measurements were taken again at the same time on the following day during the control check. In addition to weather conditions, features of the surrounding environment near and under the turbines, such as the presence of wood storage, or vegetation were also noted. Four full spectrum bat detectors (Batlogger M, Elekon) with omni-directional microphones (FG Black, Elekon) were set to record from one hour before sunset until one

hour after sunrise. The detectors were triggered by bat calls using the advance crest (CrestAdv) mode. Recordings were made at 312500 Hz sample rate and each of them logged time and temperature. The microphones were located 1.5 m above the ground. These recorders were placed at various locations near the turbines and programmed to record over two consecutive nights. The placements were as follows: condition 1) near a non-operating turbine (randomly selected from non-operating turbines due to weather conditions), condition 2) near an operating turbine classified as having historically high carcass counts based on KAB ecology reports (randomly selected from this turbine category), condition 3) near an operating turbine classified as having historically low carcass counts (randomly selected from this turbine category), and in a control area, which was selected to be near the turbines, with similar weather conditions, but far enough to avoid the turbine lights and noise, ensuring that the noise in the control area was inaudible to the human ear. The planned study design included recordings near turbines that were non-operational due to malfunction. However, during all five visits, were repaired on the same day, and the turbines were operational before the end of any working day, making this condition unattainable. As a result, this recording condition was replaced with a comparison between an operating turbine with historically high versus low bat carcass counts. The aim was to investigate whether the turbine's location could provide insights, as some turbines are known to have higher bat carcasses count near them. Bat recordings were analyzed using BatExplorer v2.1.4 and Kaleidoscope Pro (the pro version of the kaleidoscope program was provided for free by Wildlife acoustics grant program). We did not distinguish between bat call types (e.g. navigation, feeding, or social) for our analysis. Species identifications were done following the methodology described in Barataud (2015), including the parameters in Dietz and Kiefer (2014). All sounds other than bats (dogs, rain, wind, crickets, others) were considered as noise. In addition to the main study variables, turbine brand and the presence of wood storage under turbines were documented and explored as potential explanatory factors.

4.2.3. Bat Carcasses

Bat carcasses (details are shown in Appendix A, Table A.6) were collected from the daily visits of the bird watchers working at the wind farm. A total of 88 bat carcasses were observed under the turbines, and samples were collected from 72 carcasses, as the remaining 16 were in poor condition and unsuitable for sampling.

DNA was extracted with the Qiagen Blood and Tissue Extraction Kit. PCRs were performed, and the primers LCO1490 and HCO2198 were used to amplify a specific region of the COI gene (Folmer et al., 1994). The PCR reaction (25 µL) contained 0.2 µL DNTPs (25mM each), 2.5 µL

Thermo scientific 10X Taq Buffer with KCl, 0.2 Thermo scientific Taq DNA Polymerase (1 U/µL), 15.3 µL water, 4 µL DNA, 1 µL forward (10 µM) and 1 µL reverse primers (10 µM), and 0.5 µL MgCl2 (25 mM). The PCR cycle parameters consisted of one cycle at 95°C for 15 minutes, followed by 30 cycles of 30 seconds at 94°C, 90 seconds at 50°C, 90 seconds at 70°C, with a final extension 60°C for 30 minutes (Korstian et al., 2015). The positive PCR results were sent to Macrogen (Netherlands) for commercial sequencing, to identify the species of the bat carcasses. The results were later compared with the bat species identified by sound analysis to determine whether both methods lead to identical species identification. The outcomes should ideally line up, validating the species identified in the sound analysis. However, inconsistencies can occasionally arise because of DNA deterioration in the carcass, or mistakes in sound identification.

4.3. Results

The summary of the recordings identified as bats from each month is presented in Table 4.2.

Table 4.2.a. Monthly bat detections by condition.

Month	**Condition 1: Non-operating turbine**	**Condition 2: Operating turbine (high carcass)**	**Condition 3: Operating turbine (low carcass)**	**Control**
July	384	540	379	106
August	240	2,638	927	19
September	785	1,494	1,427	1,240
October	248	1,566	261	56
November	118	1,830	66	85

Table 4.2.b Monthly noise counts by condition.

Month	**Condition 1: Non-operating turbine**	**Condition 2: Operating turbine (high carcass)**	**Condition 3: Operating turbine (low carcass)**	**Control**
July	1,713	3,491	3,219	1,402
August	7,166	127	4,142	357
September	2,279	2,028	2,302	2,214
October	2,031	2,075	2,002	122
November	510	719	63	2,959

There is a significant presence of bats in the project area. The Highest bat activity overall was in September (across most conditions), and the lowest bat activity generally occurred in November as shown in Table 4.2.a. Noise levels were most variable in August, ranging from 357 to 7,166 recordings as shown in Table 4.2.b. Condition 2 (Operating turbine (high carcass)) showed consistently higher bat activity (Figure 4.2). The Control group generally showed lower bat activity than other conditions, and noise levels did not show a consistent pattern across conditions.

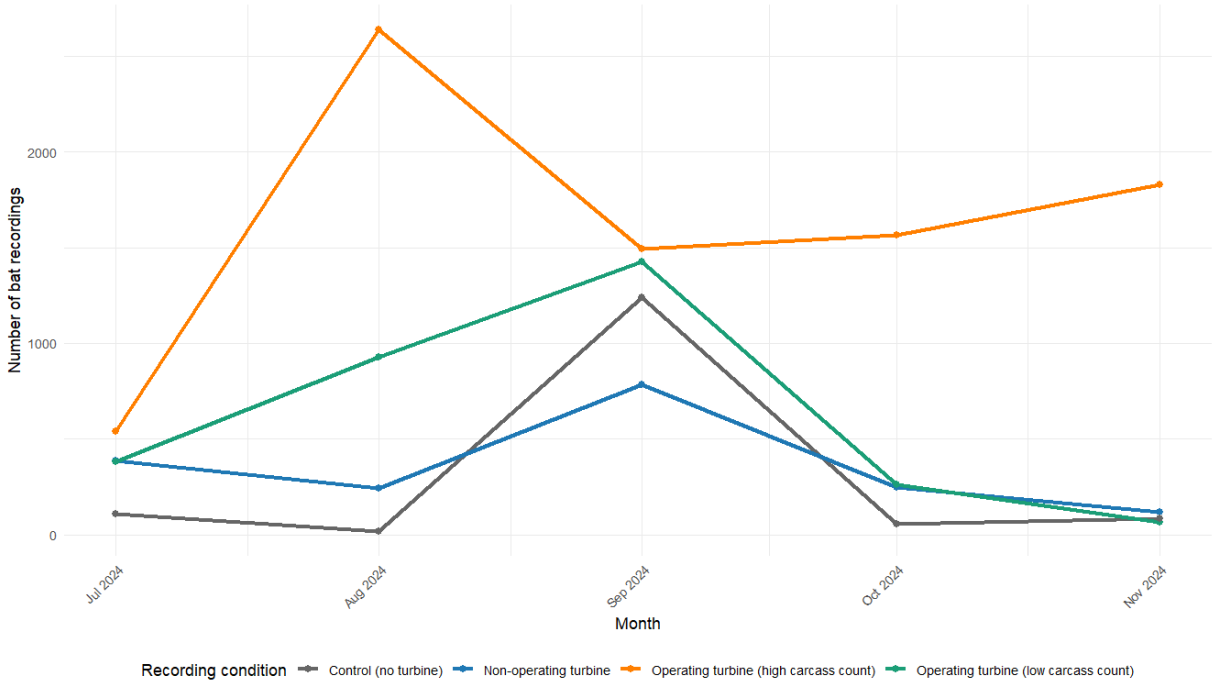


Figure 4.2. A graph showing bat passes per Month by Condition.

We looked at the correlation between bat counts and non-bat acoustic events (noise counts) to see if ambient acoustic activity could be a sign of insect prey availability. Across all recording conditions, no significant correlation was found between noise counts and bat counts ($r = -0.122$, $p = 0.607$; Figure 4.3). When examined by turbine condition, no consistent pattern emerged, suggesting that general ambient noise levels were not predictive of bat activity in this study.

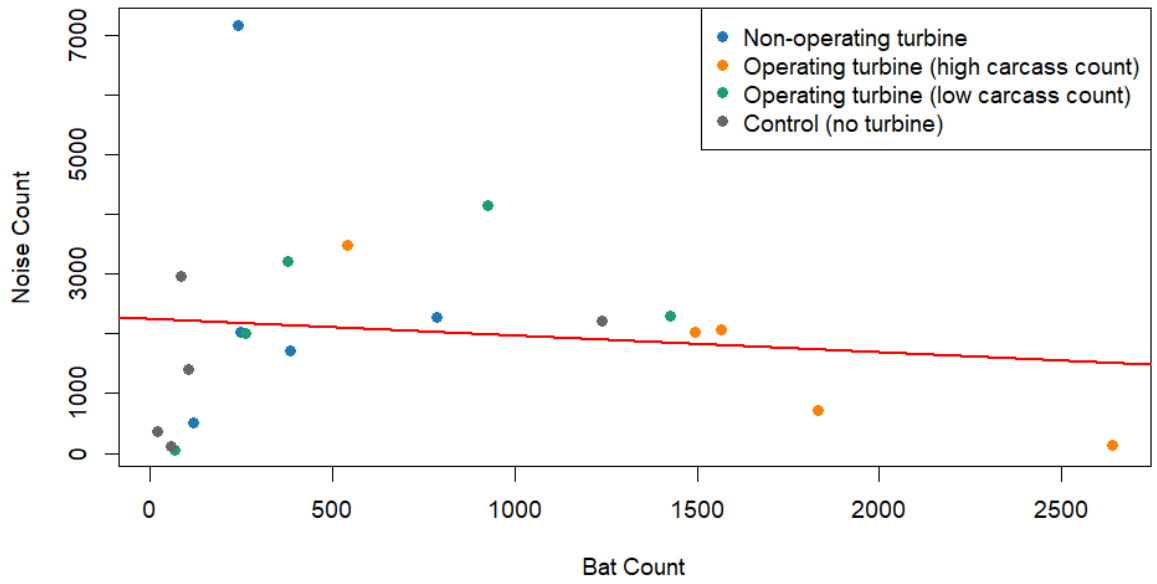


Figure 4.3. Pearson correlation and significance between bat count and noise count across all recording conditions.

A minimum of 15 species has been recorded as shown in Figure 4.4. *Pipistrellus nathusii* was the most frequently recorded species, representing around 50% of the passes. *Pipistrellus pipistrellus*, *Nyctalus noctule and Nyctalus leisleri* are the other commonly observed species (Table 3), all these abundant species are considered to have high collision risk. Overall, the species composition was similar among the conditions. Species within the genus *Myotis* are difficult to identify with certainty from acoustic data alone, which is why they are represented as *Myotis* sp. in Table 4.3. However, the species we suspected to be present, but we were not confident in terms of their identification were: *Myotis emarginatus*, *Myotis myotis*, *Myotis nattereri*, *Myotis daubentoniid*, *Myotis mystacinus*, *Myotis brandtii*, *Myotis capaccinii*. For graphical clarity, species with low overall activity were aggregated into an "Others" category in Figure 4.4. Complete species-level data are presented in Table 4.3 below.

Table 4.3. Recorded bat species, their IUCN status and their number of passes for each condition in all the visits in this study.

Scientific name	**IUCN**	**Condition 1: Non-operating turbine**	**Condition 2: Operating turbine (high carcass)**	**Condition 3: Operating turbine (low carcass)**	**Control**	**Total**
Pipistrellus nathusii	LC	926	3845	1732	804	7307
Pipistrellus pipistrellus	LC	586	2990	934	565	5075
Pipistrellus pygmaeus	LC	5	37	11	2	55
Hypsugo savii	LC	10	46	14	6	76
Miniopterus schreibersii	VU	19	125	33	4	181
Nyctalus noctula	LC	14	86	24	7	131
Nyctalus leisleri	LC	17	233	70	3	323
Eptesicus serotinus	LC	23	58	8	11	100
Nyctalus lasiopterus	VU	2	16	9	13	40
Rhinolophus blasii	VU	8	16	15	2	41
Rhinolophus ferrumequinum	LC	7	30	11	15	63
Rhinolophus hipposideros	LC	3	37	6	1	47
Rhinolophus euryale	VU	1	17	5	6	29
Myotis sp.		127	488	167	58	840
Plecotus auritus	LC	7	19	6	5	37
Barbastella barbastellus	NT	2	6	2	1	11
Tadarida teniotis	LC	18	19	13	3	53

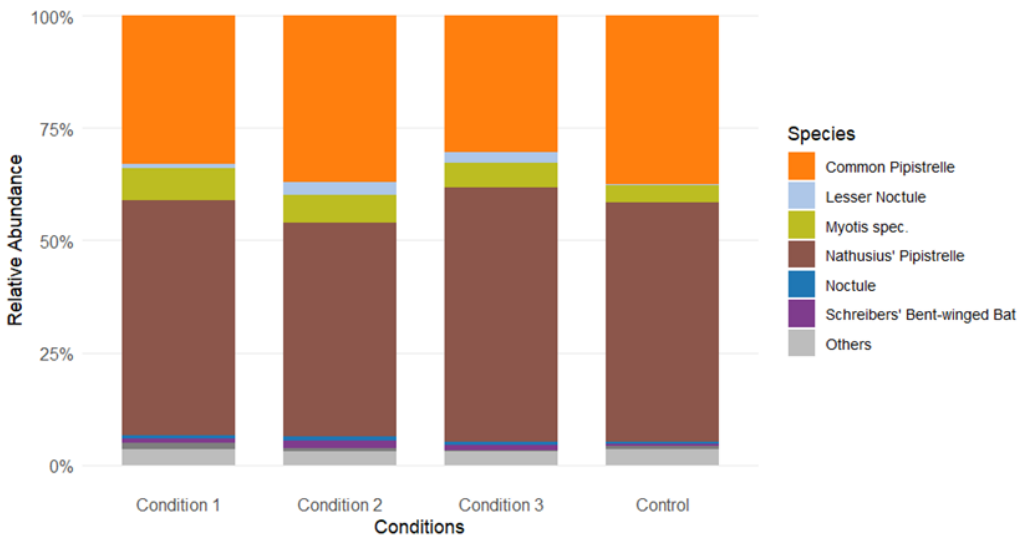


Figure 4.4. Bat species composition recorded during survey nights under different conditions. Species with fewer than 100 totall calls were grouped as ‘Others’.

4.3.1. Carcass Collection Analyses

The carcass number variation from month to month can be seen in Figure 4.5. The number of observed carcasses under turbines (as seen in Figure 4.6) only corresponds to a fraction of the bats that collide with the turbine blades. Major reasons are: (1) many of the carcasses are eaten/removed by scavenger animals, such as dogs, foxes and insects (Figure 4.7); (2) the surveys usually cover only a fraction of the surface where bats may fall; and (3) inevitably, some carcasses may go unnoticed by the surveyor.

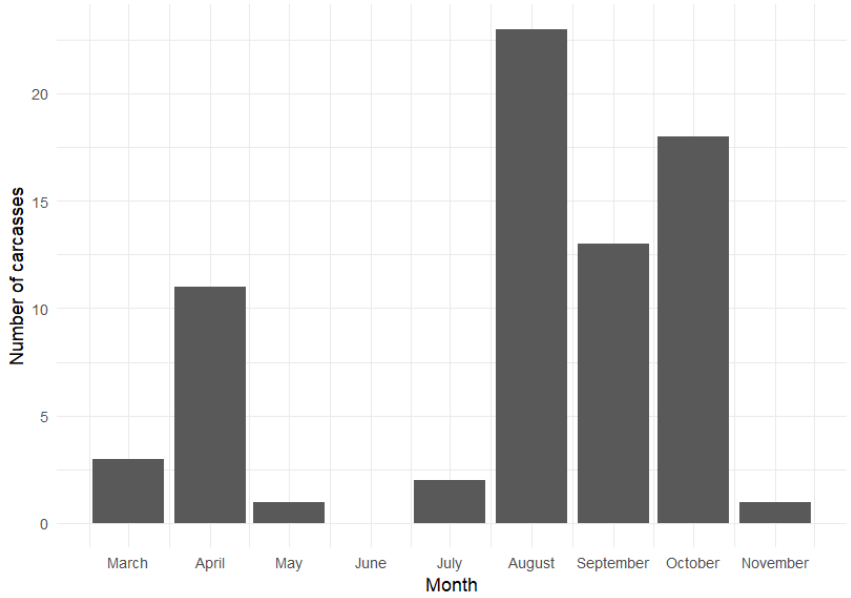


Figure 4.5. Total number of carcasses per month.



Figure 4.6. Map showing the number of carcasses found under each turbine.



Figure 4.7. Photographs taken by Emre Çetin (Bird surveyor in the wind farm) of dead bats getting attacked by insects.

The species identification from bat carcasses collected during daily visits by the bird watchers at the wind farm are presented in Figure 4.8 below.

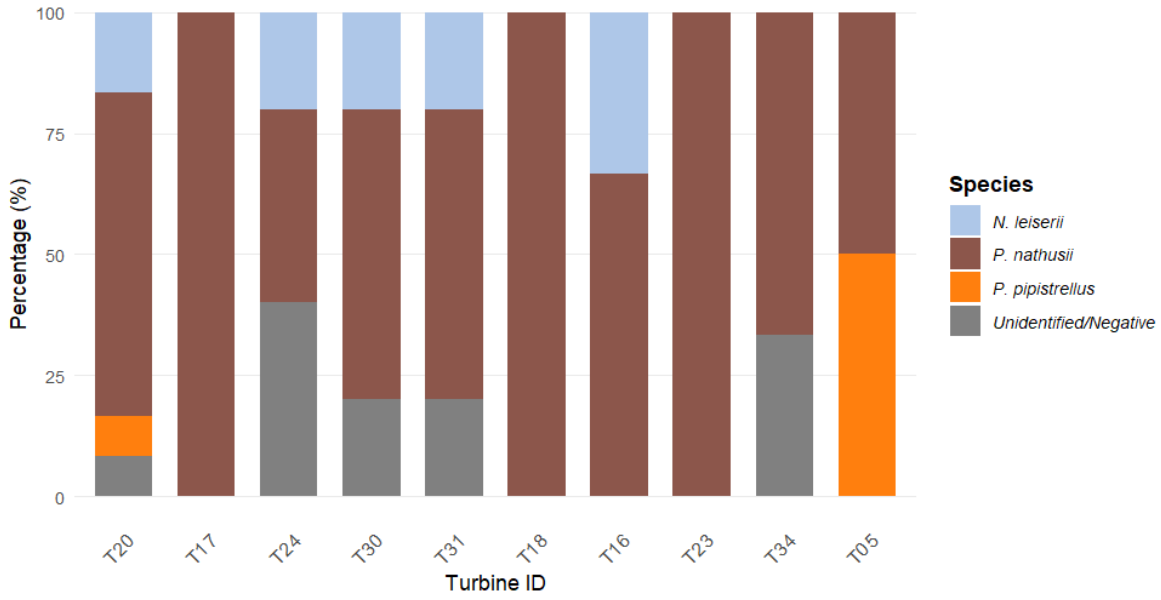


Figure 4.8. Bat carcass species composition by turbine.

More bat carcasses were detected under the turbines, around where the bat activity was much higher, with about 963 more recorded bat sounds on average during peak activity periods as shown in Figure 4.9.

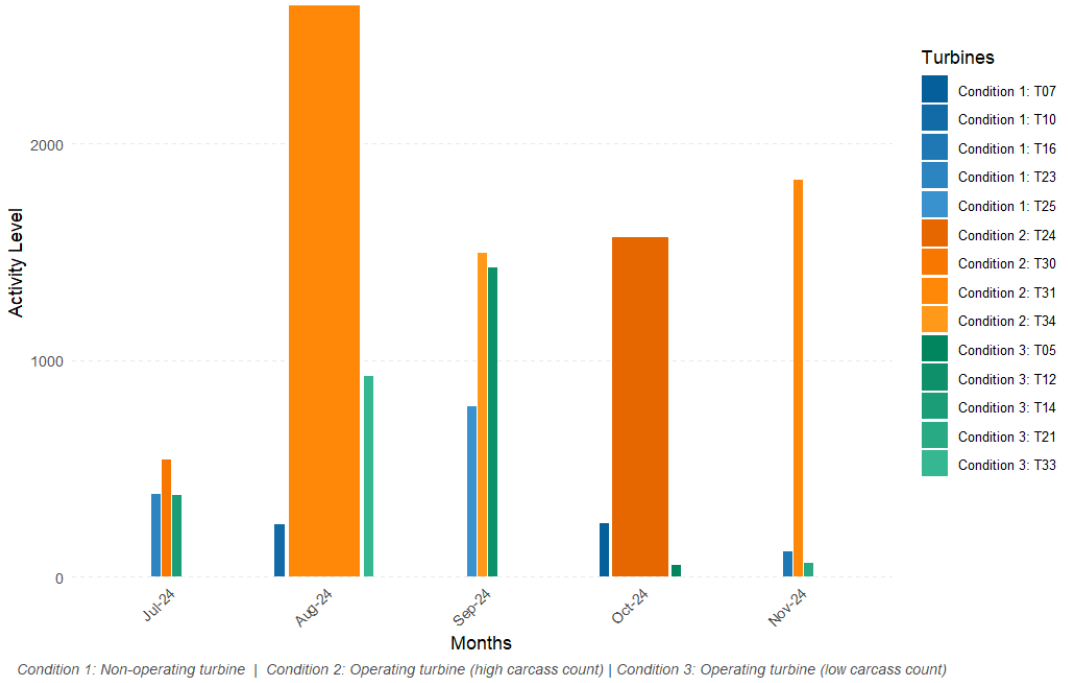


Figure 4.9. Monthly bat activity and carcass observations at turbines (July–November 2024). Bar height represents bat sounds recorded, and bar width represents carcass counts.

The graph in Figure 4.10 reveals distinct seasonal patterns and condition-specific responses in bat activity and mortality across the study period from July to November 2024. A peak in bat counts

is observed in Condition 2 (Operating Turbine, High Carcass), shown in orange, during August (reaching approximately 2,638 bat count), while simultaneously showing relatively high carcass counts throughout the study period. In contrast, Condition 3 (Operating Turbine, Low Carcass) demonstrates a more gradual seasonal decline in bat activity from summer to late autumn, with peak activity occurring in September rather than August. The Control condition (No Turbine) shows low bat activity with a notable September peak, while Condition 1 (Non-operating Turbine) maintains relatively stable, low bat counts throughout the study period.

Notably, Conditions 1 (Non-operating Turbine) and 2 (Operating Turbine, High Carcass) show similar mortality patterns throughout most of the study period, suggesting that turbine operation alone does not fully explain carcass counts. This similarity is likely driven by seasonal migration effects, particularly during late summer and early autumn, when collision risk increases regardless of turbine activity. In addition, the non-operating classification was based on turbines not producing electricity, but turbine blades may still have been spinning due to wind even when not generating power, potentially causing mortality. Finally, the monthly resolution of carcass surveys may mask short-term differences in risk associated with turbine operation.

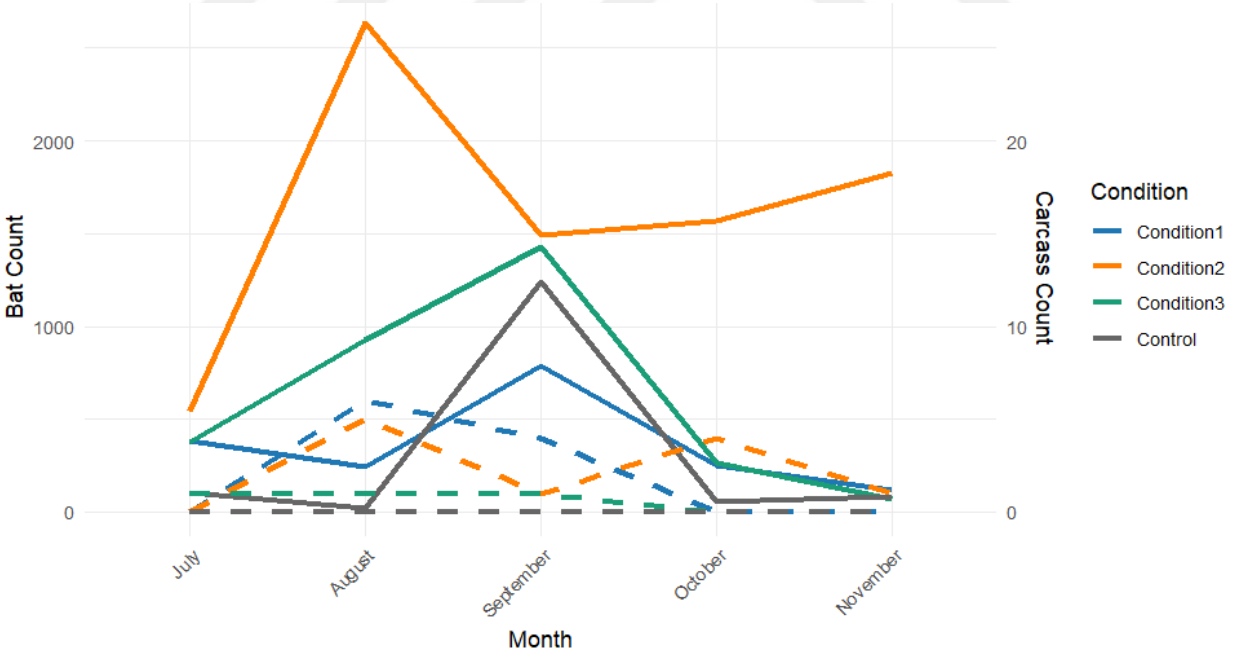


Figure 4.10. Monthly trends of bat count and carcass count. Solid lines: bat counts, dashed lines: carcass counts (scaled).

When visualizing the bat activity and carcasses count across the three turbine conditions, the graph in Figure 4.11 shows a generally positive association between bat activity and carcass numbers. When all data are considered together, this relationship is moderate ($r = 0.4755$). The turbines chosen

for condition 2 (Operating Turbine, High Carcass Number) exhibit the steepest positive slope, with higher bat activity corresponding to higher carcass numbers, indicating a stronger association under this condition. Condition 1 (non-operating) also shows a positive relationship, although with considerable uncertainty (data points are widely scattered around the regression line), suggesting that carcass occurrence is not entirely eliminated in the absence of turbine operation. Condition 3 (Operating turbine, Low Carcass) displays a shallower slope indicating a weaker association between bat activity and carcass numbers compared to turbines with historically high carcass counts.

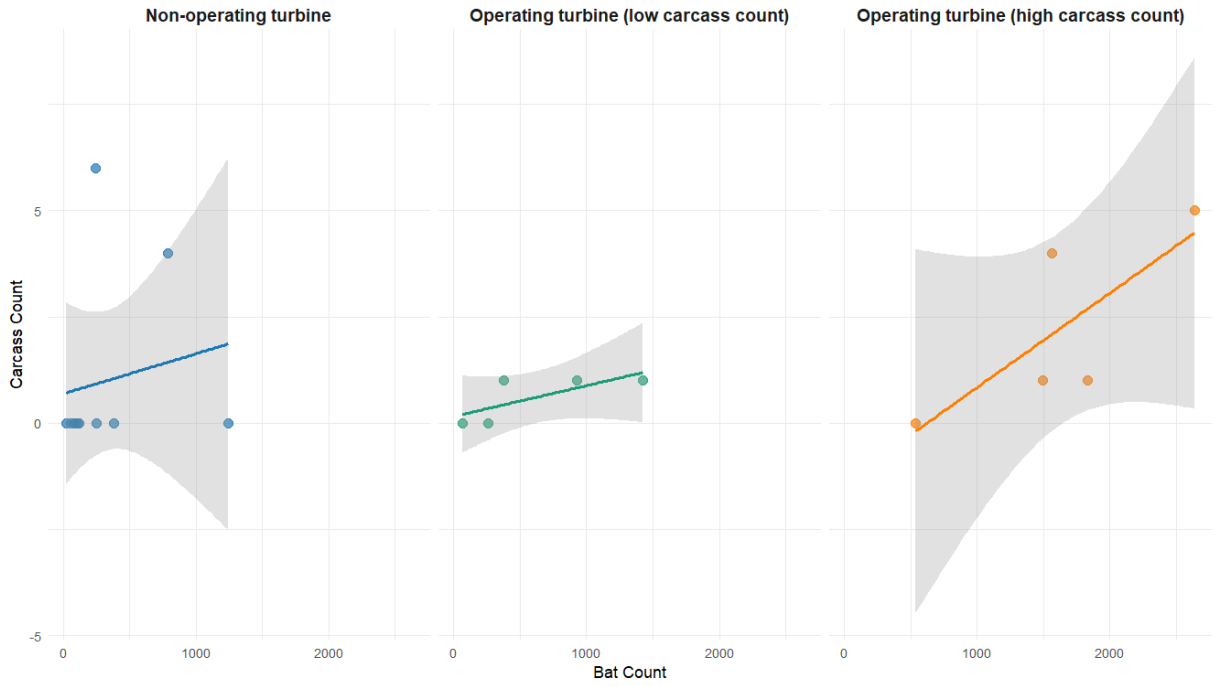


Figure 4.11. A graph showing bat activity vs carcass count by turbine condition. (Condition 1 in blue, Condition 2 in orange and Condition 3 in green).

The correlation analysis (table 4.4) reveals distinct patterns across the three experimental conditions, though statistical significance remains challenging due to the small sample size (only 5 turbines were tested by condition for 5 months). Condition 2 shows the strongest relationship between bat count and carcass count, with both Pearson ($r=0.771$, $p=0.1273$) and Spearman ($\rho=0.821$, $p=0.0886$) correlations indicating strong positive associations. Condition 3 shows a similarly strong relationship with an even higher Spearman correlation ($\rho=0.866$, $p=0.0577$) that approaches statistical significance, however, the violation of normality in carcass count data (Shapiro–Wilk $p=0.0065$) suggests the Spearman measure is more reliable than the Pearson correlation ($r=0.736$, $p=0.1565$). In contrast, Condition 1 exhibits much weaker correlations, with Pearson analysis ($r=0.353$, $p=0.5605$) showing a modest positive relationship while Spearman analysis ($\rho=0.112$, $p=0.8579$) indicates little

to no monotonic relationship; the normality violation in carcass count (p=0.0422) further limits confidence in the correlation estimates.

Table 4.4. Correlations by Condition.

Condition	Pearson correlation	p-value	Spearman correlation	p-value	Normality test (Shapiro-Wilk): Bat count p-value	Normality test (Shapiro-Wilk): carcass count p-value
Condition 1	0.353	0.560	0.112	0.858	0.219	0.042
Condition 2	0.771	0.127	0.821	0.089	0.815	0.272
Condition 3	0.736	0.156	0.866	0.0577	0.504	0.006

4.3.2. Field Survey Conditions

The conditions summarized in Table 4.5 were measured one hour before sunset when the recording devices were initially set up on the first day. They were measured again at the same time on the following day during the control check. Overnight, the conditions changed, and the presence of rain was evident in some recordings. During the summer surveys, the temperature changed between 25 °C and 28 °C. At the beginning of survey nights, the wind speed was between 1 m/s and 4 m/s and cloud coverage varied between 0 to 20%. During the autumn surveys, the temperature changed between 9 °C and 24 °C. At the beginning of survey nights, the wind speed was between 1.5 m/s and 4.7 m/s and cloud coverage varied between 10 to 100%.

Table 4.5. Monthly averages of weather conditions on recording nights.

Month	Temperature (°C)	Humidity (%)	Precipitation (mm)	Cloud Cover (%)	Wind speed (m/s)
July	27.0	65	0.0	0	1.50
August	25.5	60	0.0	15	3.50
September	23.0	85	0.5	90	3.35
October	15.5	75	0.3	40	3.10
November	9.5	75	0.0	85	4.25

Figure 4.12 below shows Pearson correlations between monthly weather variables and bat activity recorded under four sampling conditions. Bat activity showed generally positive correlations

at control sites with humidity (r=0.76), precipitation (r=0.817), and cloud cover (r=0.611), suggesting bat activity may increase during wetter conditions, though this relationship did not reach statistical significance. Wind speed displays mixed associations with bat activity, including a moderate negative correlation under non-operational conditions (r = −0.246) and a strong positive correlation under condition 2 (r = 0.770).

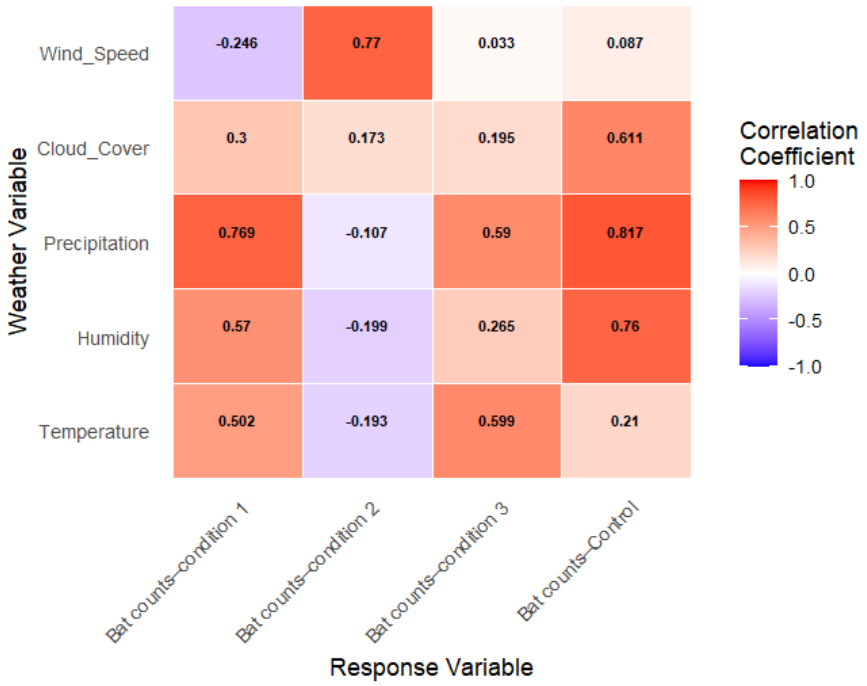


Figure 4.12. Pearson correlation coefficients (r) between monthly weather variables (rows) and bat activity (Bat counts) recorded during two sampling nights per month.

The weather conditions were not recorded during carcass search days, and the operational status of turbines at the time of carcass detection was not documented. To account for this limitation, weather data were obtained from Ventusky.com for the three nights preceding each carcass detection date.

For each carcass record, mean values of temperature, humidity, precipitation, cloud cover, and wind speed were calculated across the three preceding nights, as seen in Table 4.6 below. This temporal window was selected as a reasonable approximation of environmental conditions during potential collision or barotrauma events, given that carcass searches were conducted daily but the exact timing of bat mortality could not be determined. The uncertainty in mortality timing is influenced by both carcass persistence and observer detection efficiency during searches in the area under the turbines. Averaging weather conditions over the three nights prior to detection were chosen to reduce the risk of incorrectly assigning weather variables to the carcass event and to provide a more ecologically meaningful representation of conditions under which mortality likely occurred.

Table 4.6. Mean weather conditions averaged over the three days preceding bat carcass detection events.

Date	Temperature (°C)	Humidity (%)	Precipitation (mm)	Cloud Cover (%)	Wind speed (m/s)
3/28/2024	8.7	73.3	0.3	36.7	3.0
3/30/2024	11.0	73.3	0.3	36.7	2.3
4/1/2024	13.7	70.0	0.0	26.7	2.7
4/19/2024	17.7	60.0	0.1	60.0	2.7
4/21/2024	13.3	83.3	0.5	86.7	2.7
4/27/2024	13.3	90.0	0.0	63.3	1.3
4/29/2024	12.3	83.3	0.0	66.7	2.0
5/8/2024	11.7	90.0	0.3	40.0	2.7
7/20/2024	26.0	83.3	0.0	23.3	3.0
7/22/2024	25.3	83.3	0.0	13.3	2.7
8/10/2024	23.3	80.0	0.0	20.0	3.3
8/11/2024	23.0	80.0	0.0	20.0	2.3
8/22/2024	22.7	86.7	0.0	30.0	1.7
8/23/2024	23.0	86.7	0.0	33.3	2.0
8/25/2024	24.3	83.3	0.0	23.3	2.0
8/26/2024	24.3	80.0	0.0	13.3	2.3
8/28/2024	24.7	76.7	0.0	16.7	3.0
8/31/2024	22.0	76.7	0.0	16.7	2.7
9/4/2024	22.3	83.3	4.9	53.3	3.0
9/5/2024	22.7	80.0	1.0	23.3	2.3
9/9/2024	21.7	83.3	0.3	20.0	2.7
9/11/2024	22.0	83.3	0.4	46.7	3.3
9/13/2024	22.0	86.7	0.0	43.3	2.0
9/14/2024	22.0	90.0	0.0	43.3	2.3
9/17/2024	20.3	80.0	0.0	36.7	3.3
9/22/2024	20.0	73.3	0.4	86.7	4.0
10/4/2024	15.3	70.0	0.0	36.7	3.0
10/24/2024	12.0	83.3	0.0	50.0	4.0
11/2/2024	13.7	83.3	0.0	20.0	2.7

Date indicates the day on which the bat carcass was detected, associated weather variables represent mean values for the three preceding days.

Pearson correlation analyses revealed significant relationships between weather variables and daily bat carcass counts (Table 4.7). Wind speed showed a strong positive correlation with carcass counts ($r = 0.706$, $p < 0.001$). Temperature was significantly negatively correlated with carcass counts ($r = -0.540$, $p < 0.001$). Cloud cover had a weak but statistically significant positive correlation with carcass counts ($r = 0.269$, $p = 0.022$). In contrast, humidity and precipitation were not significantly correlated with carcass counts (humidity: $r = 0.206$, $p = 0.083$; precipitation: $r = -0.187$, $p = 0.116$).

Table 4.7. Pearson correlations between weather variables and bat carcass counts.

Weather_variables	Pearson_r	P_value	Significance
Temperature	-0.540	0.0000	***
Humidity	0.206	0.0826	
Precipitation	-0.187	0.1163	
Cloud_Cover	0.269	0.0222	*
Wind_Speed	0.706	0.0000	***

Environmental conditions under each turbine were classified based on the presence or absence of wood storage. Turbine brand was documented as a categorical variable (Nordex or Gamesa), which varies in dimensions (hub height and rotor diameter).



Figure 4.13. Photos showing wood storage by local workers in the area under a turbine.

The box plots in Figure 14 and Figure 15 visually demonstrate the patterns identified in the correlation analysis, showing differences in bat count distributions between turbine brands and wood storage conditions, though these differences are not statistically significant. The plot in Figure 15 reveals that Nordex turbines have higher bat counts than Gamesa turbines. The plot in Figure 14

illustrates a difference between wood storage conditions, where turbines with wood storage areas show higher bat counts compared to turbines without wood storage.

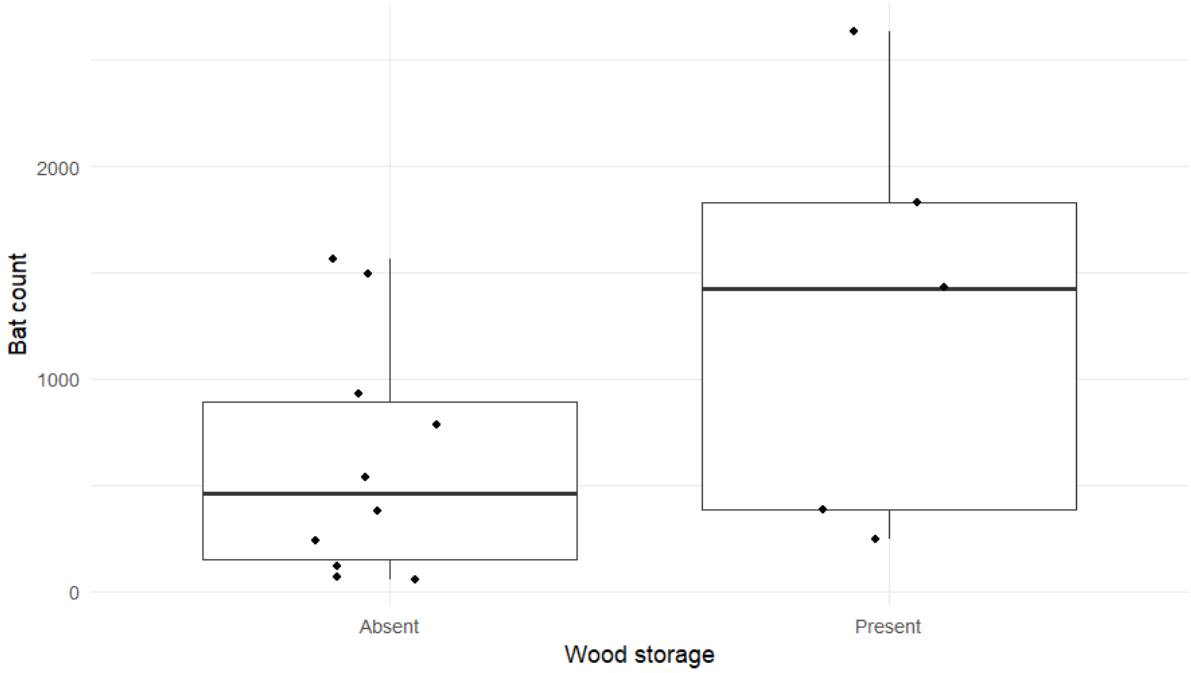


Figure 4.14. A box plot of bat count by wood storage presence.

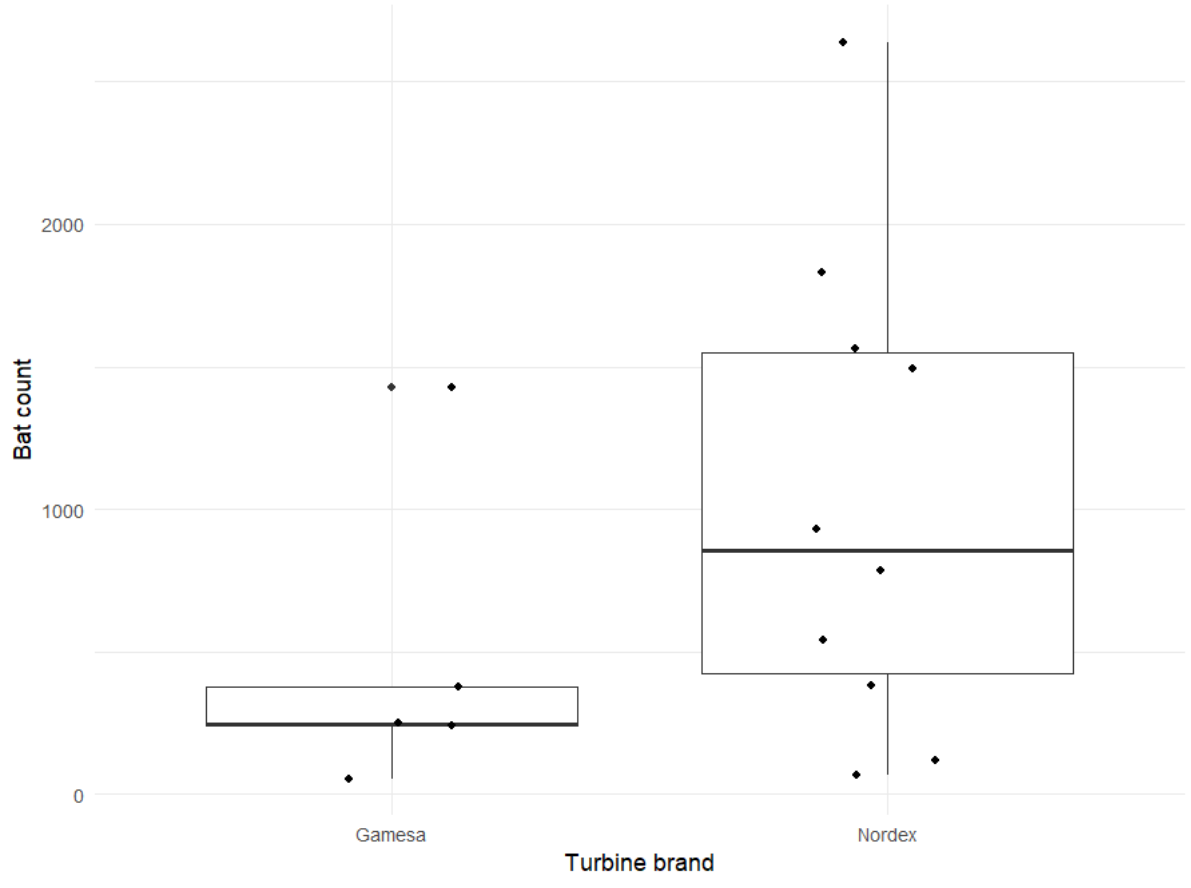


Figure 4.15. A box plot of bat count by Turbine brand.

Although descriptive statistics suggested higher bat activity at turbines with wood storage and at Nordex turbines, these differences were not statistically significant. Bat counts did not differ significantly between turbines with and without wood storage (Wilcoxon rank-sum test, $w = 13$, $p = 0.16$). Similarly, no statistically significant difference in bat counts was detected between turbine brands ($w = 12$, $p = 0.13$).

4.4. Discussion

Acoustic monitoring and carcass surveys were used to study bat activity and mortality patterns at a single wind farm in Türkiye. The relationships observed between turbine conditions, environmental factors, bat activity, and mortality patterns reveal important insights into the multifaceted nature of wind energy impacts on bat populations. However, because the study was conducted at one facility with limited replication (including a single control point), the findings are interpreted primarily as descriptive and hypothesis-generating rather than broadly generalized.

Acoustic monitoring revealed at least 15 bat species throughout the study area, with peak activity occurring in September under most turbine conditions. This temporal pattern was similar with the autumn migration and pre-hibernation behavior observed in several European bat species (Rydell et al. 2010). Most of the detected species were pipistrelle bats, specifically *Pipistrellus pipistrellus* and *P. nathusii*, as well as noctule species (*Nyctalus noctula* and *N. leisleri*), all of which are known for having high collision risk with wind turbines across Europe (Rodrigues et al., 2015). Bat activity was often higher near turbines than in the control area, except for the month of September. This showed that turbines, or more likely the ecological elements associated with turbine installation, may attract foraging or commuting bats. This can support the hypothesis that turbine infrastructure may create microclimates or vegetation margins that attract insect prey (Rydell et al., 2012). The increase in bat activity in the control site during the month of September after showing low activity in all other months remains unexplained, but it could reflect a variety of causes. This coincides with numerous species' peak fall migration, and it is possible that the control site intercepts a migratory corridor that is mainly used during this period. Alternatively, behavior caused by mating or pre-hibernation social activity may have temporarily concentrated bats in this location (Parsons et al., 2003). The brief duration of this study makes it difficult to determine if this is an annual pattern or a random incident. In addition, the use of only one control point may be limiting because it is unknown how representative that point is of the surrounding landscape; a rotating or replicated control design would better capture spatial heterogeneity and reduce the risk that “control” patterns reflect local site effects rather than a true baseline.

The DNA results revealed that *Pipistrellus nathusii* accounted for most of the identified carcasses. This species was also reported in acoustic surveys, although the acoustic sampling duration (two nights per month) prevents a thorough examination of temporal patterns in species composition. This limited temporal coverage also reduces the ability to match "mortality nights" (potentially driven by brief weather episodes) to acoustic activity measured on a small number of nights. The high carcass counts of *P. nathusii* is notable given that this species is known to migrate through Türkiye during autumn passage between Eastern European breeding grounds and overwintering sites (Petersons, 2004). The peak in overall bat activity and carcass detection occurred in September, coinciding with the expected migration period. However, the high carcass counts of *P. nathusii* could represent both the species' presence in the area and possible susceptibility during migratory transit, however discriminating between high activity and high vulnerability (greater collision risk per bat) would require finer-scale monitoring (more nights per month, turbine-operational logs, and species-specific activity at rotor height).

Considering bat activity and mortality, establishing a relationship between these two variables is not straightforward. Carcass count patterns do not directly mirror bat activity trends (Cryan et al., 2014), indicating that factors beyond simple abundance influence mortality rates. This suggests that mortality might be dependent on operational criteria, migration behavior of bats, and/or environmental conditions, creating higher risk scenarios even when overall bat activity remains moderate. These findings highlight the importance of understanding not just where bats are active but also studying their migratory routes and behaviors. While turbines with historically high carcass counts showed increased bat activity, this condition was not statistically significant. This was probably also influenced by the fact that bat behavior near turbines does not necessarily result in mortality. Bats may successfully forage near turbines without entering the rotor-swept zone, or they may avoid moving blades (Horn et al. 2008). Moreover, species-specific differences in flight behavior, echolocation skills, and responses to turbine structures are expected to influence collision risk regardless of overall activity levels (Cryan et al. 2014).

Weather variables showed no statistically significant correlations with bat activity, though trends indicated increased bat activity during humid and cloudy conditions. Humidity often correlates with insect abundance (Ciechanowski et al., 2007), while cloud cover may reduce ambient light levels preferred by some foraging bats (Saldaña-Vázquez & Munguía-Rosas, 2013). However, weather variables are naturally intercorrelated, and our limited sampling precluded significant statistical validation of these patterns. In addition, the weather data used in this chapter may not capture short, high-impact events (e.g., brief wind-gust episodes) that occur at night and could influence collision

risk disproportionately. On the other hand, analyses of weather conditions associated with carcass detection revealed more robust patterns. There was a significant positive correlation between wind speed and carcass counts ($r = 0.706$, $p < 0.001$), which is consistent with the hypothesis that higher wind speeds increase the risk of collisions through a number of mechanisms, including higher turbine blade velocities, more difficulty for bats to detect or avoid moving blades, and the possibility of barotrauma from sudden pressure changes near moving blades (Baerwald et al., 2008; Rollins et al., 2012). Nevertheless, this pattern should be interpreted cautiously because wind speed is also strongly seasonal and may vary with turbine operation status, and other weather features (e.g., gust) that were not interpreted here. Additionally, many mitigation strategies (curtailment) are designed around low-to-moderate wind speeds when bats are often most active; therefore, a positive wind–carcass correlation may reflect local context, confounding with seasonal migration, or measurement resolution rather than a general rule that "high winds cause higher bat mortality".

In addition, temperature was significantly negatively correlated with carcass counts ($r = -0.540$, $p < 0.001$), likely due to behavioral responses, as during cold nights, insects and bats may concentrate near ground level or sheltered areas where temperatures are warmer (Voigt et al., 2012), potentially increasing flight activity in the rotor-swept area where collision risk is higher. However, an alternative and likely explanation is seasonal confounding: within the study period, "cooler nights" may coincide with autumn migration peaks (especially September), producing an association even if temperature itself is not a direct driver of collision risk. Temperature may be acting as a proxy for season/migration rather than a mechanistic cause. Cloud cover showed a weak positive correlation with carcass counts ($r = 0.269$, $p = 0.022$), possibly reflecting associated overcast conditions such as precipitation, atmospheric pressure changes, and changes in wind patterns. These atmospheric variations may have an impact on bat flight behavior, orientation, or foraging efficiency, also increasing the risk of collisions (Cryan & Barclay, 2009).

The interpretation of turbine-condition effects also depends on how "non-operating" turbines functioned in practice. In some systems, turbines may be non-operational in terms of electricity production while blades still rotate freely in wind; if so, collision risk may remain non-zero. Although turbines classified as non-operating appeared stationary during field checks, rotation status could vary at night and between visits. Access to turbine operational logs (e.g., rotor speed, brake status, curtailment events) would strengthen future inference and help separate "presence of turbine structure" effects from "rotating-blade" effects.

While not statistically significant, two observations during field visits are worth mentioning. First, turbines under which farmers stored wood showed higher mean bat activity compared to turbines without wood storage, which suggests that storage areas could be creating attractive microhabitats for bats, potentially serving as roosting sites or concentrating insect prey populations.

While also not reaching statistical significance, Nordex turbines appeared to have higher bat activity compared to Gamesa turbines. This difference is likely reflected in design variations, with Nordex turbines (Vestas V136) featuring a 136-meter rotor diameter and 112-meter hub height compared to the smaller Gamesa turbines (Siemens G90) with a 97-meter rotor diameter and 78-meter hub height. The larger swept area and greater height of Nordex turbines may increase collision risk by extending the danger zone and intercepting more bat flight paths (Barclay et al., 2007), though this hypothesis requires validation with larger sample sizes. Moreover, the fact that the correlation with wood storage proves stronger than turbine brand effects might indicate that environmental modifications around turbines may have more impacts on bat mortality than technological differences between manufacturers. Future research using matched-pair designs or accounting for fine-scale habitat characteristics in statistical models would be required to determine if turbine dimensions independently influence bat activity or mortality.

In addition to providing baseline data describing species diversity, seasonal activity patterns, and weather variables at this wind farm, this study adds to the limited research on bat-wind farm interactions in Türkiye. Türkiye's location along migratory corridors connecting Eastern European breeding populations with Mediterranean and Middle Eastern wintering locations makes it a critical area for migratory bat conservation. The dominance of *P. nathusii*, a migratory bat species, in carcass counts at this particular wind farm near Türkiye's European border, a region likely serving as a key passage route during autumn migration highlights the need for targeted mitigation measures. Understanding and reducing effects on migratory bat populations should be given top priority when choosing sites, operational planning, and regulatory frameworks as wind energy development spreads throughout Türkiye.

5. CHAPTER 3: ECOLOGICAL NICHE MODELLING OF THE COMMON PIPISTRELLE

5.1. Introduction

Climate change and biodiversity loss are two of the world's most pressing issues (Shin et al., 2022). Tens of thousands of wildlife populations have declined by an average of 73% since 1970, according to the Living Planet Index (Hannah Ritchie, 2022). Over the past century, climate change has been the main factor in the extinction or loss of species (Jones et al., 2016). Bats are among the mammals most vulnerable to the effects of climate change (Sachanowicz, & Ciechanowski, 2006; Scheel, Vincent & Cameron, 1996). Due to their ability to fly, bats hold a unique position in the phylogeny of mammals (Adams, 2013). Their success and global biogeography are supported by some crucial adaptive features, including flight and echolocation (Jones & Teeling 2006). Given their increased sensitivity to disruptions at roosting places, broad-spectrum insecticides, resource depletion, deforestation, and harm to other terrestrial ecosystems, bats are frequently regarded as environmental indicators (Ransome et al., 1994; Yapa, 2017). Additionally, they are essential for ecological services like pollination, seed dispersal, forest regeneration, the control of arthropod populations in both natural and agricultural environments, and the redistribution of nutrients and energy (Hodgkison et al., 2003; Ghanem et al., 2012). Globally, bat numbers are in decline, which can be attributed to habitat degradation (such as deforestation, the growth of commercial farmlands, and urbanization), as well as artificial disturbances such as human visits to roosts, the use of pesticides (Jones et al., 2009), and wind energy.

Since the 1940s, many European bat populations have declined, with the main causes thought to be the loss or changes of semi-natural habitats and the use of pesticides linked to increased agriculture (Walsh and Harris, 1996a, b; Schober & Grimmberger, 1997). Therefore, changes in land use, driven by increased agriculture and urbanization, have eliminated valuable bat habitats while also accelerating the effects of climate change, which threaten both bats and their ecosystem services (Williams et al., 2008). According to the research conducted by Amorim et al. (2015) on *Tadarida teniotis*, the reproduction of this species in the Mediterranean region was significantly impacted by years of drought, resulting in a substantial decrease in the number of pregnant female bats. Moreover, in western North America, when temperatures were higher than average and precipitation was below average, the reproductive output of vespertilionid bat populations decreased (Adams, 2010). Although the precise effects may differ depending on the species and environmental circumstances, these

studies show that bat populations are impacted by the direct and or indirect effects of climate change. Therefore, a crucial component of managing bat conservation is studying and providing an accurate assessment of their habitat needs (Walsh & Harris, 1996a), and to ensure their survival and the continuity of the essential ecosystem services they provide (Boyles et al., 2011).

Information on species distribution, the suitability of their habitats, and their responses to climate change are necessary before setting conservation measures to prevent these impacts (Hirzel et al., 2008). Field surveys comprise the main approach with regards to assessing species distributions, however they may underestimate the accurate distribution of bats because of their nocturnal habits and the inadequate sampling of roosting locations (Kunz et al., 2011). It is also challenging to identify bats at the species level using only their general physical characteristics, which can lead to inaccurate global distribution estimates (Ramasindrazana et al., 2011). Although automated acoustic recorders, machine-learning based identification models, and theoretical advances in sound ecology (Pijanowski et al., 2011) offer potential alternatives to, or complementary tools to be used along with traditional field sampling, implementing such passive surveys across larger geographic areas can be difficult, especially due to costs and required effort. Therefore, it is urgent to create new techniques for mapping bat distribution, both currently and in the future.

Habitat suitability models (species distribution models, ecological niche models, or ENMs) are predictive geospatial models that rely on environmental variables of species occupancy and georeferenced data on species presences to offer reliable estimates on their distributions. This modelling strategy can map existing distribution and estimate future range shifts in response to environmental change (Hirzel et al., 2008; Pearson et al., 2003). Biologically significant indicators and spatial parameters that correspond with the likelihood of species presence are necessary for successful applications of ENMs (Hirzel et al., 2008). The ENMs predict species occurrence across geographies, forecast future distribution ranges in response to changing environments, and assist in prioritizing conservation targets by establishing an empirical relationship between observed species distribution and spatially explicit environmental variables (Hirzel et al., 2008; Pearson et al., 2003). (Fielding et al., 1997; Phillips et al., 2006). The ENMs have been widely used to answer problems about biogeography, conservation, evolution, project historical species distributions, and calculate the impact of climate change on the geographic ranges of various species (Soto-Centeno et al., 2015).

Based on the different roosting sites that bats choose depending on the season, seasonality and climate are essential factors in the habitat selection process (Russ et al., 2003; Vasko et al., 2020). Seasonality affects the life-history stages of bats, including mating, parturition, nursing, postnatal

care, and peak food availability (such as insect swarms) (Yapa, 2017; Pearson et al., 2003). Bats also acquire resources and conserve energy in a climate-mediated manner (Stawski et al., 2014). Consequently, bioclimatic variables are valid environmental proxies to simulate bats' primary ecological niche.

Even though there is a variety of knowledge on the usage of bat habitat in many regions (e.g., Furlonger et al., 1987; Walsh and Harris 1996a, b; Vaughan et al., 1997a, b), little to nothing is known about the preferred habitats of bats in the Mediterranean region. The common pipistrelle is known for its highly opportunistic selection of foraging locations (Vaughan et al., 1997a), in addition to being one of the most common bats in the Mediterranean region, a region that stands out among important biodiversity hotspots (Blondel et al., 2010). In this chapter, we developed ecological niche models (ENMs) for the *Pipistrellus pipistrellus* bat species under both current and future climate change scenarios. Our aim was to estimate its extent of occurrence, identify which habitats are likely to be lost or gained, and determine the key abiotic environmental factors that most influence its distribution. The impact of climate change on *P. pipistrellus* bats was evaluated, and suggestions that could reduce potential effects were developed to emphasize our primary goal of conservation of the common pipistrelle. The assumption was that, through changes in temperature, precipitation patterns, and the frequency of extreme climate events, climate change will make parts of the existing habitat less favorable for the common pipistrelle, and new habitats favorable.

5.2. Materials and Methods

5.2.1. Study Area and Presence Records

The study area covered several European countries including (Albania, Belgium, Bosnia and Herzegovina, Bulgaria, Corsica, Cyprus, Czech Republic, Denmark, France, Germany, Greece, Isle of Man, Liechtenstein, Luxembourg, Malta, Netherlands, Portugal, Romania, Serbia, Slovakia, Spain, Sweden, Switzerland, Italy, Ukraine, and the United Kingdom), extended into a part of Asia (Iran, Jordan, Lebanon, Syria, Tajikistan, Türkiye, Uzbekistan, Turkmenistan, Kazakhstan, Russia) and included a portion of Africa (Algeria, Morocco, Tunisia) corresponding to an overall surface area of ca. 22.7 million km².

We obtained 151,135 occurrence records (Figure 5.1) from several sources: 1) Prague's National Museum (Národní Muzeum), 2) colleagues' unpublished databases; and 3) the public access database Global Biodiversity Information Facility (GBIF; http://www.gbif. org; GBIF, 2019 a,b,c). For the

third source, we examined the public data critically and used only records from direct observation for which positional values had at least two decimal digits (0.01 decimal degrees, corresponding to ca. 1 km at the equator). In addition, we filtered the data further to remove records with missing or inaccurate coordinates (with coordinate uncertainty ≥ 1 km). We collected from GBIF only the presence records that were included in the period from 1960 to the day we accessed the data (16/03/2023). To homogenize the data with those derived from authors' unpublished personal databases, we removed duplicate records. After this selection, 49,891 records were used to carry out the analysis.

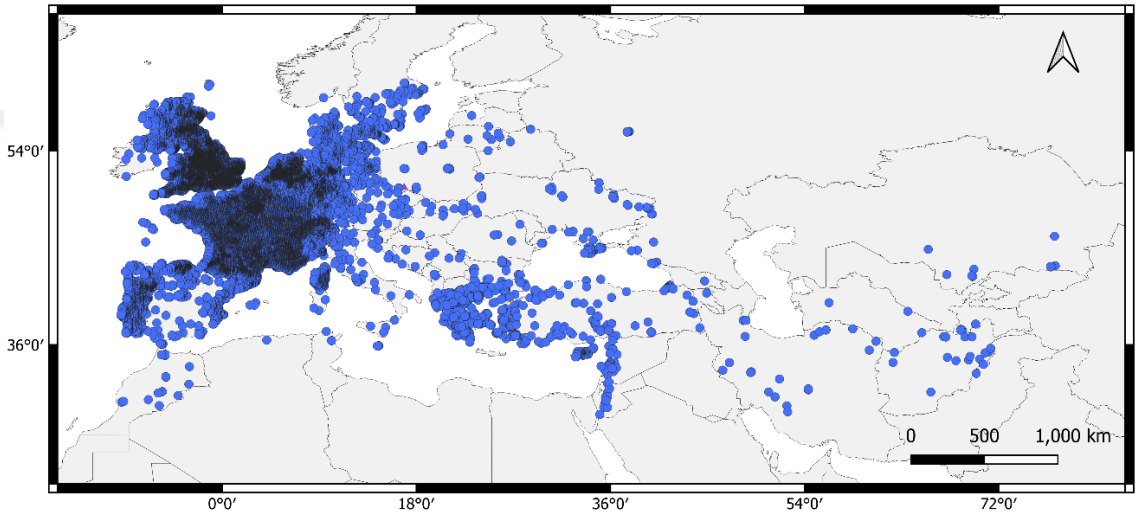


Figure 5.1. Map of all the *Pipistrellus pipistrellus* records (blue circles) obtained for this study, shown in the WGS 84 geographic coordinate reference system (EPSG:4326).

5.2.2. Preparation of the Occurrence Data

We defined a reference raster with a resolution of 2.5 arc minutes. We chose this resolution because it coincides with the resolution of many environmental layers, which we later used in the modeling process. This resolution is also not too high, so it allows reasonable computing time. To set the spatial extent (Figure 5.2), we excluded the polar regions and limited the area to match the range of the occurrence records, using the presence points extent: N: 60.29167, E: 77.16667, W: -9.416667, S: 30.20833.

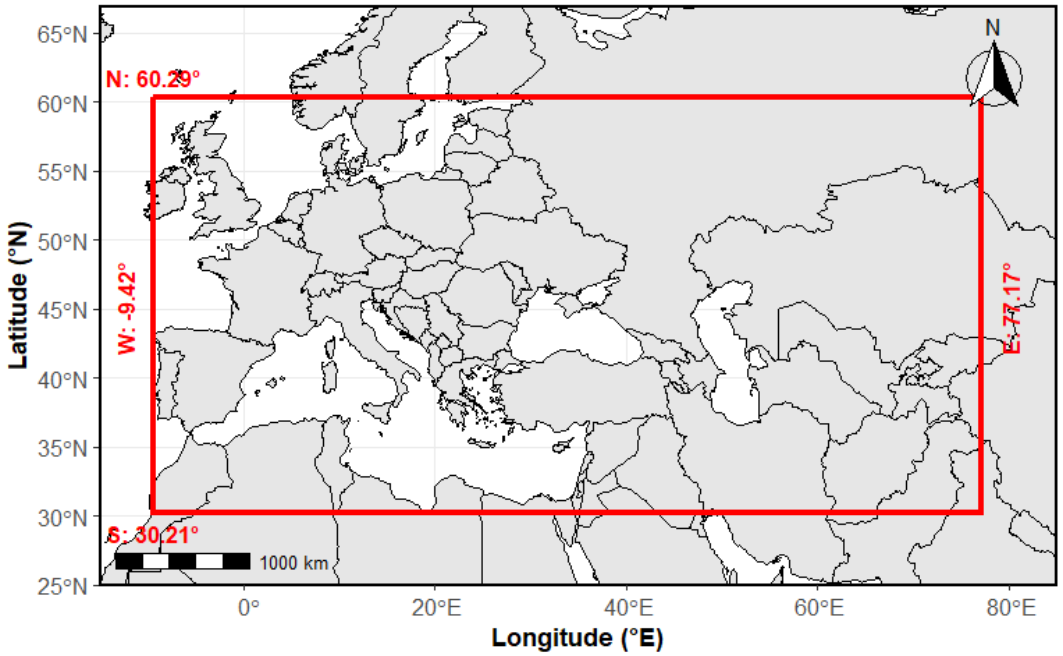


Figure 5.2: Spatial Distribution Map Covering Europe to Western Asia.

5.2.3. Preparation of the Environmental Layers for the Current Prediction Model

We considered several environmental variables as potential predictors of the geographical distribution of *Pipistrellus pipistrellus*. These variables cover factors revealed by our literature research representing six categories: climate, land cover and vegetation, topography, and light index. The 19 climatic variables , with a resolution of 2.5 arc minutes, including average monthly minimum, mean, and maximum temperature, and precipitation for 1970-2000, were obtained in GeoTIFF format from the WorldClim dataset (Hijmans et al., 2005; https://www.worldclim.org/data/worldclim21.html). Additionally, we considered wind speed variables with a resolution of 2.5 arc minutes for 1970-2000, which were also obtained in GeoTIFF format from the WorldClim dataset (Hijmans et al., 2005; https://www.worldclim.org/data/worldclim21.html). For topographic variables Digital Elevation Models (DEMs) were downloaded in GeoTIFF format from WorldClim (Hijmans et al., 2005; https://www.worldclim.org/data/worldclim21.html). These DEMs have a spatial resolution of 2.5 arc minutes and are derived from NASA's Shuttle Radar Topography Mission version 4 (SRTM v.4). Slope variable was downloaded in GeoTIFF format from EarthEnv (https://www.earthenv.org/topography) based on 2.5 arc minutes resolution from the Global Multi-resolution Terrain Elevation data 2010 (GMTED 2010). Nighttime artificial lighting was quantified using the VIIRS (Visible Infrared Imaging Radiometer Suite) Annual Nighttime Lights dataset version 2. The average masked radiance composite for 2024 was downloaded in GeoTIFF format from the Earth Observation Group (EOG) at NOAA's National Centers for Environmental

Information. This data set provides global coverage at approximately 15 arc-second spatial resolution (~500m) and represents cloud-free average radiance values with background noise and transient lights (fires, aurora) filtered out. Additionally, we considered Land Cover maps at a 300m (0.1617 arc minutes) spatial resolution for each year between 1992 and 2015. These maps were downloaded in GeoTIFF format from ESA Land Cover Climate Change Initiative (CCI) website, Centre for Environmental Data Analysis (https://catalogue.ceda.ac.uk/uuid/b382ebe6679d44b8b0e68ea4ef4b701c).
All variables were resampled to 2.5 arc-minute resolution using mean aggregation to match the spatial resolution of other environmental variables.

5.2.4. Operations on the Presence Records

A major assumption behind species distribution models (SDMs) is that presence records are generated by a systematic and random sampling methodology that appropriately covers the entire environmental and geographic extent of the research region. In reality, spatial sampling bias is common, particularly for widespread species that are under-reported due to uneven survey effort (Kramer-Schadt et al., 2013), where differences in funding and data-sharing practices between countries result in significant spatial gaps and record clustering (Beck et al., 2014). In this study, we had multiple occurrences closely related in space, in well-surveyed parts of Europe, leading to multiple occurrence data per cell of the reference raster which can give too much weight to the values of environmental variables in these cells. This leads to the model's possible capture of sampling effort patterns instead of true ecological preferences, resulting in underestimation of suitable habitats in under-sampled regions and an over-prediction in environmentally very similar regions. The data covered several adjacent cells of the reference raster, thus biasing the robustness of environmental data in favor of the high occurrence regions.

We had an approach to mitigate this issue; we applied a multi-step filtering and thinning approach. First, we used the CoordinateCleaner (Zizka et al., 2019) library in R, to flag and remove the records that have potential geolocation issues, ensuring that retained records represented biologically meaningful locations. Second, we implemented a combined geographic and environmental thinning (Figure 5.3) to reduce clustering bias in species occurrence data. This thinning was applied selectively to European countries (Group 2, shown in red), where sampling density was highest, while all occurrence records from Asia, Middle East, and North Africa (Group 1, shown in blue) were preserved to avoid further loss of information from under-sampled regions.

Geographic thinning was first performed by enforcing a minimum distance of 50 km between occurrence points, reducing spatial autocorrelation at the resolution of the environmental predictors. Environmental thinning was then applied by extracting environmental values at each occurrence point, standardizing all predictors, and calculating environmental distances across nine variables. Occurrence points with environmental distances < 0.5 standard deviations were considered environmentally redundant, and only one representative point was retained. This procedure was repeated over 10 iterations, and the iteration retaining the highest number of points while satisfying both geographic and environmental constraints was selected for subsequent modelling.

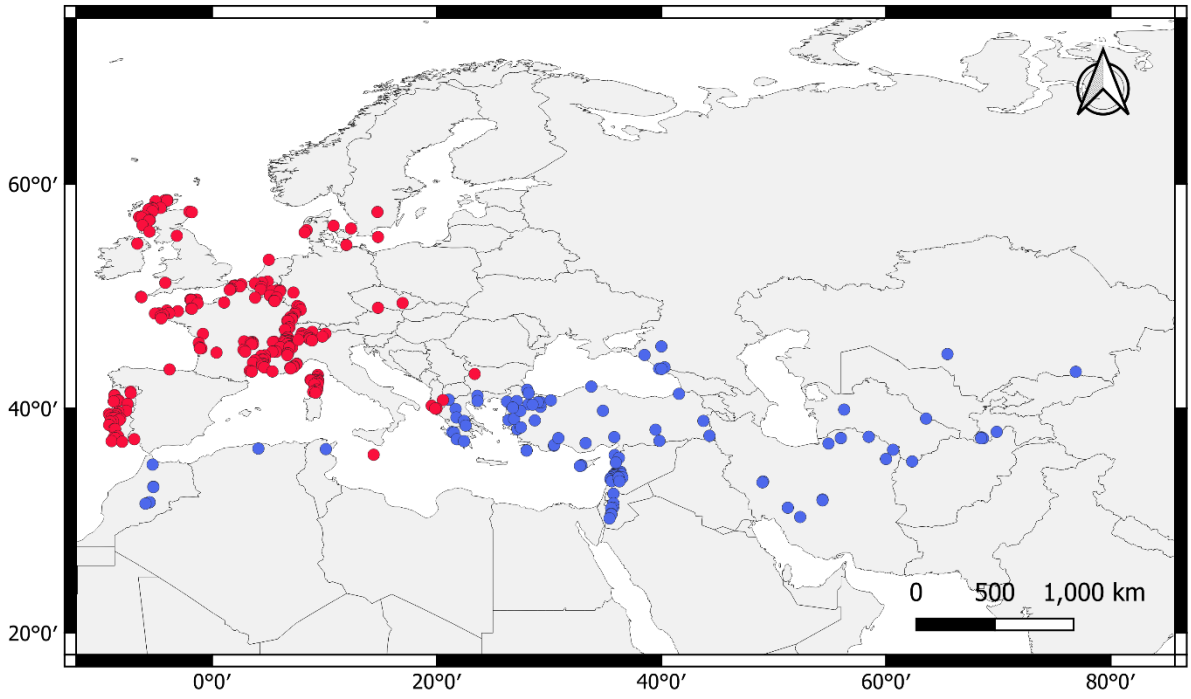


Figure 5.3. Map showing the thinning results of the presence records from Europe. red indicates thinned records from Europe (Group 2), and blue shows untouched records from Asia, the Middle East, and North Africa (Group 1).

5.2.5. Operations on the Environmental Variables

We refined our analyses by excluding variables that were not directly relevant to the study objectives or that contributed limited explanatory power. Rather than focusing solely on variables with the highest correlations, we prioritized those with theoretical or contextual relevance, even if their statistical associations appeared weaker. This strategy aimed to improve model interpretability while retaining biologically meaningful predictors.

To derive ecologically relevant predictors for *Pipistrellus pipistrellus*, we processed the ESA Climate Change Initiative (CCI) land cover dataset. Original land cover classes were reclassified into broader habitat categories that reflect the species' known ecological requirements, such as roosting opportunities in urban areas, foraging along forest edges, and prey availability near water bodies. This reclassification was applied consistently across all available years of the dataset to account for temporal variation in habitat composition. From the reclassified maps, we derived habitat variables representing key components of the common pipistrelle's ecology. These included: (i) proportion of urban areas, representing roosting habitat; (ii) landscape heterogeneity, quantified as land cover diversity within a moving window to reflect environmental complexity and potential prey abundance; (iii) water proximity, estimated from the relative occurrence of water bodies within the landscape; and (iv) edge habitat availability, quantifying the extent of transitional zones between forests and open areas, which are important for efficient foraging. To integrate these predictors into a single measure of habitat quality, we additionally computed a composite habitat suitability index, weighted according to the species' habitat preferences. These derived variables were subsequently used as environmental predictors in the species distribution modelling framework.

Land cover variables were included to represent broad habitat structure and landscape context across the study area. Although land cover information is known to be scale-dependent and may lose ecological specificity at continental extents, it was further retained to complement climatic predictors and to avoid relying exclusively on climate-based niche estimates. Land cover variables were treated as coarse descriptors of landscape composition rather than fine-scale habitat selection metrics. Their inclusion was intended to capture large-scale heterogeneity while acknowledging that their influence is expected to be weaker than that of climatic variables.

5.2.6. Selecting Ecologically Relevant Environmental Variables

Understanding the ecology, and population dynamics of a species in addition to its susceptibility to disturbance is essential for developing effective SDMs (Araújo & Guisan 2006). The predictor environmental variables (Table 5.1) included in the model were the variables that were considered to be essential and can influence the geographical distribution of *Pipistrellus pipistrellus* through physiological, ecological, and/or behavioural mechanisms, and these include variables that affect roosting suitability, thermoregulation, and seasonal survival.

Table 5.1. Environmental variables chosen to be used in MaxEnt.

Category of Environmental variables	Environmental Variables	Abbreviation	Relevance to *Pipistrellus pipistrellus*	References
Climate	Annual Mean Temperature	Bio1	Determines geographic range limits, influences foraging activity .Controls insect abundance, affects hibernation length and impacts reproductive success.	Rebelo et al., 2010 Russ et al., 2003, Sherwin et al., 2013
	Temperature Seasonality	Bio4	Variation in temperature throughout the year reflects seasonal changes in habitat conditions and prey availability.	Rebelo et al., 2010,
	Precipitation Seasonality	Bio15	High variability influence vegetation types and may cause temporally mismatched insect prey emergence.	Rebelo et al., 2010; Ancillotto et al., 2016
	Average of Summer wind speed	summer_ wind_avg	Influences foraging efficiency by affecting insect activity and bat flight patterns. Stronger winds in late summer can impact migratory patterns, restrict foraging and fat accumulation required for hibernation.	Russo & Jones, 2003
Topography	Elevation		*P. pipistrellus* is generally found in lowland and forest-edge habitats. Temperature and prey distributions are affected by altitude variations.	Rebelo et al., 2010, Dietz et al., 2009

Table 5.1 continued

Category of Environmental variables	Environmental Variables	Abbreviation	Relevance to *Pipistrellus pipistrellus*	References
Topography	Slope		Flat slope areas facilitate feeding and commuting, while steep slopes can restrict foraging corridors and insect availability.	Boughey et al., 2011, Frey-Ehrenbold et al., 2013
Light	Nighttime artificial lighting	VIIRS	This measure captures the intensity of artificial lighting that can influence bat foraging behavior, prey availability, and habitat selection patterns	Mathews et al., 2015
Land Cover (2015)	Proportion of urban areas		Shows the presence of foraging areas and roosts in urban environments.	Hale et al., 2012,
	Landscape heterogeneity		Diversity of land cover types, reflecting ecological complexity and food availability.	Boughey et al., 2011, Heim et al., 2017
	Water proximity		The distance to water bodies, essential for foraging as water sources support insect populations.	Russo & Jones, 2003
	Edge habitat availability		Ecotones such as forest edges and hedgerows concentrate insect prey and are preferred foraging corridors for *P. pipistrellus*.	Verboom & Huitema 1997, Boughey et al. 2011
	Habitat index		Composite index integrating various habitat features into a single measure of habitat quality, reflecting species-specific habitat preferences.	Razgour et al. 2013, Rebelo et al. 2010

We selected the most recent year of available data (2015) to ensure that the land cover variables used in the model reflect the current landscape conditions.

5.2.7. Standardizing the Variables

We standardized the environmental variables prior to model fitting in R to ensure comparability across different measurement scales and to optimize model performance. For variables assumed to follow approximately normal distributions (temperature, wind speed, and light), we applied standard Z-score standardization based on the mean and the standard deviation. For variables prone to skewness or containing extreme outliers (precipitation seasonality, elevation, slope, and land-cover metrics), we implemented robust standardization using the median and median absolute deviation (MAD), which is less sensitive to outliers and provides more stable scaling for non-normal distributions.

5.2.8. Ecological Interactions for the Species Distribution Model

In addition to evaluating the individual contributions of environmental predictors, we incorporated interactions between key environmental variables to enhance the ecological realism of the model. The inclusion of predictor interactions is critical in species distribution models (SDMs), as the effects of one environmental factor often depend on the presence or magnitude of another, a concept that can substantially influence species distribution patterns (Guisan et al., 2006). For instance, the interaction between Urban Proportion x Water Proximity (Urban_Water Int) reflects the dynamic relationship between roosting habitats in urban areas and the availability of water bodies for foraging. While urban areas provide critical roosting sites, the proximity to water may enhance foraging efficiency, balancing both habitat functions. Similarly, the interaction between Edge Habitat x Landscape Heterogeneity (Edge_Heter Int) highlights the role of landscape complexity in supporting diverse habitats and increasing prey abundance, thereby enhancing the foraging potential at habitat edges. These interaction terms were integrated into the species distribution model to test whether they improved predictive performance and provided a more comprehensive representation of habitat suitability for *Pipistrellus pipistrellus*.

5.3. Results

5.3.1. Correlation Matrix

Based on the correlation matrix in Figure 5.4, several strong correlations ($r > 0.6$) were identified among the environmental variables, indicating potential redundancy. The most pronounced correlations were observed between topographic variables, with elevation and slope showing a strong positive correlation ($r = 0.77$), suggesting that steeper terrain is typically associated with higher elevations in the study area. Moreover, the habitat suitability index was strongly correlated with both edge habitat ($r = 0.95$) and landscape heterogeneity ($r = 0.62$). This high correlation indicates that areas with more edge habitat tend to coincide with regions of higher habitat quality and increased landscape heterogeneity.

Variables exceeding the |0.6| correlation threshold were considered redundant and flagged for potential removal to prevent model overfitting and improve ecological interpretability. This preprocessing step ensured that only environmentally distinct variables contributing unique information were retained for species distribution modeling.

11 variables were retained for subsequent model reconstruction: Light, temperature seasonality, precipitation seasonality, Slope, Average Summer wind speed, Urban Proportion, Edge habitat availability, landscape heterogeneity, Annual mean temperature, the interaction between Urban Proportion and Water Proximity, and the interaction between edge habitat and landscape heterogeneity.

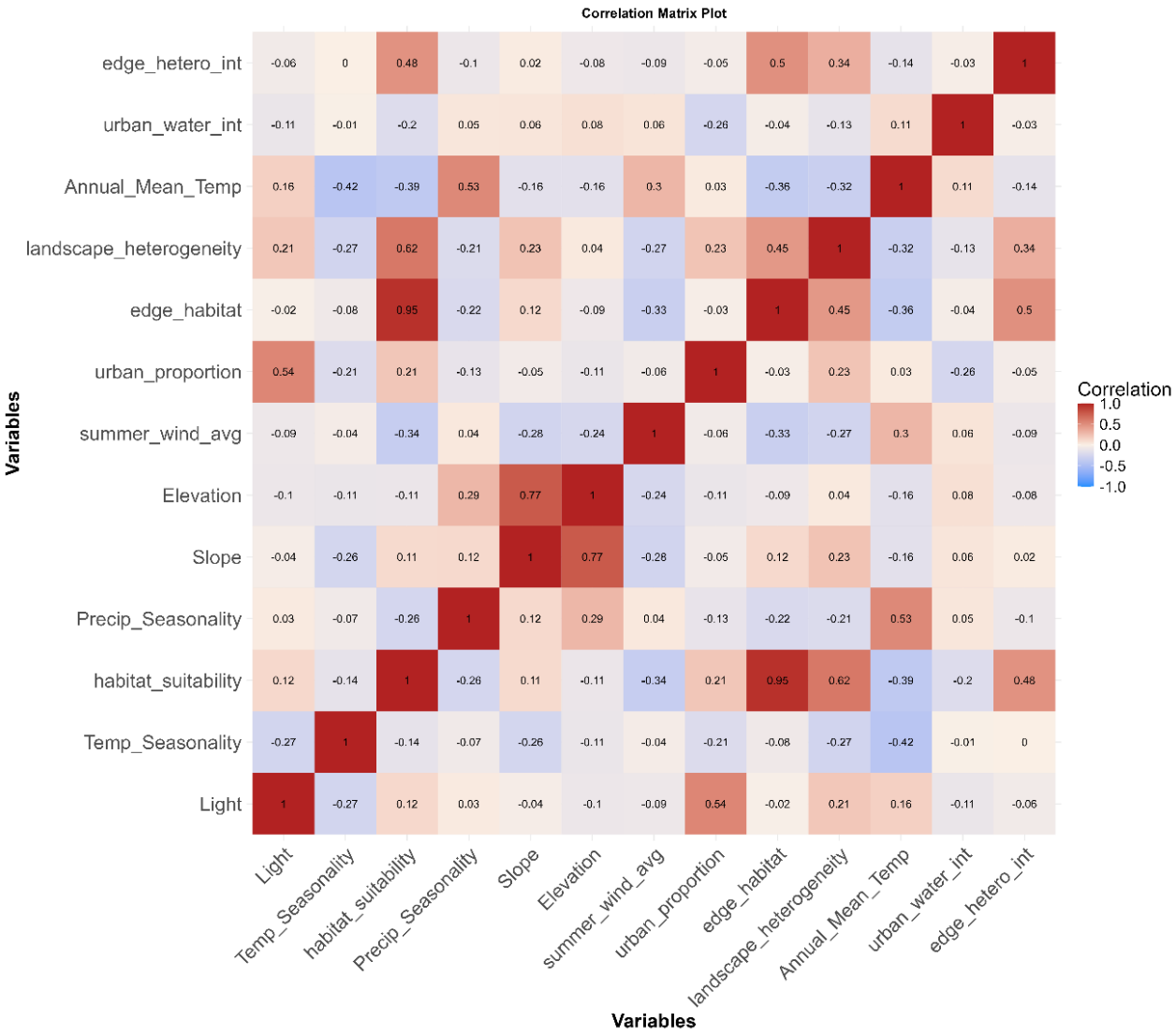


Figure 5.4. Correlation matrix of all the environmental variables.

Afterwards, we conducted a Variance Inflation Factor (VIF) analysis (Figure 5.5) to further assess and address any remaining multicollinearity among variables. This additional analysis led to the elimination of two more variables (Urban Proportion and the interaction between Urban Proportion and Water Proximity) that showed high VIF score. This final step resulted in a set of nine environmental predictors, ensuring minimal multicollinearity while maintaining the explanatory power of our variable set.

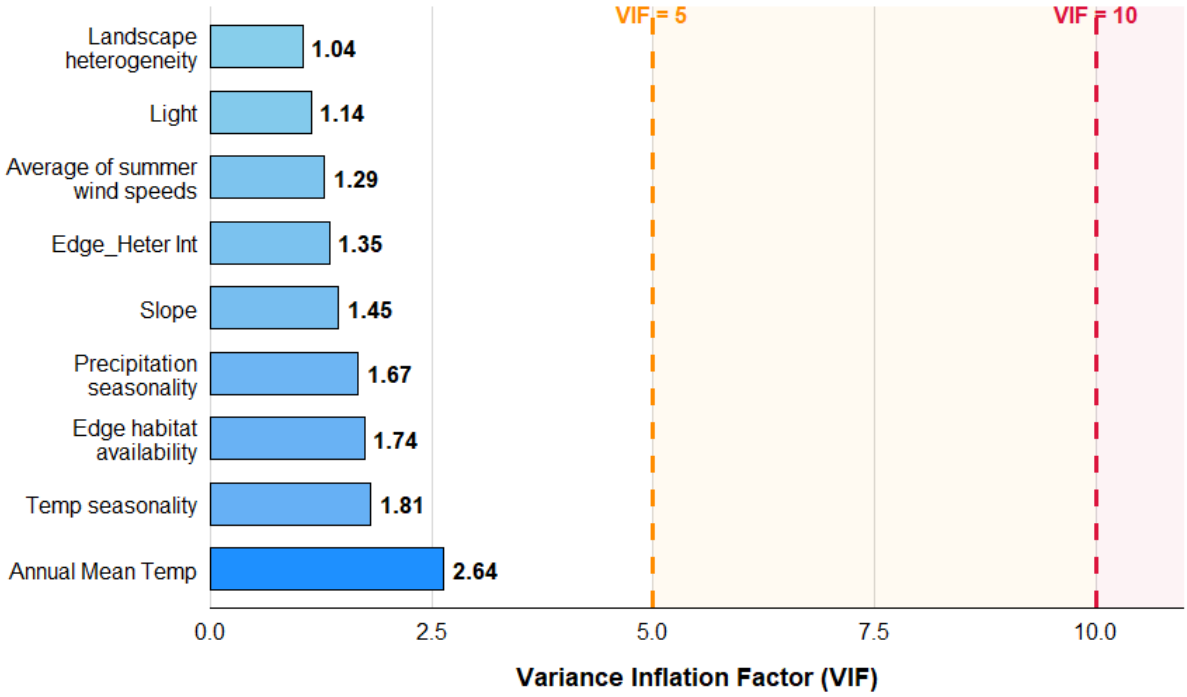


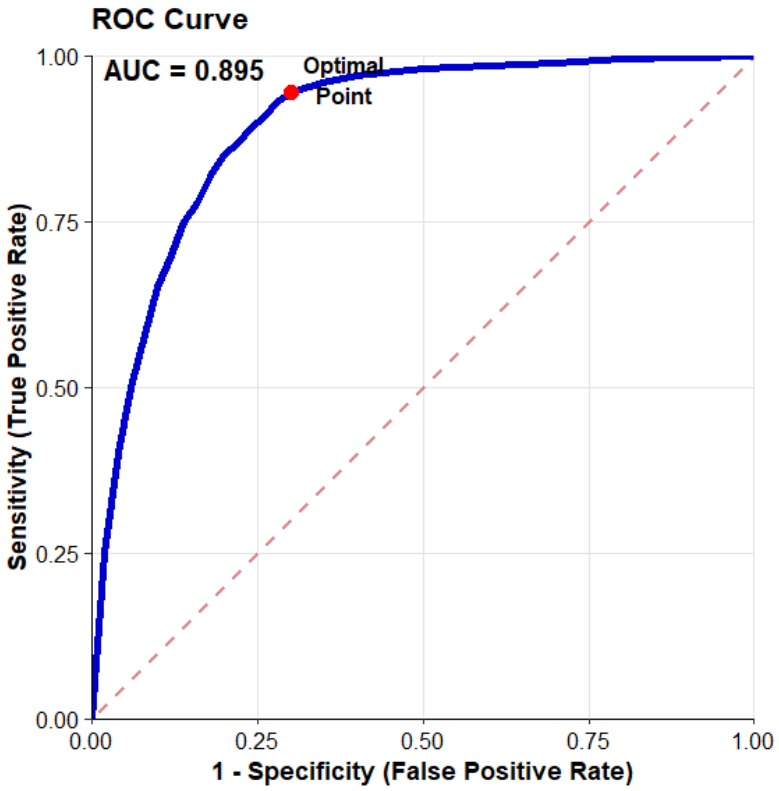
Figure 5.5. Variance inflation factor (VIF) scores for selected variables.

5.3.2. MaxEnt Operations

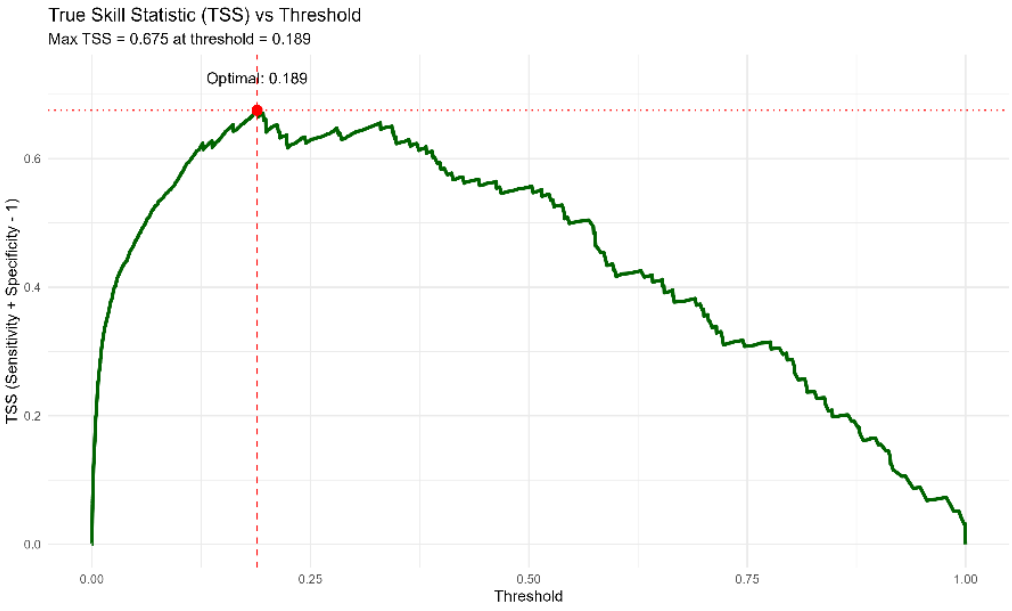
The dataset for modeling was randomly split into 75% training and 25% independent test sets, with background points split proportionally. The MaxEnt model was trained with 5,000 maximum iterations and a convergence threshold of 0.00001 to ensure model stability. The final model demonstrated very good predictive performance with an independent test AUC of 0.895 (Figure 5.6.a) and a True Skill Statistic (TSS) of 0.675 (Figure 5.6.b), indicating strong discriminatory ability. The model exhibited minimal overfitting (AUC difference = -0.002) and high sensitivity (0.968) at the optimal threshold (0.148) (Figure 5.6.c), effectively identifying 96.8% of suitable habitat areas. The MaxEnt model employed two complementary metrics to assess variable importance in predicting *Pipistrellus pipistrellus* habitat suitability. Despite relatively low precision (0.111), the high sensitivity (0.968) suggests the model successfully captures the broad environmental habitats suitable for *P. pipistrellus*, while identifying all potentially suitable areas is prioritized over minimizing false positives. Percent contribution (Figure 5.7) measured how much each variable contributed during model training, while permutation importance evaluated the decrease in model performance when each variable's values are randomly shuffled, providing a more robust assessment of true predictive power. Notable differences between these metrics were observed: temperature seasonality remained dominant in both measures (45.4% contribution vs. 42.5% permutation importance), confirming its critical role, while light pollution showed higher contribution (21.1%) than permutation importance

(8.1%), suggesting it was heavily utilized during training but less functionally essential for predictions. Conversely, annual mean temperature demonstrated greater permutation importance (21.7%) relative to its contribution (6.9%), indicating its fundamental role in maintaining model accuracy despite being less prominent during the training algorithm's variable selection process.

(a)



(b)



(c)

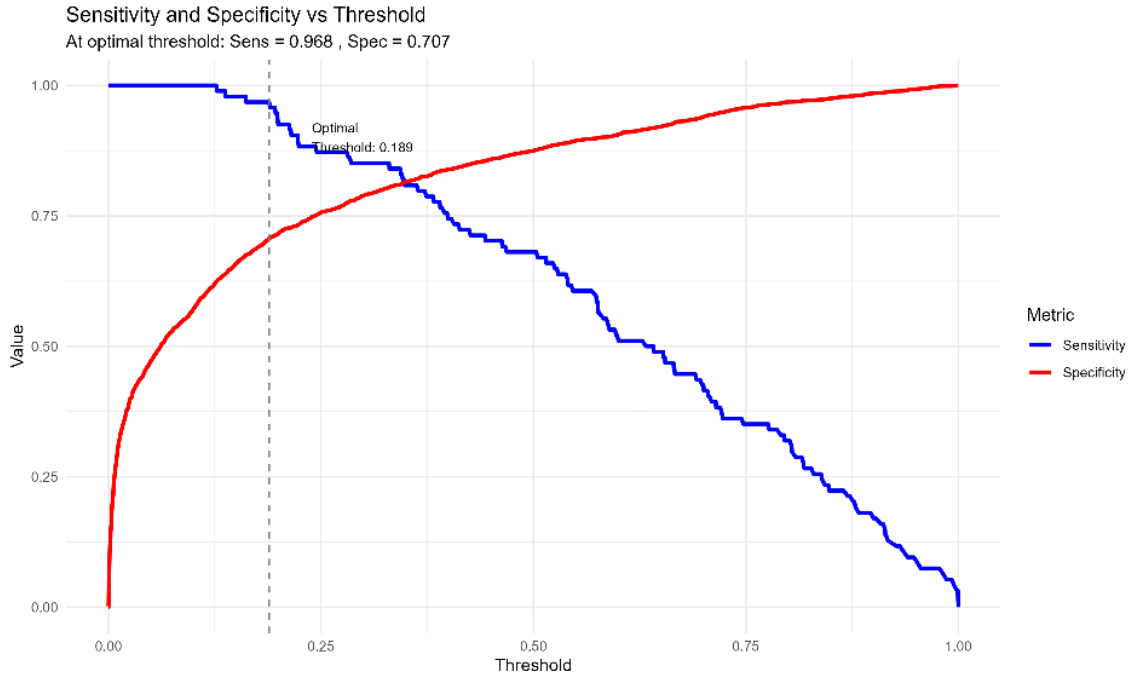


Figure 5.6. MaxEnt model performance evaluation showing (a) ROC curve with AUC = 0.895, (b) True Skill Statistic optimization, (c) sensitivity and specificity trade-offs.

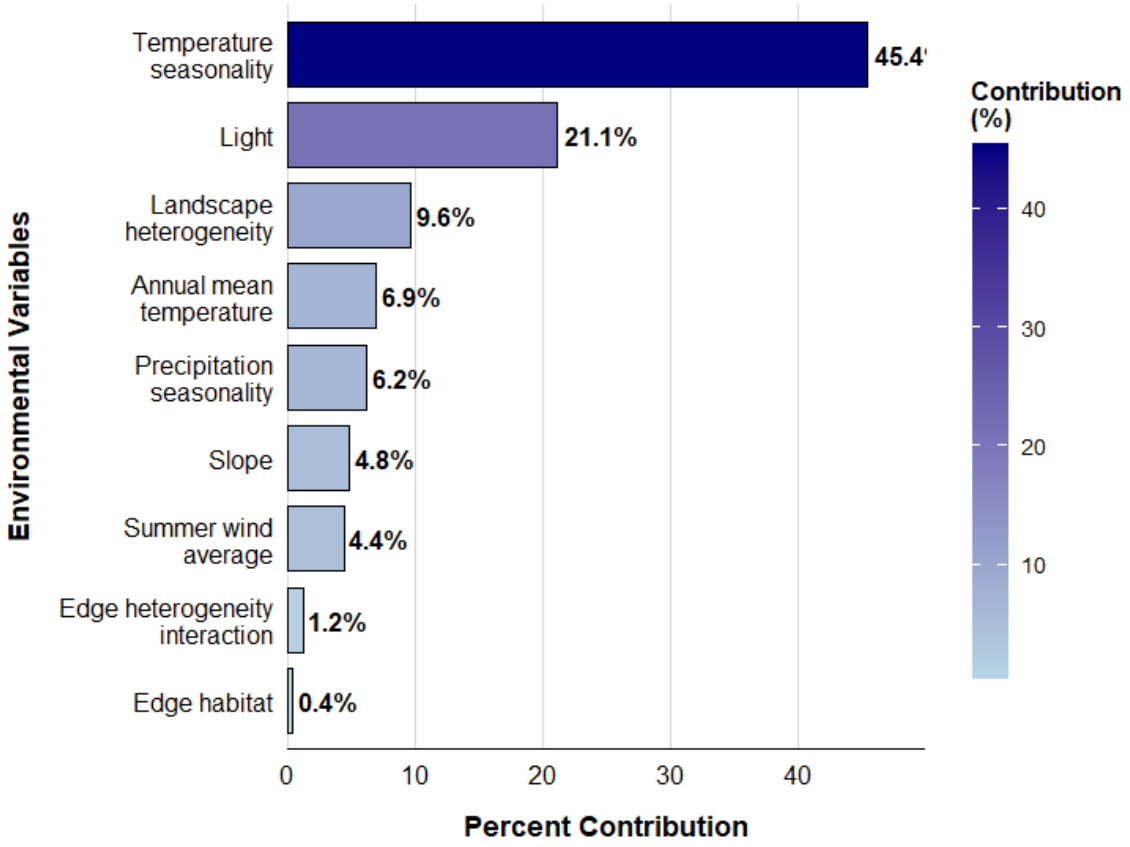


Figure 5.7. Variables contributions to Maxent (%).

The resulting habitat suitability map is presented as a binary habitat suitability map in Figure 5.8 and as a continuous habitat suitability map in Figure 5.9. The distribution of training (black) and test (brown) points across both suitable and unsuitable zones validates model performance, with most occurrence records falling within predicted suitable habitat. This spatial pattern identifies priority conservation areas while highlighting regions where habitat connectivity may be limited.

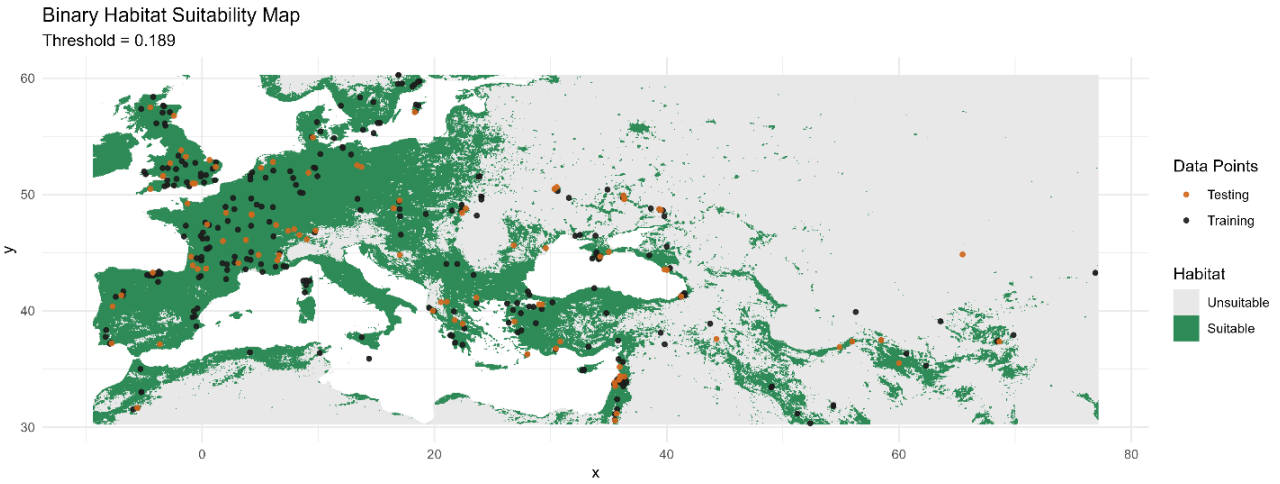


Figure 5.8. Binary Habitat Suitability map.

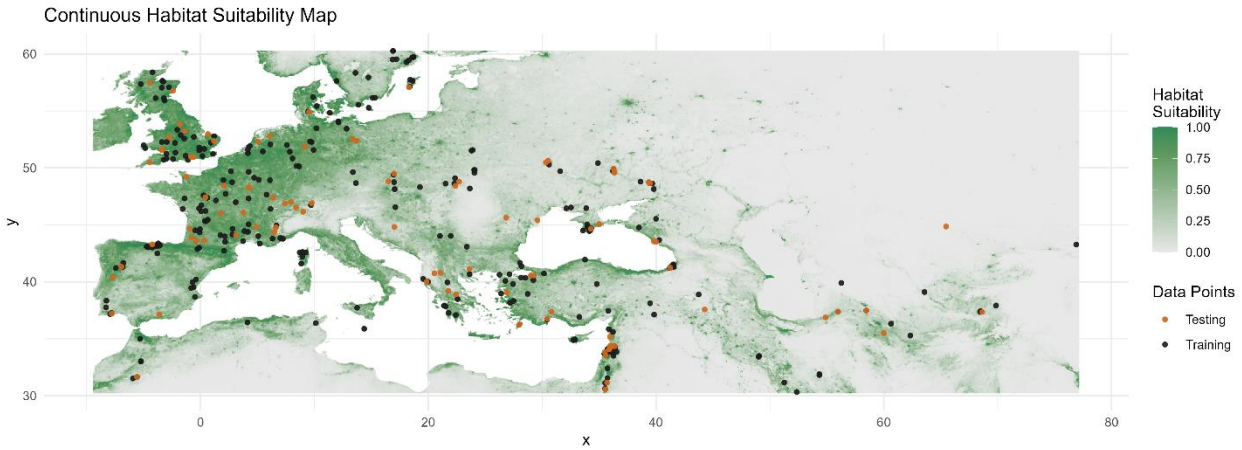


Figure 5.9. Continuous Habitat Suitability map.

5.3.3. Future Projections

In this part we predicted the future distribution of *Pipistrellus pipistrellus* under climate change scenarios. Based on the CMIP6, future (2041 and 2060) climate projections of climatic variables reconstructed from the SSP2-4.5 climate scenario were obtained in GeoTIFF format, based on 2.5 arc minutes resolution, from the WorldClim dataset (Hijmans et al., 2005; https://www.worldclim.org/data/cmip6/cmip6_clim2.5m.html) from multiple Global Climate Models (GCMs), including ACCESS-CM2, EC-Earth3-Veg, HadGEM3-GC31-LL, MIROC6, and MPI-ESM1-2-HR.

Topographic variables were retained unchanged in future projections, as they remain constant over the years. Light pollution levels were maintained at 2024 values as standardized future projections for VIIRS nighttime lights are not available. Average summer wind speed was maintained at current levels as WorldClim CMIP6 future scenarios do not include wind speed projections. Land cover variables (urban proportion, edge habitat, landscape heterogeneity) were held constant at 2015 levels for future projections, despite their potential to change over time, as compatible high-resolution future land cover scenarios matching the ESA CCI classification system were not available for the study period. While acknowledging this limitation, these land cover variables were essential to maintain model integrity, especially landscape heterogeneity as it was a significant predictor in our original habitat suitability model and the exclusion of this variable would compromise the model's performance.

We applied our trained MaxEnt model to future climate projections, and we used an ensemble modeling approach with five different Global Climate Models (HadGEM3-GC31-LL, ACCESS-CM2, MPI-ESM1-2-HR, MIROC6, and EC-Earth3-Veg) to generate separate habitat suitability predictions for each climate scenario.

The maps in Figure 5.10 display habitat suitability projections for the period 2041-2060, generated by five different climate models: EC-Earth3-Veg, MIROC6, MPI-ESM1-2-HR, ACCESS-CM2, and HadGEM3-GC31-L. The five climate models show remarkably similar spatial patterns of habitat suitability. All models consistently predict higher suitability (darker green areas) in similar geographic regions and lower suitability (lighter areas) in the same locations across the domain. The overall distribution patterns are quite consistent between the models, suggesting strong agreement among these models regarding where suitable habitat will likely occur in the 2041-2060 period. While there may be subtle differences in the intensity of suitability values between models, the fundamental

spatial patterns appear highly concordant, which indicates relatively low uncertainty in the projected habitat distribution for *Pipistrellus pipistrellus*.

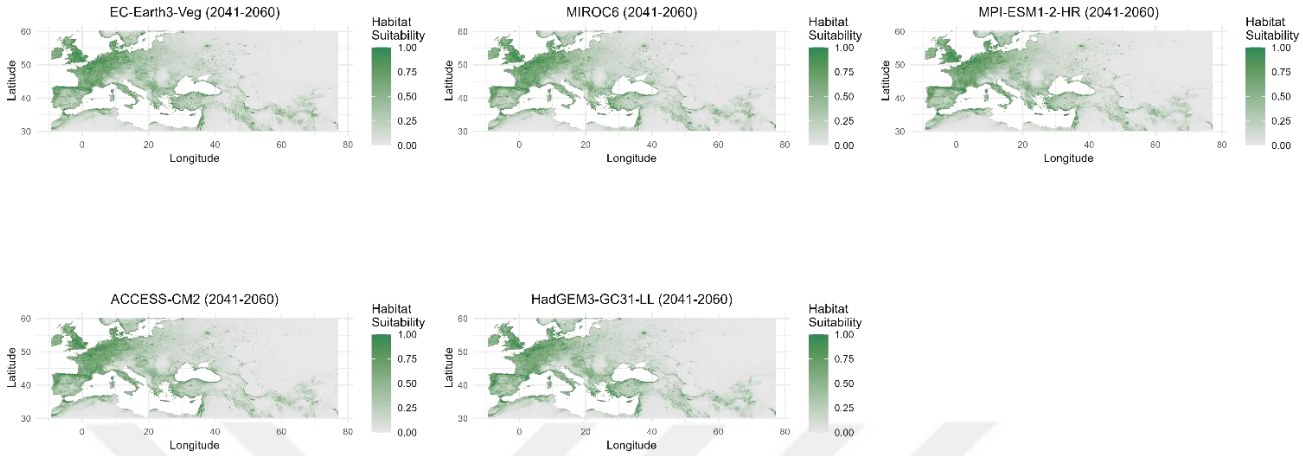


Figure 5.10. Habitat suitability projections for 2041-2060 across five global climate models.

The ensemble mean prediction map for 2041-2060 showed in Figure 5.11 represents the averaged habitat suitability across all five climate models, providing a consensus view of future habitat conditions. This approach smooths out any minor differences between individual models and provides a more robust prediction by combining the strengths of multiple climate projections.

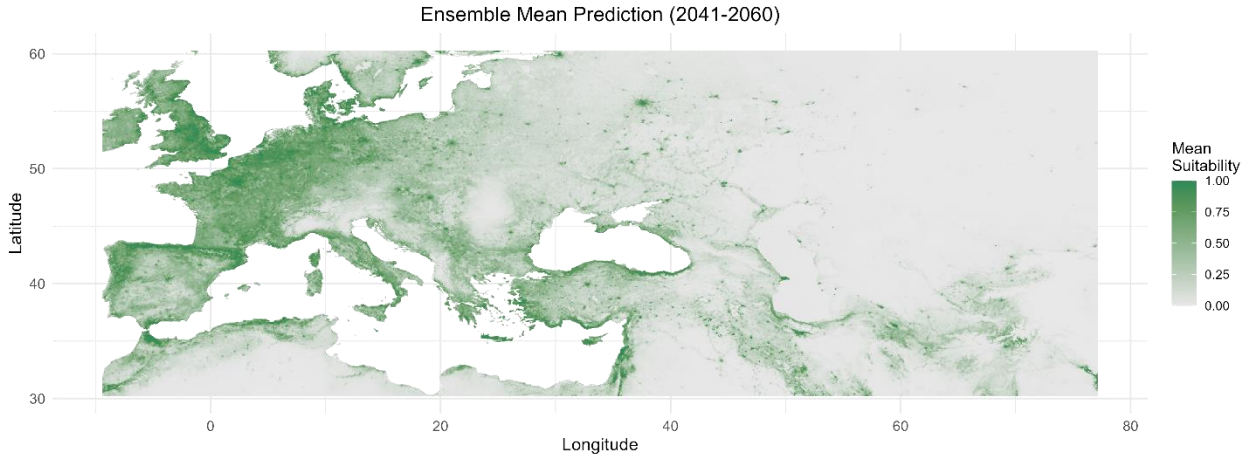


Figure 5.11. Ensemble mean habitat suitability projection (2041-2060).

The habitat change map in Figure 5.12 compares current predicted suitable habitats with future projected suitable habitats under climate scenarios for 2041-2060. Green areas show stable habitat

areas, primarily distributed across the British Isles, Scandinavia, and portions of central Europe, where suitable conditions are predicted currently and projected to persist under future climate scenarios. Red patches indicate habitat loss areas which are sparse and localized, appearing as isolated patches scattered throughout Central and Southern Europe, particularly around the Iberian Peninsula and parts of the Mediterranean basin where currently predicted, suitable areas are projected to become unsuitable under future climate conditions, representing areas where existing populations may face risks. Blue areas reveal newly suitable habitats that are not predicted under current conditions but are projected to become available under future climate scenarios, with gains appearing in Eastern Europe and Western Russia, particularly in the steppe zone, indicating potential colonization opportunities as preferable for *P. pipistrellus* climate conditions shift east and north, while gray areas indicate regions that are unsuitable in both current and future scenarios.

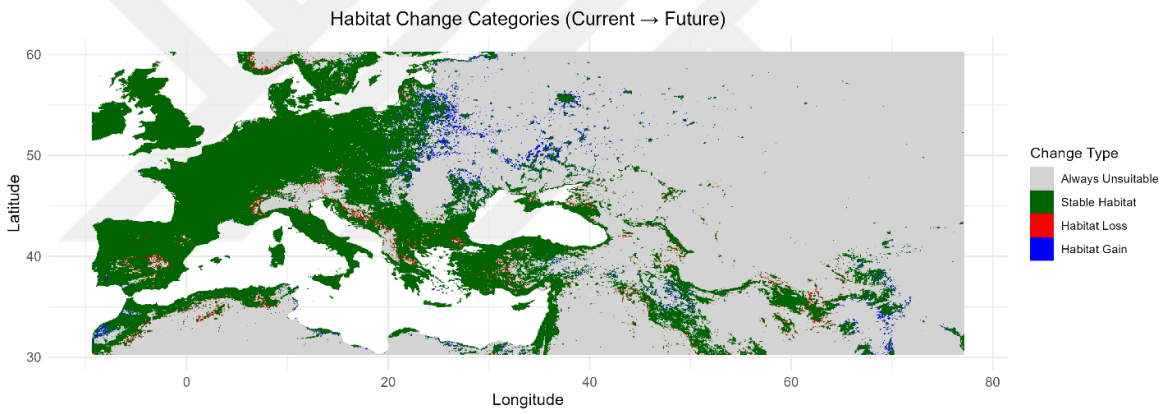


Figure 5.12. Projected habitat change categories from current to future conditions (2041-2060).

5.4. Discussion

Species distribution modeling for *Pipistrellus pipistrellus* addresses interconnected questions in conservation biogeography, extending beyond simple habitat mapping to explain mechanistic drivers of species occurrence and resilience under environmental change. With ongoing pressures like habitat fragmentation, urbanization, and climate change, SDMs provide essential insights into the relative importance of environmental drivers that shape a species' occurrence patterns. The high predictive performance achieved in our modeling (AUC = 0.895, TSS = 0.675) demonstrated robust discriminatory capacity that enables reliable habitat predictions.

In line with previous biogeographic classifications of European bats (Rebelo et al., 2010), our results indicate that the distribution of *P. pipistrellus* is primarily constrained by broad-scale climatic factors. Temperature seasonality emerged as the dominant predictor (45.4% contribution, 42.5% permutation importance), highlighting the species' sensitivity to thermal variability rather than mean temperature alone. Seasonal temperature changes influence hibernation energetics, reproduction timing, and insect prey phenology, thereby playing a key role in synchronizing physiological processes with resource availability (Humphries et al., 2002). This result supports the view that temperate bat species can survive across wide thermal ranges as long as seasonal conditions remain moderate and predictable.

The high permutation importance of temperature seasonality indicates that this variable provides information that is not easily compensated for by other predictors. In contrast, the significant difference between contribution and permutation importance for annual mean temperature (6.9% vs. 21.7%, respectively) suggests that absolute thermal limits impose fundamental constraints on distribution boundaries, despite appearing less prominent during model training. This pattern indicates that, while *P. pipistrellus* has significant thermal tolerance across its range, absolute temperature limits impose hard constraints on distribution boundaries. Under projected warmer future scenarios, these thermal thresholds could shift dramatically, potentially expanding suitable habitat into previously marginal areas while also approaching critical upper limits in southern refugia.

Although land cover and anthropogenic variables were included in the models, their interpretation requires caution at the continental scale considered here. Previous work has shown that the relative importance of environmental predictors is scale-dependent, with climatic variables dominating at broad extents and habitat variables becoming more influential at regional and local scales (Pearson & Dawson, 2003). Land cover variables were nevertheless retained to capture large-scale habitat constraints relevant to bat ecology and to avoid an exclusively climate-driven niche representation.

The significant influence of anthropogenic variables, particularly light pollution (21.1% contribution) and the urban-water proximity interaction, reflects the species' tendencies to adapt within human-modified landscapes. However, the relatively low permutation importance of light pollution (8.1%) may indicate the presence of compensatory mechanisms, such as behavioral plasticity or alternative foraging strategies, although causal relationships cannot be inferred from correlative models alone. The importance of landscape heterogeneity and edge habitat variables highlights the species' ecological adaptability and resource allocation strategies. *P. pipistrellus*

exhibits greater habitat tolerance than morphologically similar related species, allowing it to take advantage of diverse foraging opportunities across habitat boundaries and heterogeneous landscapes. This ecological plasticity, while providing resilience against localized disturbances, also exposes the species to cumulative impacts across multiple habitat types. The interaction term between edge habitat and landscape heterogeneity indicates non-additive effects in which habitat complexity improves edge utilization, implying advanced spatial resource exploitation strategies.

Our ensemble modeling approach using five Global Climate Models provides robust uncertainty assessment for future habitat projections. The strong agreement between individual GCM predictions indicates consistent climatic controls on habitat suitability across different models. However, this agreement may mask deeper uncertainties in climate projections, particularly for extreme weather events and threshold responses that could have a significant impact on populations. The habitat change analyses reveals critical conservation implications for *P. pipistrellus* population dynamics. While stable refugia in northern and western Europe may buffer populations against climate change, the fragmented nature of newly suitable habitats raises concerns about colonization success. Although the species shows moderate dispersal capacity (typically 10-50 km seasonal movements, occasionally up to 200 km), landscape connectivity remains important for accessing distant suitable places, particularly given the projected rate of climate-driven habitat shifts.

The persistence of unsuitable conditions across Mediterranean regions, despite our efforts to address sampling bias through weighted sampling approaches, may suggest bioclimatic constraints in addition to methodological artifacts. Rather than simple latitudinal migration, our results reveal complex range dynamics where stable suitable habitat remains extensive and well connected across northern and western Europe, while newly suitable areas under future climate scenarios appear as scattered, fragmented patches. This fragmentation of potential expansion zones, rather than core habitat areas, may limit the species' ability to colonize newly available habitats despite their moderate dispersal capacity. This finding emphasizes that even adaptable taxa may face connectivity constraints under climate change, particularly when accessing newly suitable areas, which suggests that successful adaptation will depend on maintaining connectivity between stable refugia and the scattered patches of newly suitable habitat. Although *P. pipistrellus* is not currently considered a conservation-dependent species, these findings highlight the importance of maintaining landscape connectivity to support future range adjustments under climate change, rather than identifying discrete conservation areas per se.

6. CONCLUSION, LIMITATIONS AND FUTURE RECOMMENDATIONS

This thesis demonstrates the value of integrating multiple analytical approaches, phylogeography, field monitoring, and habitat suitability modeling to generally assess bat conservation status in a biogeographically critical region.

The mitochondrial DNA analyses presented in the first Chapter revealed high haplotype diversity in all geographic regions (Hd > 0.80)., with clear geographic structuring also evident in phylogenetic analyses. Western Europe and North Africa had the highest nucleotide diversity, while European Türkiye and the British Isles showed the lowest diversity. The low diversity in the British Isles is compatible with expectations for peripheral, recently colonized populations in the northwestern end of the species' distribution. In contrast, despite the region's central geographic location, the similarly low diversity in European Türkiye calls for more research. Although haplotype and nucleotide diversity estimates are theoretically independent of sample size, uneven sampling can still influence diversity estimates in geographically structured populations, therefore, the smaller sample size from Thrace Türkiye (n = 27) compared to Anatolia (n = 55) may have contributed to the reduced diversity observed for the latter. However, the high haplotype and nucleotide diversity in North Africa despite a much smaller sample size (n = 9) suggests that sampling effects alone cannot explain the observed patterns. Instead, this high diversity may reflect long-term population persistence in North Africa, potentially indicating a North African refugium that preserved distinct mitochondrial lineages during Pleistocene climatic oscillations (Husemann et al., 2014). Alternatively, reduced diversity in European Türkiye can also reflect obstacles to gene flow between Anatolian and European groups. These results point to complex phylogeographic history, where regions with higher nucleotide diversity may represent long-term stable populations or contact zones between distinct lineages, while areas with lower diversity may reflect more recent colonization, founder effects, or population bottlenecks (Hewitt, 2004).

Clear geographic structuring was evident in phylogenetic analyses also, with distinct clustering patterns supporting regional differentiation. However, haplotype networks proved more informative for visualizing relationships among closely related populations, as they explicitly represent ancestral haplotypes that persist in contemporary populations. In intraspecific analyses, like this study, phylogenetic tree reconstruction forces all sampled haplotypes to terminal positions, and cannot accommodate ancestral haplotypes at internal nodes, an assumption clearly violated when central nodes in haplotype networks represent extant ancestral lineages. The presence of these ancestral

haplotypes in contemporary populations, particularly observable in regions like Anatolia and the Middle East, indicates ongoing connectivity with refugial source populations and highlights the importance of these regions for maintaining evolutionary diversity.

In comparison to mitochondrial patterns, nuclear DNA markers showed weaker and more heterogeneous spatial structure, indicating possible sex-biased dispersal with increased male-mediated gene flow. However, conclusive findings regarding patterns of genome-wide connection are not possible due to the small number of nuclear markers examined. Türkiye's biogeographic location between high-diversity Western European populations and the Middle Eastern/Asian regions of the species' distribution makes it a potentially key corridor. Whether Turkish populations represent different evolutionary lineages that require more research or serve primarily as a genetic link between European and Asian populations, has significant implications for understanding regional population dynamics.

The genetic structuring also provides context for interpreting wind turbine mortality. If high gene flow connects populations, individual wind farm mortality may be partially compensated through immigration, though cumulative impacts across multiple facilities along migratory routes could still have population-level effects. Resolving this question requires more nuclear marker analyses to assess contemporary gene flow patterns.

Chapter 2 provided the first systematic assessment of bat-wind farm interactions in Türkiye, revealing that *Pipistrellus nathusii*, a migratory species traversing Türkiye during autumn passage between Eastern European breeding grounds and southern wintering areas, comprised the majority of both acoustic detections and wind turbine fatalities, followed by *P. pipistrellus*. This finding has significant conservation implications given Türkiye's position along critical migratory corridors. The strong correlation between wind speed and mortality, coupled with elevated mortality during cooler temperatures, highlights temporal windows of increased collision risk and provides useful information for operational mitigation, such as seasonal or weather-based curtailment. However, the single-season, limited-intensity sampling design (two nights per month) constrained statistical power and precluded assessment of inter-annual variation in activity and mortality patterns.

The species distribution models developed in Chapter 3 predicted a net loss of suitable habitat for *P. pipistrellus* under future climate scenarios (2.8% loss versus 0.9% gain), with projected northward range shifts consistent with warming trends documented across temperate taxa. However, the models' heavy reliance on European occurrence data, combined with the challenge of adequately

representing urbanization, a critical habitat feature for this synanthropic species, introduces uncertainty in predictions for Türkiye and Asia. The finding that light pollution, intended as a proxy for urban habitat, contributed relatively little to model predictions suggests either that this proxy inadequately captures urban habitat suitability or that other unmeasured factors (building density, roost site availability) are more important determinants of *P. pipistrellus* distribution.

Finally, while *P. nathusii* accounted for the highest number of turbine-related fatalities, *P. pipistrellus* is the most killed bat species in wind farms in Türkiye overall and the second most affected species at the studied wind farm. This 'recent' mortality pattern gains additional importance when considered alongside genetic and biogeographic insights. If Turkish *P. pipistrellus* populations exhibit partial genetic differentiation, turbine-related mortality could disproportionately impact specific demographic or evolutionary units. Even in the presence of substantial gene flow, repeated mortality events across multiple wind farms may reduce population resilience over time. Predicted distributional shifts under climate change further amplify these concerns. Our models indicate that *P. pipistrellus* is likely to follow suitable climatic conditions northward. However, species distribution models assume that present-day relationships between species occurrence and environmental variables remain constant under future conditions, an assumption that may be violated by increasing anthropogenic pressures, such as wind energy development, which can eventually coincide spatially with areas projected to become climatically suitable.

Genetic studies should prioritize multi-locus nuclear DNA analyses across the study region to resolve contemporary gene flow patterns, assess male-mediated connectivity, and detect signatures of local adaptation. Expanded sampling in underrepresented regions, particularly Central Asia and the Middle East, would improve resolution of Türkiye's role as a potential genetic bridge or contact zone.

Wind farm monitoring should expand to multi-year studies at multiple facilities to quantify inter-annual variation, assess cumulative impacts across migratory corridors, and validate observed patterns. Incorporating real-time turbine operational monitoring, and experimental curtailment protocols (varying cut-in speeds and operational schedules under different weather conditions) would provide direct evidence for mitigation efficacy. Monitoring additional wind farms across different Turkish regions would identify particularly high-risk facilities or landscape contexts.

Distribution modeling should incorporate explicit urbanization variables (building density, human population density, distance to urban centers) and test whether they improve predictions beyond light pollution. Developing region-specific models or approaches allowing environmental

relationships to vary spatially would address extrapolation concerns. Incorporating projections of future land use and urbanization patterns, rather than holding anthropogenic variables constant, would better reflect real-world conditions or urban-associated species.

Integrative approaches linking genetics with mortality monitoring could assess whether wind farm fatalities disproportionately affect genetic lineages through genetic analysis of carcasses to determine population origin. Combining distribution models with spatial data on planned wind energy development would identify convergent threat zones where habitat suitability, genetic importance, and mortality risk coincide. Extending this framework to additional bat species would test generality and broaden conservation applications across Türkiye's diverse bat fauna.

REFERENCES

Adams, A. M. (2013). *Assessing and analyzing bat activity with acoustic monitoring: Challenges and interpretations*. The University of Western Ontario (Canada).

Adams, R. A. (2010). Bat reproduction declines when conditions mimic climate change projections for western North America. *Ecology, 91*(8), 2437–2445.

Adams, R. A., & Hayes, M. A. (2008). Water availability and successful lactation by bats as related to climate change in arid regions of western North America. *Journal of Animal Ecology, 77*, 1115–1121.

Alsos, I. G., Ehrich, D., Thuiller, W., Eidesen, P. B., Tribsch, A., Schönswetter, P., … Brochmann, C. (2012). Genetic consequences of climate change for northern plants. *Proceedings of the Royal Society B: Biological Sciences, 279*(1735), 2042–2051.

Altringham, J. D. (2011). *Bats: From evolution to conservation*. Oxford University Press.

Amorim, F., Mata, V. A., Beja, P., & Rebelo, H. (2015). Effects of a drought episode on the reproductive success of European free-tailed bats (*Tadarida teniotis*). *Mammalian Biology, 80*(3), 228–236.

Ancillotto, L., Santini, L., Ranc, N., Maiorano, L., & Russo, D. (2016). Extraordinary range expansion in a common bat: The potential roles of climate change and urbanisation. *The Science of Nature, 103*(3), 15.

Araújo, M. B., & Guisan, A. (2006). Five (or so) challenges for species distribution modelling. *Journal of Biogeography, 33*(10), 1677–1688.

Araújo, M. B., Pearson, R. G., Thuiller, W., & Erhard, M. (2005). Validation of species–climate impact models under climate change. *Global Change Biology, 11*(9), 1504–1513.

Arnett, E. B. (2005). *Relationships between bats and wind turbines in Pennsylvania and West Virginia: An assessment of bat fatality search protocols, patterns of fatality, and behavioral*

interactions with wind turbines. Final report submitted to the Bats and Wind Energy Cooperative. Bat Conservation International, Austin, TX, USA.

Arnett, E. B., Brown, W. K., Erickson, W. P., Fiedler, J. K., Hamilton, B. L., Henry, T. H., … Tankersley, R. D., Jr. (2008). Patterns of bat fatalities at wind energy facilities in North America. *The J*ournal *of Wildlife Management, 72*(1), 61–78.

Arnett, E. B., Huso, M. M., Schirmacher, M. R., & Hayes, J. P. (2011). Altering turbine speed reduces bat mortality at wind-energy facilities. *Frontiers in Ecology and the Environment, 9*(4), 209–214.

Avise, J. C. (2000). *Phylogeography: The history and formation of species*. Harvard University Press.

Baerwald, E. F., & Barclay, R. M. (2009). Geographic variation in activity and fatality of migratory bats at wind energy facilities. *Journal of Mammalogy, 90*(6), 1341–1349.

Baerwald, E. F., D'Amours, G. H., Klug, B. J., & Barclay, R. M. (2008). Barotrauma is a significant cause of bat fatalities at wind turbines. *Current Biology, 18*(16), R695–R696.

Baerwald, E. F., Edworthy, J., Holder, M., & Barclay, R. M. (2009). A large-scale mitigation experiment to reduce bat fatalities at wind energy facilities. *The Journal of Wildlife Management, 73*(7), 1077–1081.

Baker, P. J., & Harris, S. (2007). Urban mammals: What does the future hold? An analysis of the factors affecting patterns of use of residential gardens in Great Britain. *Mammal Review, 37*(4), 297–315.

Balloux, F. (2010). The worm in the fruit of the mitochondrial DNA tree. *Heredity, 104*(5), 419.

Barataud, M. (2015). *Acoustic ecology of European bats: Species identification and studies of their habitats and foraging behaviour*. Biotope Editions.

Barclay, R. M., Baerwald, E. F., & Gruver, J. C. (2007). Variation in bat and bird fatalities at wind energy facilities: Assessing the effects of rotor size and tower height. *Canadian Journal of Zoology, 85*(3), 381–387.

Barclay, R. M., & Harder, L. D. (2003). Life histories of bats: Life in the slow lane. In T. H. Kunz & M. B. Fenton (Eds.), *Bat ecology* (pp. 209–253). University of Chicago Press.

Barlow, K. E., & Jones, G. (1997). Differences in songflight calls and social calls between two phonic types of the vespertilionid bat *Pipistrellus pipistrellus*. *Journal of Zoology, 241*(2), 315–324.

Barlow, K. E., Jones, G., & Barratt, E. M. (1997). Can skull morphology be used to predict ecological relationships between bat species? A test using two cryptic species of pipistrelle. *Proceedings of the Royal Society of London. Series B: Biological Sciences, 264*(1388), 1695–1700.

Barnosky, A. D., Matzke, N., Tomiya, S., Wogan, G. O. U., Swartz, B., Quental, T. B., … Ferrer, E. A. (2011). Has the Earth's sixth mass extinction already arrived? *Nature, 471*(7336), 51–57.

Barratt, E. M., Deaville, R., Burland, T. M., Bruford, M. W., Jones, G., Racey, P. A., & Wayne, R. K. (1997). DNA answers the call of pipistrelle bat species. *Nature, 387*(6629), 138–139.

Beck, J., Böller, M., Erhardt, A., & Schwanghart, W. (2014). Spatial bias in the GBIF database and its effect on modeling species' geographic distributions. *Ecological Informatics, 19*, 10–15.

Behr, O., Brinkmann, R., Niermann, I., & Korner-Nievergelt, F. (2011). *Fledermausfreundliche Betriebsalgorithmen für Windenergieanlagen: Entwicklung von Methoden zur Untersuchung und Reduktion des Kollisionsrisikos von Fledermäusen an Onshore-Windenergieanlagen*. Umwelt und Raum.

Bellard, C., Bertelsmeier, C., Leadley, P., Thuiller, W., & Courchamp, F. (2012). Impacts of climate change on the future of biodiversity. *Ecology Letters, 15*(4), 365–377.

Benda, P., & Horáček, I. (1998). Bats (Mammalia: Chiroptera) of the Eastern Mediterranean. Part 1. Review of distribution and taxonomy of bats in Turkey. *Acta Societatis Zoologicae Bohemicae, 62*, 255–313.

Benda, P., Hulva, P., Andreas, M., & Uhrin, M. (2003). Notes on the distribution of *Pipistrellus pipistrellus* complex in the Eastern Mediterranean. *Vespertilio, 7*, 87–95.

Bermingham, E., & Moritz, C. (1998). Comparative phylogeography: Concepts and applications. *Molecular Ecology, 7*(4), 367–369.

Bilgin, R., Çoraman, E., Karataş, A., & Morales, J. C. (2009). Phylogeography of the greater horseshoe bat *Rhinolophus ferrumequinum* in southeastern Europe and Anatolia. *Acta Chiropterologica, 11*(1), 53–60.

Bilgin, R., Gürün, K., Rebelo, H., Puechmaille, S. J., Maracı, Ö., Presetnik, P., … Juste, J. (2016). Circum-Mediterranean phylogeography of a bat coupled with past environmental niche modeling. *Molecular Phylogenetics and Evolution, 99*, 323–336.

Bilgin, R., Karataş, A., Coraman, E., Pandurski, I., Papadatou, E., & Morales, J. C. (2006). Molecular taxonomy and phylogeography of *Miniopterus schreibersii*. *Biological Journal of the Linnean Society, 87*(4), 577–582.

Bilgin, R., Keşişoğlu, A., & Rebelo, H. (2012). Distribution patterns of bats in the Eastern Mediterranean Region through a climate change perspective. *Acta Chiropterologica, 14*(2), 425–437.

Blondel, J., Aronson, J., Bodiou, J. Y., & Boeuf, G. (2010). *The Mediterranean region: Biological diversity in space and time*. Oxford University Press.

Boston, E. S., Puechmaille, S. J., Clissmann, F., & Teeling, E. C. (2014). Further evidence for cryptic north-western refugia in Europe? *Acta Chiropterologica, 16*(2), 263–277.

Bouckaert, R., Vaughan, T. G., Barido-Sottani, J., Duchêne, S., Fourment, M., Gavryushkina, A., … Drummond, A. J. (2019). BEAST 2.5: An advanced software platform for Bayesian evolutionary analysis. *PLoS Computational Biology, 15*(4), e1006650.

Boughey, K. L., Lake, I. R., Haysom, K. A., & Dolman, P. M. (2011). Effects of landscape-scale woodland configuration on roost location for bats. *Biological Conservation, 144*(9), 2300–2310.

Boyla, K. A. (2024). *Database* (access restricted). KAB Ecology Consultancy.

Boyles, J. G., Cryan, P. M., McCracken, G. F., & Kunz, T. H. (2011). Economic importance of bats in agriculture. *Science, 332*(6025), 41–42.

Bradshaw, W. E., & Holzapfel, C. M. (2006). Evolutionary response to rapid climate change. *Science, 312*(5779), 1477–1478.

Burland, T. M., Barratt, E. M., Beaumont, M. A., & Racey, P. A. (1999). Population genetic structure and gene flow in *Plecotus auritus*. *Proceedings of the Royal Society B, 266*(1422), 975–980.

Burland, T. M., & Wilmer, J. W. (2001). Seeing in the dark: Molecular approaches to bat population studies. *Biological Reviews, 76*(3), 389–409.

Burgin, C. J., Colella, J. P., Kahn, P. L., & Upham, N. S. (2018). How many species of mammals are there? *Journal of Mammalogy, 99*(1), 1–14.

Castella, V., Ruedi, M., & Excoffier, L. (2001). Contrasted patterns of mitochondrial and nuclear structure among nursery colonies of the bat *Myotis myotis*. *Journal of Evolutionary Biology, 14*(5), 708–720.

Chen, I.-C., Hill, J. K., Ohlemüller, R., Roy, D. B., & Thomas, C. D. (2011). Rapid range shifts of species associated with high levels of climate warming. *Science, 333*(6045), 1024–1026.

Chojnowski, J. L., Kimball, R. T., & Braun, E. L. (2008). Introns outperform exons in analyses of basal avian phylogeny using clathrin heavy chain genes. *Gene, 410*(1), 89–96.

Ciechanowski, M., Zając, T., Biłas, A., & Dunajski, R. (2007). Spatiotemporal variation in activity of bat species differing in hunting tactics: Effects of weather, moonlight, food abundance, and structural clutter. *Canadian Journal of Zoology, 85*(12), 1249–1263.

Council, G. W. E. (2021). *Global wind report 2021*. Global Wind Energy Council.

Cryan, P. M. (2008). Mating behavior as a possible cause of bat fatalities at wind turbines. *The Journal of Wildlife Management, 72*(3), 845–849.

Cryan, P. M., & Barclay, R. M. (2009). Causes of bat fatalities at wind turbines: Hypotheses and predictions. *Journal of Mammalogy, 90*(6), 1330–1340.

Cryan, P. M., Gorresen, P. M., Hein, C. D., Schirmacher, M. R., Diehl, R. H., Huso, M. M., … Dalton, D. C. (2014). Behavior of bats at wind turbines. *Proceedings of the National Academy of Sciences of the United States of America, 111*(42), 15126–15131.

Cryan, P. M., Jameson, J. W., Baerwald, E. F., Willis, C. K. R., Barclay, R. M., Snider, E. A., & Crichton, E. G. (2012). Evidence of late-summer mating readiness and early sexual maturation in migratory tree-roosting bats found dead at wind turbines. *PLoS ONE, 7*(10), e47586.

Davidson-Watts, I., & Jones, G. (2006). Differences in foraging behaviour between *Pipistrellus pipistrellus* (Schreber, 1774) and *Pipistrellus pygmaeus* (Leach, 1825). *Journal of Zoology, 268*(1), 55–62.

Davidson-Watts, I., Walls, S., & Jones, G. (2006). Differential habitat selection by *Pipistrellus pipistrellus* and *Pipistrellus pygmaeus* identifies distinct conservation needs for cryptic species of echolocating bats. *Biological Conservation, 133*(1), 118–127.

Davis, M., Faurby, S., & Svenning, J.-C. (2018). Mammal diversity will take millions of years to recover from the current biodiversity crisis. *Proceedings of the National Academy of Sciences of the United States of America, 115*(44), 11262–11267.

Dietz, C., von Helversen, O., Nill, D., Lina, P. H. C., & Hutson, A. M. (2009). *Bats of Britain, Europe and Northwest Africa*. A & C Black.

Dietz, C., & Kiefer, A. (2014). *Die Fledermäuse Europas: Kennen, bestimmen, schützen*. Kosmos Naturführer.

Dirzo, R., Young, H. S., Galetti, M., Ceballos, G., Isaac, N. J. B., & Collen, B. (2014). Defaunation in the Anthropocene. *Science, 345*(6195), 401–406.

Drummond, A. J., & Rambaut, A. (2007). BEAST: Bayesian evolutionary analysis by sampling trees. *BMC Evolutionary Biology, 7*, 214.

Edwards, S. V., & Beerli, P. (2000). Perspective: Gene divergence, population divergence, and the variance in coalescence time in phylogeographic studies. *Evolution, 54*(6), 1839–1854.

Elith, J., & Leathwick, J. R. (2009). Species distribution models: Ecological explanation and prediction across space and time. *Annual Review of Ecology, Evolution, and Systematics, 40*, 677–697.

Ellerbrok, J. S., Farwig, N., Peter, F., & Voigt, C. C. (2024). Forest bat activity declines with increasing wind speed in proximity of operating wind turbines. *Global Ecology and Conservation, 49*, e02782.

Engler, R., Hordijk, W., & Guisan, A. (2012). The MIGCLIM R package: Seamless integration of dispersal constraints into projections of species distribution models. *Ecography, 35*(10), 872–878.

EUROBATS. (2014). *Report of the Intersessional Working Group on Wind Turbines and Bat Populations* (Doc. EUROBATS.StC 9-AC19.12). Heraklion, Greece.

Ezard, T. H. G., & Travis, J. M. J. (2006). The impact of habitat loss and fragmentation on genetic drift and fixation time. *Oikos, 114*(2), 367–375.

Federal Ministry for the Environment, Nature Conservation and Nuclear Safety. (2007). *The national strategy for biological diversity*. BMU.

Fiedler, J. K., Henry, T. H., Nicholson, C. P., & Tankersley, R. D. (2007). *Results of bat and bird mortality monitoring at the expanded Buffalo Mountain Windfarm, 2005*. Tennessee Valley Authority, Knoxville, TN, USA.

Fielding, A. H., & Bell, J. F. (1997). A review of methods for the assessment of prediction errors in conservation presence/absence models. *Environmental Conservation, 24*(1), 38–49.

Foley, N. M., Thong, V. D., Soisook, P., Goodman, S. M., Armstrong, K. N., Jacobs, D. S., … Teeling, E. C. (2015). How and why overcome the impediments to resolution: Lessons from rhinolophid and hipposiderid bats. *Molecular Biology and Evolution, 32*(2), 313–333.

Frey-Ehrenbold, A., Bontadina, F., Arlettaz, R., & Obrist, M. K. (2013). Landscape connectivity, habitat structure and activity of bat guilds in farmland-dominated matrices. *Journal of Applied Ecology, 50*(1), 252–261.

Frick, W. F., Baerwald, E. F., Pollock, J. F., Barclay, R. M. R., Szymanski, J. A., Weller, T. J., … McGuire, L. P. (2017). Fatalities at wind turbines may threaten population viability of a migratory bat. *Biological Conservation, 209*, 172–177.

Frick, W. F., Kingston, T., & Flanders, J. (2020). A review of the major threats and challenges to global bat conservation. *Annals of the New York Academy of Sciences, 1469*(1), 5–25.

Friedenberg, N. A., & Frick, W. F. (2021). Assessing fatality minimization for hoary bats amid continued wind energy development. *Biological Conservation, 262*, 109309.

Furlonger, C. L., Dewar, H. J., & Fenton, M. B. (1987). Habitat use by foraging insectivorous bats. *Canadian Journal of Zoology, 65*(2), 284–288.

Furman, A., Postawa, T., Öztunç, T., & Çoraman, E. (2010). Cryptic diversity of the bent-wing bat, *Miniopterus schreibersii* (Chiroptera: Vespertilionidae), in Asia Minor. *BMC Evolutionary Biology, 10*, 121.

Galtier, N., Nabholz, B., Glémin, S., & Hurst, G. D. D. (2009). Mitochondrial DNA as a marker of molecular diversity: A reappraisal. *Molecular Ecology, 18*(22), 4541–4550.

Ghanem, S. J., & Voigt, C. C. (2012). Increasing awareness of ecosystem services provided by bats. In *Advances in the Study of Behavior* (Vol. 44, pp. 279–302). Academic Press.

Goldenberg, S. Z., Cryan, P. M., Gorresen, P. M., & Fingersh, L. J. (2021). Behavioral patterns of bats at a wind turbine confirm seasonality of fatality risk. *Ecology and Evolution, 11*(9), 4843–4853.

Graham, C. H., Ron, S. R., Santos, J. C., Schneider, C. J., & Moritz, C. (2004). Integrating phylogenetics and environmental niche models to explore speciation mechanisms in dendrobatid frogs. *Evolution, 58*(8), 1781–1793.

Guest, E. E., Stamps, B. F., Durish, N. D., Hale, A. M., Hein, C. D., Morton, B. P., … Fritts, S. R. (2022). An updated review of hypotheses regarding bat attraction to wind turbines. *Animals, 12*(3), 343.

Guisan, A., Lehmann, A., Ferrier, S., Austin, M., Overton, J. M. C., Aspinall, R., & Hastie, T. (2006). Making better biogeographical predictions of species' distributions. *Journal of Applied Ecology, 43*(3), 386–392.

Hale, J. D., Fairbrass, A. J., Matthews, T. J., Davies, G., & Sadler, J. P. (2015). The ecological impact of city lighting scenarios: Exploring gap crossing thresholds for urban bats. *Global Change Biology, 21*(7), 2467–2478.

Hale, A. M., Hein, C. D., & Straw, B. R. (2021). Acoustic and genetic data can reduce uncertainty regarding populations of migratory tree-roosting bats impacted by wind energy. *Animals, 12*(1), 81.

Hallmann, C. A., Sorg, M., Jongejans, E., Siepel, H., Hofland, N., Schwan, H., … de Kroon, H. (2017). More than 75 percent decline over 27 years in total flying insect biomass in protected areas. *PLoS One, 12*(10), e0185809.

Hammond, R. L., Macasero, W., Flores, B., Mohammed, O. B., Wacher, T., & Bruford, M. W. (2001). Phylogenetic reanalysis of the Saudi gazelle and its implications for conservation. *Conservation Biology, 15*(4), 1123–1133.

Ritchie, H. (2022). *Living Planet Index: What does it really mean?* Our World in Data.

Häussler, U., Nagel, A., Braun, M., & Arnold, A. (2000). External characters discriminating sibling species of European pipistrelles, *Pipistrellus pipistrellus* and *P. pygmaeus*. *Myotis, 37*, 27–40.

Hegerl, G. C., Zwiers, F. W., Braconnot, P., Gillett, N. P., Luo, Y., Orsini, J. A. M., … Planton, S. (2007). *Understanding and attributing climate change*. Cambridge University Press.

Heim, O., Lorenz, L., Kramer-Schadt, S., Jung, K., Voigt, C. C., & Eccard, J. A. (2017). Landscape- and scale-dependent spatial niches of bats foraging above intensively used arable fields. *Ecological Processes, 6*, 24.

Hewitt, G. M. (1999). Post-glacial re-colonization of European biota. *Biological Journal of the Linnean Society, 68*(1–2), 87–112.

Hewitt, G. (2000). The genetic legacy of the Quaternary ice ages. *Nature, 405*(6789), 907–913.

Hijmans, R. J., Cameron, S. E., Parra, J. L., Jones, P. G., & Jarvis, A. (2005). Very high resolution interpolated climate surfaces for global land areas. *International Journal of Climatology, 25*(15), 1965–1978.

Hirzel, A. H., & Le Lay, G. (2008). Habitat suitability modelling and niche theory. *Journal of Applied Ecology, 45*(5), 1372–1381.

Ho, S. Y. W., Shapiro, B., Phillips, M. J., Cooper, A., & Drummond, A. J. (2007). Evidence for time dependency of molecular rate estimates. *Systematic Biology, 56*, 515–522.

Hodgkison, R., Balding, S. T., Zubaid, A., & Kunz, T. H. (2003). Fruit bats (*Chiroptera: Pteropodidae*) as seed dispersers and pollinators in a lowland Malaysian rainforest. *Biotropica, 35*(4), 491–502.

Hoffmann, M., Hilton-Taylor, C., Angulo, A., Böhm, M., Brooks, T. M., Butchart, S. H. M., … Veloso, A. (2010). The impact of conservation on the status of the world's vertebrates. *Science, 330*(6010), 1503–1509.

Hoffmann, A. A., & Sgrò, C. M. (2011). Climate change and evolutionary adaptation. *Nature, 470*(7335), 479–485.

Holderegger, R., & Wagner, H. H. (2008). Landscape genetics. *BioScience, 58*(3), 199–207.

Horáček, I., & Jahelková, H. (2005). History of the *Pipistrellus pipistrellus* group in Central Europe in light of its fossil record. *Acta Chiropterologica, 7*(2), 189–204.

Horn, J. W., Arnett, E. B., & Kunz, T. H. (2008). Behavioral responses of bats to operating wind turbines. *The Journal of Wildlife Management, 72*(1), 123–132.

Hosseinian Yousefkhani, S. S., Rastegar-Pouyani, E., & Aliabadian, M. (2016). Ecological niche differentiation and taxonomic distinction between *Eremias strauchi* subspecies on the Iranian Plateau. *Italian Journal of Zoology, 83*(3), 408–416.

Hudson, R. R. (1990). Gene genealogies and the coalescent process. *Oxford Surveys in Evolutionary Biology, 7*, 1–44.

Hulva, P., Benda, P., Hanák, V., Evin, A., & Horáček, I. (2007). New mitochondrial lineages within the *Pipistrellus pipistrellus* complex from Mediterranean Europe. *Folia Zoologica, 56*(4), 378–388.

Hulva, P., Fornůsková, A., Chudárková, A., Evin, A., Allegrini, B., Benda, P., & Bryja, J. (2010). Mechanisms of radiation in a bat group from the genus *Pipistrellus*. *Molecular Ecology, 19*(24), 5417–5431.

Hulva, P., Horáček, I., Strelkov, P. P., & Benda, P. (2004). Molecular architecture of the *Pipistrellus pipistrellus/P. pygmaeus* complex. *Molecular Phylogenetics and Evolution, 32*(3), 1023–1035.

Humphries, M. M., Thomas, D. W., & Speakman, J. R. (2002). Climate-mediated energetic constraints on the distribution of hibernating mammals. *Nature, 418*(6895), 313–316.

Hunter, C. M., Caswell, H., Runge, M. C., Regehr, E. V., Amstrup, S. C., & Stirling, I. (2010). Climate change threatens polar bear populations. *Ecology, 91*(10), 2883–2897.

Huso, M. M. P., & Hayes, J. P. (2009). *Effectiveness of changing wind turbine cut-in speed to reduce bat fatalities*. Unpublished report.

Huso, M., Conkling, T., Dalthorp, D., Davis, M., Smith, H., Fesnock, A., & Katzner, T. (2021). Relative energy production determines effect of repowering on wildlife mortality. *Journal of Applied Ecology, 58*(6), 1284–1290.

Husemann, M., Schmitt, T., Zachos, F. E., Ulrich, W., & Habel, J. C. (2014). Palaearctic biogeography revisited: Evidence for a North African refugium. *Journal of Biogeography, 41*(1), 81–94.

Jaarola, M., & Searle, J. B. (2002). Phylogeography of field voles (*Microtus agrestis*) in Eurasia inferred from mitochondrial DNA sequences. *Molecular Ecology, 11*(12), 2613–2621.

Jarvis, E. D., Mirarab, S., Aberer, A. J., Li, B., Houde, P., Li, C., … Zhang, G. (2014). Whole-genome analyses resolve early branches in the tree of life of modern birds. *Science, 346*(6215), 1320–1331.

Jones, G., & Teeling, E. C. (2006). The evolution of echolocation in bats. *Trends in Ecology & Evolution, 21*(3), 149–156.

Jones, G., Jacobs, D. S., Kunz, T. H., Willig, M. R., & Racey, P. A. (2009). *Carpe noctem*: The importance of bats as bioindicators. *Endangered Species Research, 8*(1–2), 93–115.

Jones, G., & Van Parijs, S. M. (1993). Bimodal echolocation in pipistrelle bats: Are cryptic species present? *Proceedings of the Royal Society of London. Series B: Biological Sciences, 251*(1331), 119–125.

Jones, K. R., Watson, J. E. M., Possingham, H. P., & Klein, C. J. (2016). Incorporating climate change into spatial conservation prioritisation: A review. *Biological Conservation, 194*, 121–130.

Johnson, G. D., Perlik, M. K., Erickson, W. P., & Strickland, M. D. (2004). Bat activity, composition, and collision mortality at a large wind plant in Minnesota. *Wildlife Society Bulletin, 32*(4), 1278–1288.

Jukes, T. H., & Cantor, C. R. (1969). Evolution of protein molecules. In *Mammalian protein metabolism* (Vol. 3, pp. 21–132). Academic Press.

Kerth, G., Mayer, F., & Petit, E. (2002). Extreme sex-biased dispersal in the communally breeding, nonmigratory Bechstein's bat (*Myotis bechsteinii*). *Molecular Ecology, 11*(8), 1491–1498.

Kiesecker, J. M., Evans, J. S., Fargione, J., Doherty, K., Foresman, K. R., Kunz, T. H., … Niemuth, N. D. (2011). Win-win for wind and wildlife: A vision to facilitate sustainable development. *PLoS One, 6*(4), e17566.

Knowles, L. L., & Maddison, W. P. (2002). Statistical phylogeography. *Molecular Ecology, 11*(12), 2623–2635.

Korner-Nievergelt, F., Brinkmann, R., Niermann, I., & Behr, O. (2013). Estimating bat and bird mortality occurring at wind energy turbines from covariates and carcass searches using mixture models. *PLoS One, 8*(7), e67997.

Kryštufek, B., & Vohralík, V. (2001). *Mammals of Turkey and Cyprus*. Zgodovinsko društvo za južno Primorsko.

Kunz, T. H., Arnett, E. B., Cooper, B. M., Erickson, W. P., Larkin, R. P., Mabee, T., … Szewczak, J. M. (2007a). Assessing impacts of wind-energy development on nocturnally active birds and bats: A guidance document. *The Journal of Wildlife Management, 71*, 2449–2486.

Kunz, T. H., Arnett, E. B., Erickson, W. P., Hoar, A. R., Johnson, G. D., Larkin, R. P., Strickland, M. D., Thresher, R. W., & Tuttle, M. D. (2007b). Ecological impacts of wind energy development on bats: Questions, research needs, and hypotheses. *Frontiers in Ecology and the Environment, 5*, 315–324.

Kunz, T. H., Braun de Torrez, E., Bauer, D., Lobova, T., & Fleming, T. H. (2011). Ecosystem services provided by bats. *Annals of the New York Academy of Sciences, 1223*(1), 1–38.

Kramer-Schadt, S., Niedballa, J., Pilgrim, J. D., Schröder, B., Lindenborn, J., Reinfelder, V., … Wilting, A. (2013). The importance of correcting for sampling bias in MaxEnt species distribution models. *Diversity and Distributions, 19*(11), 1366–1379.

Lagrange, H., Rico, P., Bas, Y., Ughetto, A. L., Melki, F., & Kerbiriou, C. (2013). Mitigating bat fatalities from wind-power plants through targeted curtailment: Results from four years of testing CHIROTECH©. *Book of Abstracts, Conference on Wind Energy (CWE)*, Stockholm.

Lausen, C. L., Lentini, P., Dulc, S., Rensel, L., Threlfall, C. G., de Freitas, E., & Kellner, M. (2023). Bat boxes as roosting habitat in urban centres: Thinking outside the box. In *Urban bats: Biology, ecology, and human dimensions* (pp. 75–93). Springer International Publishing.

Latch, E. K., Dharmarajan, G., Glaubitz, J. C., & Rhodes, O. E., Jr. (2006). Relative performance of Bayesian clustering software for inferring population substructure and individual assignment at low levels of population differentiation. *Conservation Genetics, 7*(2), 295–302.

Lehnert, L. S., Kramer-Schadt, S., Schönborn, S., Lindecke, O., Niermann, I., & Voigt, C. C. (2014). Wind farm facilities in Germany kill noctule bats from near and far. *PLoS One, 9*(8), e103106.

Leigh, J. W., Bryant, D., & Nakagawa, S. (2015). POPART: Full-feature software for haplotype network construction. *Methods in Ecology and Evolution, 6*(9), 1110–1116.

Lewis, R. E., & Harrison, D. L. (1962). Notes on bats from the Republic of Lebanon. *Proceedings of the Zoological Society of London, 138*(3), 473–486.

Liu, C., White, M., & Newell, G. (2013). Selecting thresholds for the prediction of species occurrence with presence-only data. *Journal of Biogeography, 40*(4), 778–789.

Long, C. V., Flint, J. A., & Lepper, P. A. (2011). Insect attraction to wind turbines: Does colour play a role? *European Journal of Wildlife Research, 57*, 323–331.

Mammal Diversity Database. (2025). *Mammal Diversity Database* (Version 1.12). American Society of Mammalogists. https://www.mammaldiversity.org

Măntoiu, D. Ş., Kravchenko, K., Lehnert, L. S., Vlaschenko, A., Moldovan, O. T., Mirea, I. C., … Voigt, C. C. (2020). Wildlife and infrastructure: Impact of wind turbines on bats in the Black Sea coast region. *European Journal of Wildlife Research, 66*(3), 1–13.

Mathews, F., Roche, N., Aughney, T., Jones, N., Day, J., Baker, J., & Langton, S. (2015). Barriers and benefits: Implications of artificial night-lighting for the distribution of common bats in Britain and Ireland. *Philosophical Transactions of the Royal Society B: Biological Sciences, 370*(1667), 20140124.

Mayer, F., & Helversen, O. V. (2001a). Sympatric distribution of two cryptic bat species across Europe. *Biological Journal of the Linnean Society, 74*(3), 365–374.

Mayer, F., & Helversen, O. V. (2001b). Cryptic diversity in European bats. *Proceedings of the Royal Society of London. Series B: Biological Sciences, 268*(1478), 1825–1832.

McMahon, C. R., & Burton, H. R. (2005). Climate change and seal survival: Evidence for environmentally mediated changes in elephant seal (*Mirounga leonina*) pup survival. *Proceedings of the Royal Society B: Biological Sciences, 272*(1566), 923–928.

Médail, F., & Diadema, K. (2009). Glacial refugia influence plant diversity patterns in the Mediterranean Basin. *Journal of Biogeography, 36*(7), 1333–1345.

Moritz, C. (1994). Defining “evolutionarily significant units” for conservation. *Trends in Ecology & Evolution, 9*(10), 373–375.

Nabholz, B., Glémin, S., & Galtier, N. (2008). Strong variations of mitochondrial mutation rate across mammals: The longevity hypothesis. *Molecular Biology and Evolution, 25*, 120–130.

Newbold, T., Hudson, L. N., Hill, S. L. L., Contu, S., Lysenko, I., Senior, R. A., … Purvis, A. (2015). Global effects of land use on local terrestrial biodiversity. *Nature, 520*(7545), 45–50.

Nogués-Bravo, D., Rodríguez-Sánchez, F., Orsini, L., de Boer, E., Jansson, R., Morlon, H., … Jackson, S. T. (2018). Cracking the code of biodiversity responses to past climate change. *Trends in Ecology & Evolution, 33*(10), 765–776.

Northrup, J. M., & Wittemyer, G. (2013). Characterising the impacts of emerging energy development on wildlife, with an eye towards mitigation. *Ecology Letters, 16*(1), 112–125.

Park, K. J., Altringham, J. D., & Jones, G. (1996). Assortative roosting in the two phonic types of *Pipistrellus pipistrellus* during the mating season. *Proceedings of the Royal Society of London. Series B: Biological Sciences, 263*(1376), 1495–1499.

Parmesan, C., & Yohe, G. (2003). A globally coherent fingerprint of climate change impacts across natural systems. *Nature, 421*(6918), 37–42.

Parsons, K. N., Jones, G., Davidson-Watts, I., & Greenaway, F. (2003). Swarming of bats at underground sites in Britain: Implications for conservation. *Biological Conservation, 111*(1), 63–70.

Pearson, R. G., & Dawson, T. P. (2003). Predicting the impacts of climate change on the distribution of species: Are bioclimate envelope models useful? *Global Ecology and Biogeography, 12*(5), 361–371.

Pereira, H. M., Leadley, P. W., Proença, V., Alkemade, R., Scharlemann, J. P. W., Fernandez-Manjarrés, J. F., … Walpole, M. (2010). Scenarios for global biodiversity in the 21st century. *Science, 330*(6010), 1496–1501.

Petersons, G. (2004). Seasonal migrations of north-eastern populations of Nathusius' pipistrelle *Pipistrellus nathusii* (Chiroptera). *Myotis, 41–42*, 29–56.

Petit, R. J., & Excoffier, L. (2009). Gene flow and species delimitation. *Trends in Ecology & Evolution, 24*(7), 386–393.

Petit, J. R., Jouzel, J., Raynaud, D., Barkov, N. I., Barnola, J. M., Basile, I., … Stievenard, M. (1999). Climate and atmospheric history of the past 420,000 years from the Vostok ice core, Antarctica. *Nature, 399*(6735), 429–436.

Phillips, S. J., Anderson, R. P., & Schapire, R. E. (2006). Maximum entropy modeling of species geographic distributions. *Ecological Modelling, 190*(3–4), 231–259.

Pierson, E. D. (1998). Tall trees, deep holes, and scarred landscapes: Conservation biology of North American bats. In T. H. Kunz & P. A. Racey (Eds.), *Bat biology and conservation* (pp. 309–325). Smithsonian Institution Press.

Pijanowski, B. C., Villanueva-Rivera, L. J., Dumyahn, S. L., Farina, A., Krause, B. L., Napoletano, B. M., … Pieretti, N. (2011). Soundscape ecology: The science of sound in the landscape. *BioScience, 61*(3), 203–216.

Piorkowski, M. D., Farnsworth, A. J., Fry, M., Rohrbaugh, R. W., Fitzpatrick, J. W., & Rosenberg, K. V. (2012). Research priorities for wind energy and migratory wildlife. *The Journal of Wildlife Management, 76*(3), 451–456.

Puechmaille, S. J., Gouilh, M. A., Piyapan, P., Yokubol, M., Mie, K. M., Bates, P. J. J., … Teeling, E. C. (2011). The evolution of sensory divergence in the context of limited gene flow in the bumblebee bat. *Nature Communications, 2*, 573.

Prugnolle, F., & De Meeûs, T. (2002). Inferring sex-biased dispersal from population genetic tools: A review. *Heredity, 88*(3), 161–165.

R Core Team. (2023). *R: A Language and Environment for Statistical Computing.* R Foundation for Statistical Computing, Vienna, Austria. Available online: https://www.R-project.org/ (accessed on 3 May 2023).

Ramasindrazana, B., Goodman, S. M., Schoeman, M. C., & Appleton, B. (2011). Identification of cryptic species of *Miniopterus* bats (Chiroptera: Miniopteridae) from Madagascar and the Comoros using bioacoustics overlaid on molecular genetic and morphological characters. *Biological Journal of the Linnean Society*, 104(2), 284–302.

Rambaut, A., Drummond, A. J., Xie, D., Baele, G., & Suchard, M. A. (2018). Posterior summarization in Bayesian phylogenetics using Tracer 1.7. *Systematic Biology*, 67(5), 901–904.

Ransome, R. D., & McOwat, T. P. (1994). Birth timing and population changes in greater horseshoe bat colonies (*Rhinolophus ferrumequinum*) are synchronized by climatic temperature. *Zoological Journal of the Linnean Society*, 112(3), 337–351.

Razgour, O., Hanmer, J., & Jones, G. (2011). Using multi-scale modelling to predict habitat suitability for species of conservation concern: the grey long-eared bat as a case study. *Biological Conservation*, 144(12), 2922–2930.

Rebelo, H., Tarroso, P., & Jones, G. (2010). Predicted impact of climate change on European bats in relation to their biogeographic patterns. *Global Change Biology*, 16, 561–576.

Richardson, S. M. (2016). *The effect of wind turbines on bats in Britain.* University of Exeter, United Kingdom.

Richardson, S. M., Lintott, P. R., Hosken, D. J., Economou, T., & Mathews, F. (2021). Peaks in bat activity at turbines and the implications for mitigating the impact of wind energy developments on bats. *Scientific Reports*, 11(1), 3636.

Rivers, N. M., Butlin, R. K., & Altringham, J. D. (2005). Genetic population structure of Natterer's bats explained by mating at swarming sites and philopatry. *Molecular Ecology*, 14(14), 4299–4312.

Rodrigues, L., Bach, L., Dubourg-Savage, M. J., Karapandža, B., Kovač, D., Kervyn, T., et al. (2015). *Guidelines for consideration of bats in wind farm projects: Revision 2014.* EUROBATS Publication Series No. 6. UNEP/EUROBATS Secretariat, Bonn, Germany.

Rollins, K. E., Meyerholz, D. K., Johnson, G. D., Capparella, A. P., & Loew, S. S. (2012). A forensic investigation into the etiology of bat mortality at a wind farm: barotrauma or traumatic injury? *Veterinary Pathology*, 49(2), 362–371.

Roman, J., Santhuff, S. D., Moler, P. E., & Bowen, B. W. (1999). Population structure and cryptic evolutionary units in the alligator snapping turtle. *Conservation Biology*, 13(1), 135–142.

Root, T. L., Price, J. T., Hall, K. R., Schneider, S. H., Rosenzweig, C., & Pounds, J. A. (2003). Fingerprints of global warming on wild animals and plants. *Nature*, 421(6918), 57–60.

Rossiter, S. J., Benda, P., Dietz, C., Zhang, S., & Jones, G. (2007). Rangewide phylogeography in the greater horseshoe bat inferred from microsatellites: implications for population history, taxonomy and conservation. *Molecular Ecology*, 16(22), 4699–4714.

Rozas, J., Ferrer-Mata, A., Sánchez-DelBarrio, J. C., Guirao-Rico, S., Librado, P., Ramos-Onsins, S. E., & Sánchez-Gracia, A. (2017). DnaSP 6: DNA sequence polymorphism analysis of large data sets. *Molecular Biology and Evolution*, 34(12), 3299–3302.

Ruedi, M., & Castella, V. (2003). Genetic consequences of the ice ages on nurseries of the bat *Myotis myotis*: a mitochondrial and nuclear survey. *Molecular Ecology*, 12(6), 1527–1540.

Russ, J. M., Briffa, M., & Montgomery, W. I. (2003). Seasonal patterns in activity and habitat use by bats (*Pipistrellus* spp. and *Nyctalus leisleri*) in Northern Ireland, determined using a driven transect. *Journal of Zoology*, 259(3), 289–299.

Russo, D., & Jones, G. (2003). Use of foraging habitats by bats in a Mediterranean area determined by acoustic surveys: conservation implications. *Ecography*, 26(2), 197–209.

Rydell, J., Bach, L., Dubourg-Savage, M. J., Green, M., Rodrigues, L., & Hedenström, A. (2010). Bat mortality at wind turbines in northwestern Europe. *Acta Chiropterologica*, 12(2), 261–274.

Rydell, J., Engström, H., Hedenström, A., Kyed Larsen, J., Pettersson, J., & Green, M. (2012). The effect of wind power on birds and bats: a synthesis. *Naturvårdsverket*.

Sachanowicz, K., & Ciechanowski, M. (2006). First winter record of the migratory bat *Pipistrellus nathusii* (Keyserling & Blasius, 1839) (Chiroptera: Vespertilionidae) in Poland: yet more evidence of global warming? *Mammalia*, 70(1–2), 113–116.

Saldaña-Vázquez, R. A., & Munguía-Rosas, M. A. (2013). Lunar phobia in bats and its ecological correlates: a meta-analysis. *Mammalian Biology*, 78(3), 216–219.

Salguero, M. D. M., De la Cruz, A., Muñoz, A. R., & Muñoz Arroyo, G. (2023). Bat mortality in wind farms of southern Europe: temporal patterns and implications in the current context of climate change. *Biodiversity and Conservation*, 32(12), 3953–3971.

Salicini, I., Ibáñez, C., & Juste, J. (2011). Multilocus phylogeny and species delimitation within the Natterer's bat species complex in the Western Palearctic. *Molecular Phylogenetics and Evolution*, 61(3), 888–898.

Scheel, D., Vincent, T. L. S., & Cameron, G. N. (1996). Global warming and the species richness of bats in Texas. *Conservation Biology*, 10(2), 452–464.

Schmitt, T. (2007). Molecular biogeography of Europe: Pleistocene cycles and postglacial trends. *Frontiers in Zoology*, 4, 11.

Schober, W., & Grimmberger, E. (1997). *The bats of Europe and North America.* London: TFH Publications.

Sherwin, H. A., Montgomery, W. I., & Lundy, M. G. (2013). The impact and implications of climate change for bats. *Mammal Review*, 43(3), 171–182.

Shin, Y. J., Midgley, G. F., Archer, E. R., Arneth, A., Barnes, D. K. A., Chan, L., et al. (2022). Actions to halt biodiversity loss generally benefit the climate. *Global Change Biology*, 28(9), 2846–2874.

Saitou, N., & Nei, M. (1987). The neighbor-joining method: a new method for reconstructing phylogenetic trees. *Molecular biology and evolution*, *4*(4), 406-425.

Slatkin, M. (1987). Gene flow and the geographic structure of natural populations. *Science*, 236(4803), 787–792.COPS

Soto-Centeno, J. A., O'Brien, M., & Simmons, N. B. (2015). The importance of late Quaternary climate change and karst on distributions of Caribbean mormoopid bats. *American Museum Novitates*, 3847, 1–32.

Speakman, J. R., Thomas, D. W., Kunz, T. H., & Fenton, M. B. (2003). Bat ecology. In *Physiological ecology and energetics of bats* (pp. 430–490). Chicago: University of Chicago Press.

Straka, T. M., Fritze, M., & Voigt, C. C. (2020). The human dimensions of a green–green dilemma: lessons learned from the wind energy–wildlife conflict in Germany. *Energy Reports*, 6, 1768–1777.

Tamura, K., Stecher, G., & Kumar, S. (2021). MEGA11: molecular evolutionary genetics analysis version 11. *Molecular Biology and Evolution*, 38(7), 3022–3027.

Thomas, C. D., Cameron, A., Green, R. E., Bakkenes, M., Beaumont, L. J., Collingham, Y. C., … & Williams, S. E. (2004). Extinction risk from climate change. *Nature*, 427(6970), 145–148.

Thompson, M., Beston, J. A., Etterson, M., Diffendorfer, J. E., & Loss, S. R. (2017). Factors associated with bat mortality at wind energy facilities in the United States. *Biological Conservation*, 215, 241–245.

Tougard, C., Renvoisé, E., Petitjean, A., & Quéré, J. P. (2008). New insight into the colonization processes of common voles: inferences from molecular and fossil evidence. *PLoS One*, 3(10), e3532.

Tsang, S. M., Cirranello, A. L., Bates, P. J., & Simmons, N. B. (2016). The roles of taxonomy and systematics in bat conservation. In *Bats in the Anthropocene: Conservation of bats in a changing world* (pp. 503–538). Springer, Cham.

Vaughan, N., Jones, G., & Harris, S. (1997a). Habitat use by bats (Chiroptera) assessed by means of a broad-band acoustic method. *Journal of Applied Ecology*, 716–730.

Vaughan, N., Jones, G., & Harris, S. (1997b). Identification of British bat species by multivariate analysis of echolocation call parameters. *Bioacoustics*, 7(3), 189–207.

Vasko, V., Blomberg, A. S., Vesterinen, E. J., Suominen, K. M., Ruokolainen, L., Brommer, J. E., … & Lilley, T. M. (2020). Within-season changes in habitat use of forest-dwelling boreal bats. *Ecology and Evolution*, 10(9), 4164–4174.

Verboom, B., & Huitema, H. (1997). The importance of linear landscape elements for the pipistrelle *Pipistrellus pipistrellus* and the serotine bat *Eptesicus serotinus*. *Landscape Ecology*, 12(2), 117–125.

Voigt, C. C., Sörgel, K., & Dechmann, D. K. (2010). Refueling while flying: foraging bats combust food rapidly and directly to power flight. *Ecology*, 91(10), 2908–2917.

Voigt, C. C., Lehnert, L. S., Petersons, G., Adorf, F., & Bach, L. (2015). Wildlife and renewable energy: German politics cross migratory bats. *European Journal of Wildlife Research*, 61(2), 213–219.

Voigt, C. C., Lindecke, O., Schönborn, S., Kramer-Schadt, S., & Lehmann, D. (2016). Habitat use of migratory bats killed during autumn at wind turbines. *Ecological Applications*, 26(3), 771–78

Wakeley, J., & Sargsyan, O. (2009). Extensions of the coalescent effective population size. *Genetics*, 181(1), 341–345.

Walsh, A. L., & Harris, S. (1996a). Foraging habitat preferences of vespertilionid bats in Britain. *Journal of Applied Ecology*, 508–518.

Walsh, A. L., & Harris, S. (1996b). Factors determining the abundance of vespertilionid bats in Britain: geographical, land class and local habitat relationships. *Journal of Applied Ecology*, 519–529.

Walther, G. R., Post, E., Convey, P., Menzel, A., Parmesan, C., Beebee, T. J., … & Bairlein, F. (2002). Ecological responses to recent climate change. *Nature*, 416(6879), 389–395.

Warren, D. L., Glor, R. E., & Turelli, M. (2010). ENMTools: a toolbox for comparative studies of environmental niche models. *Ecography*, 33(3), 607–611.

Wellig, S. D., Nusslé, S., Miltner, D., Kohle, O., Glaizot, O., Braunisch, V., … & Arlettaz, R. (2018). Mitigating the negative impacts of tall wind turbines on bats: Vertical activity profiles and relationships to wind speed. *PLOS One*, 13(3), e0192493.

Williams-Guillén, K., Perfecto, I., & Vandermeer, J. (2008). Bats limit insects in a neotropical agroforestry system. *Science*, 320(5872), 70–70.

Yalden, D. W., & Morris, P. A. (1975). *Lives of bats*. David & Charles.

Yapa, W. B. (2017). First record of a wrinkle-lipped free-tailed bat *Chaerephon plicatus* Buchannan, 1800 (Mammalia: Chiroptera: Molossidae) colony in Sri Lanka, with notes on echolocation calls and taxonomy. *Journal of Threatened Taxa*, 9(4), 10115–10120.

Zizka, A., Silvestro, D., Andermann, T., Azevedo, J., Duarte Ritter, C., Edler, D., … & Antonelli, A. (2019). CoordinateCleaner: Standardized cleaning of occurrence records from biological collection databases. *Methods in Ecology and Evolution*, 10(5), 744–751.

APPENDIX A: INFORMATION ON THE SAMPLES OF THE STUDY

Table A.1. Summary of sample origin, geographic information (country and/or city), sample type, and ownership information for specimens used in Chapter 1.

Samples source	Country (and cities)	Number of samples	Sample type	Rights Holders
Petr Benda (77 samples)	Albania	4	Internal organ: pectoral muscle	P. Benda, F.Spitzenberger, M.Uhrin & E.Weib
	Bosnia and Herzegovina	1	Internal organ: pectoral muscle	M.Kusbesova
	Bulgaria	1	Internal organ: pectoral muscle	P.Benda
	Czech Republic	4	Internal organ: pectoral muscle	M.Vlasin & P. Lachman
	Greece	4	Internal organ: pectoral muscle	M.Andreas, P.Benda & M.Uhrin
	Iran	10	Internal organ: pectoral muscle	M.Andreas, P.Benda, A. Reiter & M.Uhrin
	Jordan	9	Internal organ: pectoral muscle	P.Benda, J.Obuch & A. Reiter
	Lebanon	18	Internal organ: pectoral muscle	I.Horacek, P.Hulva, R.lucan, P.Nemec, P. Benda, M.Uhrin & T.Bartonicka
	Morocco	6	Internal organ: pectoral muscle	P. Benda, J.Cerveny, A.Konochy, A. Reiter, M.Sevcik & M.Uhrin
	Romania	1	Internal organ: pectoral muscle	NA
	Slovakia	6	Internal organ: pectoral muscle	P. Benda
	Syria	1	Internal organ: pectoral muscle	M.Andreas, P.Benda, A. Reiter & M.weinfurtova
	Tajikistan	7	Internal organ: pectoral muscle	P.Benda , A. Reiter & M.Uhrin
	Ukraine	4	Internal organ: pectoral muscle	NA

Samples source	Country (and cities)	Number of samples	Sample type	Rights Holders
KAB Ecology (143 samples)	Balikesir /Türkiye	2	Internal organ (not specified)	KAB Ecology
	Bursa/ Türkiye	3	Internal organ (not specified)	KAB Ecology
	Izmir/ Türkiye	10	Internal organ (not specified)	KAB Ecology
	Vize / Türkiye	30	Wings	KAB Ecology
	Tekirdag / Türkiye	9	Internal organ (not specified) and/or wings	KAB Ecology
	Mersin/ Türkiye	1	Internal organ (not specified)	KAB Ecology
	Çanakkale/ Türkiye	31	Internal organ (not specified)	KAB Ecology
	Istanbul/Türkiye	47	Internal organ (not specified)	KAB Ecology
	Yalova/Türkiye	10	Internal organ (not specified)	KAB Ecology
Tarkan Yorulmaz (33 samples)	Adana/ Türkiye	2	Buccal swab specimens	Tarkan Yorulmaz
	Diyarbakır /Türkiye	1	Buccal swab specimens	Tarkan Yorulmaz
	Şanlıurfa /Türkiye	4	Buccal swab specimens	Tarkan Yorulmaz
	Manisa/Türkiye	2	Buccal swab specimens	Tarkan Yorulmaz
	Izmir/ Türkiye	2	Buccal swab specimens	Tarkan Yorulmaz
	Yozgat /Türkiye	2	Buccal swab specimens	Tarkan Yorulmaz
	Kocaeli /Türkiye	2	Buccal swab specimens	Tarkan Yorulmaz
	Yalova/Türkiye	1	Buccal swab specimens	Tarkan Yorulmaz
	Bursa/Türkiye	2	Buccal swab specimens	Tarkan Yorulmaz
	Edirne/ Türkiye	3	Buccal swab specimens	Tarkan Yorulmaz
	Antalya/ Türkiye	5	Buccal swab specimens	Tarkan Yorulmaz
	Hamitköyü /Türkiye	2	Buccal swab specimens	Tarkan Yorulmaz
	Artvin / Türkiye	1	Buccal swab specimens	Tarkan Yorulmaz
	Van/ Türkiye	1	Buccal swab specimens	Tarkan Yorulmaz
	Hakkâri / Türkiye	1	Buccal swab specimens	Tarkan Yorulmaz
	Kastamonu/ Türkiye	2	Buccal swab specimens	Tarkan Yorulmaz

Table A.2. Geographic and clade-based summary of mtDNA haplotypes identified in the haplotype network.

Clade	Sample name	Longitude	Latitude	mtDNA Haplotypes	Geographic region
Anatolia	Izmir_308	27.501	38.335	Hap_12	Anatolia
Anatolia	Izmir_318	27.501	38.335	Hap_12	Anatolia
Anatolia	Kapadokia_6125	35.810	37.450	Hap_13	Anatolia
Anatolia	Manisa_23	27.179	38.150	Hap_14	Anatolia
Anatolia	Manisa_27	27.179	38.150	Hap_14	Anatolia
Anatolia	Bursa_713	28.156	40.375	Hap_15	Anatolia
Anatolia	Yalova_703	29.270	40.555	Hap_15	Anatolia
Anatolia	Çanakkale_611	27.438	39.795	Hap_16	Anatolia
Anatolia	Tekirdag_866	27.130	40.670	Hap_17	European Türkiye
Anatolia	Izmir_309	27.501	38.335	Hap_18	Anatolia
Anatolia	Tayakadin_622	28.058	41.673	Hap_19	European Türkiye
Anatolia	Bandirma_106	28.532	40.347	Hap_20	Anatolia
Anatolia	Bandirma_115	28.532	40.347	Hap_20	Anatolia
Anatolia	Bandirma_118	28.532	40.347	Hap_20	Anatolia
Anatolia	Bursa_215	28.156	40.375	Hap_20	Anatolia
Anatolia	Yalova_717	29.270	40.555	Hap_20	Anatolia
Anatolia	Tayakadin_617	28.058	41.672	Hap_20	European Türkiye
Anatolia	Izmir_731	27.501	38.335	Hap_21	Anatolia
Anatolia	Greece_23	28.001	36.260	Hap_22	Southern Europe
Anatolia	Greece_6076	26.400	38.967	Hap_23	Southern Europe
Anatolia	Izmir_305	27.501	38.335	Hap_24	Anatolia
Anatolia	Izmir_307	27.501	38.335	Hap_25	Anatolia
Anatolia	Çanakkale_305	27.438	39.794	Hap_26	Anatolia
Anatolia	Izmir_300	27.501	38.335	Hap_27	Anatolia
Anatolia	Bursa_726	28.156	40.375	Hap_28	Anatolia
Anatolia	Izmir_29	27.501	38.335	Hap_29	Anatolia

Clade	Sample name	Longitude	Latitude	mtDNA Haplotypes	Geographic region
Anatolia	Izmir_32	27.501	38.335	Hap_29	Anatolia
Anatolia	Izmir_730	27.501	38.335	Hap_29	Anatolia
Anatolia	Yozgat_30	39.830	37.119	Hap_30	Anatolia
Anatolia	Çanakkale_320	27.438	39.795	Hap_31	Anatolia
Anatolia	Çanakkale_602	27.438	39.795	Hap_32	Anatolia
Anatolia	Bursa_208	28.156	40.375	Hap_33	Anatolia
Anatolia	Antalya_5	33.258	36.915	Hap_34	Anatolia
Anatolia	Bursa_714	28.156	40.375	Hap_34	Anatolia
Anatolia	Çanakkale_312	27.439	39.795	Hap_34	Anatolia
Anatolia	Çanakkale_624	27.439	39.795	Hap_34	Anatolia
Anatolia	Kapadokia_6126	34.850	38.583	Hap_35	Anatolia
Anatolia	Yozgat_11	39.830	37.120	Hap_35	Anatolia
Anatolia	Yozgat_14	39.830	37.120	Hap_35	Anatolia
Anatolia	Çanakkale_302	27.439	39.795	Hap_36	Anatolia
Anatolia	Yozgat_08	39.830	37.120	Hap_37	Anatolia
British Isles	Italy_273578	14.460	41.700	Hap_127	Southern Europe
British Isles	England_273522	-1.450	53.470	Hap_128	British Isles
British Isles	Italy_273581	9.500	45.480	Hap_129	Southern Europe
British Isles	England_273514	-1.250	53.140	Hap_130	British Isles
British Isles	England_273520	0.120	51.500	Hap_131	British Isles
British Isles	England_273528	-1.700	50.470	Hap_132	British Isles
British Isles	Ireland_273531	-6.250	53.300	Hap_133	British Isles
British Isles	Ireland_273572	-6.250	53.300	Hap_133	British Isles
British Isles	Italy_273579	8.490	45.490	Hap_134	Southern Europe
British Isles	England_273519	0.800	51.480	Hap_136	British Isles
British Isles	England_273516	-1.640	46.980	Hap_137	British Isles

Clade	Sample name	Longitude	Latitude	mtDNA Haplotypes	Geographic region
British Isles	England_273529	-3.410	50.390	Hap_137	British Isles
British Isles	England_273530	-2.370	53.320	Hap_137	British Isles
British Isles	England_273515	-0.450	52.200	Hap_138	British Isles
British Isles	England_273517	-6.250	53.300	Hap_139	British Isles
British Isles	Ireland_273569	-6.250	53.300	Hap_139	British Isles
British Isles	England_273527	0.500	53.200	Hap_140	British Isles
British Isles	England_273523	-1.250	52.490	Hap_141	British Isles
British Isles	England_273525	-0.900	52.470	Hap_142	British Isles
British Isles	England_273518	-2.690	47.580	Hap_143	British Isles
British Isles	Ireland_273534	-6.250	53.300	Hap_143	British Isles
British Isles	Ireland_273506	-6.250	53.300	Hap_144	British Isles
British Isles	Ireland_273507	-7.120	53.510	Hap_144	British Isles
British Isles	Ireland_273508	-7.210	53.590	Hap_144	British Isles
British Isles	Ireland_273532	-6.150	52.580	Hap_144	British Isles
British Isles	Ireland_273533	-6.190	52.510	Hap_144	British Isles
British Isles	Ireland_273535	-6.250	53.300	Hap_144	British Isles
British Isles	Ireland_273536	-6.160	53.280	Hap_144	British Isles
British Isles	Ireland_273570	-6.250	53.300	Hap_144	British Isles
British Isles	Northern Ireland_273537	-5.540	54.340	Hap_144	British Isles
British Isles	France_273543	-1.640	46.980	Hap_143	Western Europe
British Isles	France_273544	-1.640	46.980	Hap_137	Western Europe
British Isles	France_273551	-1.640	46.980	Hap_143	Western Europe
British Isles	France_273561	-2.690	47.580	Hap_143	Western Europe
British Isles	France_273567	2.750	44.810	Hap_135	Western Europe

Clade	Sample name	Longitude	Latitude	mtDNA Haplotypes	Geographic region
Central Asia	Iran_6078	60.633	36.317	Hap_121	Middle East
Central Asia	Tajikistan_3	68.467	37.350	Hap_122	Central Asia
Central Asia	Iran_6080	55.983	37.367	Hap_123	Middle East
Central Asia	Tajikistan_2	68.467	37.350	Hap_124	Central Asia
Central Asia	Turkmenistan_38	58.090	38.099	Hap_125	Central Asia
Central Asia	Turkmenistan_24	58.080	38.098	Hap_126	Central Asia
Central Asia	Turkmenistan_26	58.085	38.095	Hap_126	Central Asia
Eastern Europe	Russia_6097	39.800	43.550	Hap_59	Eastern Europe
Eastern Europe	Russia_6093	40.000	45.533	Hap_60	Eastern Europe
Eastern Europe	Russia_6094	40.000	45.533	Hap_60	Eastern Europe
Eastern Europe	Iran_6052	55.983	37.367	Hap_61	Middle East
Eastern Europe	Russia_6098	40.283	43.667	Hap_62	Eastern Europe
Eastern Europe	Russia_6089	40.283	43.667	Hap_63	Eastern Europe
Eastern Europe	Russia_6092	40.000	45.533	Hap_64	Eastern Europe
Eastern Europe	Ukraine_76	34.983	44.983	Hap_65	Eastern Europe
Eastern Europe	Russia_6100	38.500	44.767	Hap_66	Eastern Europe
Eastern Europe	Ukraine_74	33.900	44.500	Hap_67	Eastern Europe
Eastern Europe	Ukraine_77	33.900	44.500	Hap_67	Eastern Europe
Eastern Europe	Russia_6090	40.000	45.533	Hap_68	Eastern Europe
Eastern Europe	Russia_6099	38.500	44.767	Hap_69	Eastern Europe
Eastern Europe	Russia_6096	39.800	43.550	Hap_70	Eastern Europe
Eastern Europe	Russia_6091	40.000	45.533	Hap_71	Eastern Europe
Eastern Europe	Ukraine_75	35.217	44.950	Hap_71	Eastern Europe
Middle East	Jordan_12	35.383	30.200	Hap_10	Middle East
Middle East	Jordan_13	35.516	30.616	Hap_10	Middle East
Middle East	Jordan_15	35.700	31.160	Hap_11	Middle East

Clade	Sample name	Longitude	Latitude	mtDNA Haplotypes	Geographic region
Middle East	Iran_6077	54.350	31.817	Hap_40	Middle East
Middle East	Jordan_48	35.550	30.560	Hap_41	Middle East
Middle East	Russia_6095	39.800	43.550	Hap_42	Eastern Europe
Middle East	Syria_6121	36.533	33.850	Hap_43	Middle East
Middle East	Syria_6122	36.533	33.850	Hap_44	Middle East
Middle East	Jordan_55	35.730	31.550	Hap_45	Middle East
Middle East	Syria_6116	36.183	33.833	Hap_45	Middle East
Middle East	Syria_6117	36.183	33.833	Hap_46	Middle East
Middle East	Cyprus_6086	32.867	34.917	Hap_47	Middle East
Middle East	Cyprus_6087	32.867	34.917	Hap_48	Middle East
Middle East	Lebanon_57	35.860	34.160	Hap_49	Middle East
Middle East	Lebanon_6081	35.900	34.067	Hap_49	Middle East
Middle East	Kapadokia_6123	34.850	38.583	Hap_50	Anatolia
Middle East	Kapadokia_6124	35.810	37.450	Hap_51	Anatolia
Middle East	Lebanon_11	35.800	33.900	Hap_52	Middle East
Middle East	Lebanon_41	35.470	33.690	Hap_52	Middle East
Middle East	Lebanon_58	35.816	34.000	Hap_52	Middle East
Middle East	Lebanon_6085	36.017	34.267	Hap_52	Middle East
Middle East	Lebanon_6082	35.917	34.117	Hap_53	Middle East
Middle East	Lebanon_44	35.130	34.000	Hap_54	Middle East
Middle East	Lebanon_6083	35.467	33.700	Hap_54	Middle East
Middle East	Lebanon_30	36.000	34.400	Hap_55	Middle East
Middle East	Lebanon_31	35.883	34.001	Hap_56	Middle East
Middle East	Lebanon_1	35.950	34.250	Hap_57	Middle East
Middle East	Lebanon_6084	35.600	33.550	Hap_58	Middle East
Middle East	Akbez	36.517	36.850	Hap_7	Anatolia
Middle East	Syria_6118	36.217	35.600	Hap_8	Middle East
Middle East	Syria_6120	36.217	35.600	Hap_8	Middle East
Middle East	Syria_6119	36.217	35.600	Hap_9	Middle East

Clade	Sample name	Longitude	Latitude	mtDNA Haplotypes	Geographic region
Mixed Cluster	Albania_27	20.550	40.750	Hap_100	Southern Europe
Mixed Cluster	Slovakia_6101	22.350	49.100	Hap_101	Central Europe
Mixed Cluster	Slovakia_6110	17.350	48.433	Hap_102	Central Europe
Mixed Cluster	CzechRepublic_6063	14.667	48.667	Hap_103	Central Europe
Mixed Cluster	CzechRepublic_6128	15.900	48.833	Hap_103	Central Europe
Mixed Cluster	GermanyandSlovakia_6068	17.350	48.433	Hap_103	Central Europe
Mixed Cluster	Türkiye (Kıyıköy)_29	28.050	41.670	Hap_103	European Türkiye
Mixed Cluster	Türkiye (Kıyıköy)_590	28.050	41.670	Hap_103	European Türkiye
Mixed Cluster	CzechRepublic_6064	14.667	48.667	Hap_104	Central Europe
Mixed Cluster	Greece_273554	21.000	40.770	Hap_105	Southern Europe
Mixed Cluster	Albania_4	19.983	40.002	Hap_106	Southern Europe
Mixed Cluster	Albania_5	19.550	40.250	Hap_106	Southern Europe
Mixed Cluster	Türkiye (Yalova)_38	29.013	40.560	Hap_107	Anatolia
Mixed Cluster	Türkiye (Yalova)_701	29.013	40.560	Hap_107	Anatolia
Mixed Cluster	Türkiye (Tayakadın)_627	28.180	41.370	Hap_108	European Türkiye
Mixed Cluster	Türkiye (Tayakadın)_654	28.180	41.370	Hap_109	European Türkiye
Mixed Cluster	Türkiye (Tayakadın)_647	28.180	41.370	Hap_110	European Türkiye
Mixed Cluster	Germany_6069	14.267	51.417	Hap_111	Central Europe
Mixed Cluster	Türkiye ((Bursa)_43	28.530	40.347	Hap_112	Anatolia
Mixed Cluster	Türkiye (Bursa)_712	28.530	40.347	Hap_112	Anatolia
Mixed Cluster	CzechRepublic_6065	13.383	49.633	Hap_113	Central Europe
Mixed Cluster	Poland_6088	16.867	50.583	Hap_114	Central Europe

Clade	Sample name	Longitude	Latitude	mtDNA Haplotypes	Geographic region
Mixed Cluster	Slovakia_6102	22.350	49.100	Hap_115	Central Europe
Mixed Cluster	Slovakia_6108	21.517	48.617	Hap_116	Central Europe
Mixed Cluster	Slovakia_6111	17.350	48.433	Hap_117	Central Europe
Mixed Cluster	Türkiye (Çanakkale)_319	27.441	39.797	Hap_118	Anatolia
Mixed Cluster	Türkiye (Çanakkale)_327	27.441	39.797	Hap_118	Anatolia
Mixed Cluster	Türkiye (Çanakkale)_612	27.441	39.797	Hap_119	Anatolia
Mixed Cluster	Lebanon_50	36.001	33.850	Hap_120	Middle East
Mixed Cluster	Türkiye (Kıyıköy)_416	28.050	41.670	Hap_120	European Türkiye
Mixed Cluster	Türkiye (Kıyıköy)_420	28.050	41.670	Hap_120	European Türkiye
Mixed Cluster	Türkiye (Kıyıköy)_422	28.050	41.670	Hap_120	European Türkiye
Mixed Cluster	Türkiye (Kıyıköy)_523	28.050	41.670	Hap_120	European Türkiye
Mixed Cluster	Türkiye (Tayakadın)_619	28.180	41.370	Hap_120	European Türkiye
Mixed Cluster	Türkiye (Tayakadın)_629	28.180	41.370	Hap_120	European Türkiye
Mixed Cluster	Türkiye (Tayakadın)_630	28.180	41.370	Hap_120	European Türkiye
Mixed Cluster	Türkiye (Tayakadın)_632	28.180	41.370	Hap_120	European Türkiye
Mixed Cluster	Türkiye (Tayakadın)_637	28.180	41.370	Hap_120	European Türkiye
Mixed Cluster	Türkiye (Tayakadin)_646	28.180	41.370	Hap_120	European Türkiye
Mixed Cluster	Türkiye (Tekirdağ)_871	27.130	40.670	Hap_120	European Türkiye

Clade	Sample name	Longitude	Latitude	mtDNA Haplotypes	Geographic region
Mixed Cluster	CzechRepublic_67	17.003	49.500	Hap_120	Central Europe
Mixed Cluster	Slovakia_66	19.270	48.320	Hap_120	Central Europe
Mixed Cluster	SlovakiaandCzechRepublic_6062	15.400	50.550	Hap_120	Central Europe
Mixed Cluster	Iran_51	58.467	37.483	Hap_126	Middle East
Mixed Cluster	Iran_6079	58.467	37.483	Hap_126	Middle East
Mixed Cluster	France_273542	-1.640	46.980	Hap_165	Western Europe
Mixed Cluster	Italy_273577	10.120	45.320	Hap_76	Southern Europe
Mixed Cluster	Italy_273580	10.120	45.320	Hap_76	Southern Europe
Mixed Cluster	Slovakia_6103	22.350	49.100	Hap_77	Central Europe
Mixed Cluster	CzechRepublic_6059	16.133	49.117	Hap_78	Central Europe
Mixed Cluster	CzechRepublic_6060	16.133	49.117	Hap_79	Central Europe
Mixed Cluster	Slovakia_6104	22.350	49.100	Hap_80	Central Europe
Mixed Cluster	Türkiye (Yalova)_711	29.013	40.560	Hap_81	Anatolia
Mixed Cluster	Romania_73	26.830	45.630	Hap_82	Eastern Europe
Mixed Cluster	Greece_273557	21.000	40.770	Hap_83	Southern Europe
Mixed Cluster	Greece_6070	21.067	40.783	Hap_83	Southern Europe
Mixed Cluster	Slovakia_6109	17.350	48.433	Hap_84	Central Europe
Mixed Cluster	Türkiye (Bandırma)_109	26.770	40.074	Hap_85	Anatolia
Mixed Cluster	Türkiye (Bursa)_213	28.530	40.347	Hap_85	Anatolia
Mixed Cluster	Türkiye (Çanakkale)_313	27.441	39.797	Hap_86	Anatolia
Mixed Cluster	Türkiye (Tayakadın)_620	28.180	41.370	Hap_87	European Türkiye
Mixed Cluster	Türkiye (Bursa)_719	28.530	40.347	Hap_88	Anatolia

Clade	Sample name	Longitude	Latitude	mtDNA Haplotypes	Geographic region
Mixed Cluster	Albania_46	19.860	40.001	Hap_89	Southern Europe
Mixed Cluster	Greece_6072	23.617	41.133	Hap_89	Southern Europe
Mixed Cluster	Tajikistan_20	68.500	37.430	Hap_90	Central Asia
Mixed Cluster	Greece_273556	21.000	40.770	Hap_91	Southern Europe
Mixed Cluster	GermanyandCzechRepublicandPoland_6067	15.400	50.550	Hap_92	Central Europe
Mixed Cluster	Türkiye (Edirne)_49	26.258	40.640	Hap_93	European Türkiye
Mixed Cluster	Türkiye (Edirne)_51	26.258	40.640	Hap_93	European Türkiye
Mixed Cluster	Türkiye (Edirne)_52	26.258	40.640	Hap_93	European Türkiye
Mixed Cluster	Türkiye (Edirne)_54	26.258	40.640	Hap_93	European Türkiye
Mixed Cluster	Türkiye (Edirne)_55	26.258	40.640	Hap_93	European Türkiye
Mixed Cluster	Slovakia_6106	21.517	48.617	Hap_94	Central Europe
Mixed Cluster	Türkiye (Çanakkale)_301	27.441	39.797	Hap_94	Anatolia
Mixed Cluster	Türkiye (Çanakkale)_625	27.441	39.797	Hap_94	Anatolia
Mixed Cluster	Türkiye (Yalova)_714	29.013	40.560	Hap_94	Anatolia
Mixed Cluster	Türkiye (Tekirdağ)_878	27.130	40.670	Hap_94	European Türkiye
Mixed Cluster	Türkiye (Tekirdağ)_856	27.130	40.670	Hap_94	European Türkiye
Mixed Cluster	Slovakia_6105	21.517	48.617	Hap_95	Central Europe
Mixed Cluster	Türkiye (Çanakkale)_315	27.441	39.797	Hap_95	Anatolia
Mixed Cluster	Slovakia_6107	21.517	48.617	Hap_96	Central Europe
Mixed Cluster	GermanyandCzechRepublic_6061	16.133	49.117	Hap_97	Central Europe

Clade	Sample name	Longitude	Latitude	mtDNA Haplotypes	Geographic region
Mixed Cluster	Slovakia_71	17.110	46.550	Hap_98	Central Europe
Mixed Cluster	Slovakia_72	17.110	46.550	Hap_98	Central Europe
Mixed Cluster	CzechRepublic_6066	13.383	49.633	Hap_99	Central Europe
Non clustered	Northern Ireland_273505	-5.550	54.340	Hap_1	British Isles
Non clustered	Spain_6113	-6.283	36.517	Hap_38	Western Europe
Non clustered	Spain_6114	-6.283	36.517	Hap_39	Western Europe
Non clustered	Greece_273555	21.000	40.770	Hap_72	Southern Europe
Non clustered	Greece_6071	21.067	40.783	Hap_72	Southern Europe
Non clustered	Greece_6074	22.583	38.483	Hap_73	Southern Europe
Non clustered	Greece_6075	22.583	38.483	Hap_74	Southern Europe
Non clustered	Greece_6073	22.583	38.483	Hap_75	Southern Europe
North Africa 1	Algeria_6057	4.117	36.433	Hap_2	North Africa 1
North Africa 1	Morocco_6053	-5.233	33.033	Hap_3	North Africa 1
North Africa 1	Morocco_6055	-5.233	33.033	Hap_4	North Africa 1
North Africa 1	Tunisia_6058	10.133	36.383	Hap_5	North Africa 1
North Africa 1	Morocco_6054	-5.233	33.033	Hap_6	North Africa 1
North Africa 2	Morocco_6051	-5.933	31.517	Hap_173	North Africa 2
North Africa 2	Morocco_56	-5.230	33.001	Hap_174	North Africa 2
North Africa 2	Morocco_6050	-5.233	33.033	Hap_174	North Africa 2
North Africa 2	Morocco_6056	-5.233	33.033	Hap_175	North Africa 2
Southern Europe	Malta	14.383	35.883	Hap_170	Southern Europe
Southern Europe	Sicily	13.940	37.780	Hap_171	Southern Europe
Southern Europe	Corsica	8.900	41.983	Hap_172	Southern Europe
Western Europe	France_273538	-2.450	47.510	Hap_157	Western Europe

Clade	Sample name	Longitude	Latitude	mtDNA Haplotypes	Geographic region
Western Europe	France_273539	-2.450	47.510	Hap_156	Western Europe
Western Europe	France_273540	-2.450	47.510	Hap_157	Western Europe
Western Europe	France_273541	-2.450	47.510	Hap_157	Western Europe
Western Europe	France_273545	-1.640	46.980	Hap_157	Western Europe
Western Europe	France_273546	-1.690	46.980	Hap_166	Western Europe
Western Europe	France_273547	-1.690	46.980	Hap_152	Western Europe
Western Europe	France_273548	-2.450	47.510	Hap_157	Western Europe
Western Europe	France_273549	2.190	43.410	Hap_158	Western Europe
Western Europe	France_273550	2.190	43.410	Hap_145	Western Europe
Western Europe	France_273552	2.190	43.410	Hap_153	Western Europe
Western Europe	France_273553	2.190	43.410	Hap_162	Western Europe
Western Europe	France_273558	2.750	44.490	Hap_161	Western Europe
Western Europe	France_273559	2.750	44.810	Hap_154	Western Europe
Western Europe	England_273524	2.800	44.780	Hap_157	British Isles
Western Europe	France_273560	2.750	44.810	Hap_157	Western Europe
Western Europe	France_273562	2.800	44.780	Hap_157	Western Europe
Western Europe	France_273563	2.750	44.810	Hap_155	Western Europe
Western Europe	France_273564	2.750	44.810	Hap_157	Western Europe
Western Europe	France_273565	2.750	44.810	Hap_160	Western Europe
Western Europe	France_273566	2.750	44.810	Hap_154	Western Europe
Western Europe	France_273568	2.750	44.810	Hap_167	Western Europe
Western Europe	France_273571	2.760	44.790	Hap_159	Western Europe
Western Europe	France_273573	2.800	44.780	Hap_163	Western Europe
Western Europe	France_273574	2.800	44.780	Hap_159	Western Europe

Clade	Sample name	Longitude	Latitude	mtDNA Haplotypes	Geographic region
Western Europe	France_273575	2.760	44.790	Hap_159	Western Europe
Western Europe	France_273576	4.700	43.600	Hap_168	Western Europe
Western Europe	Portugal_273509	-8.900	40.350	Hap_151	Western Europe
Western Europe	Portugal_273510	-8.900	40.350	Hap_149	Western Europe
Western Europe	England_273521	-0.270	52.800	Hap_164	British Isles
Western Europe	England_273526	-0.270	52.800	Hap_164	British Isles
Western Europe	Portugal_273512	-8.900	40.350	Hap_147	Western Europe
Western Europe	Portugal_273513	-8.900	40.350	Hap_150	Western Europe
Western Europe	Portugal_273514	-8.900	40.350	Hap_149	Western Europe
Western Europe	Spain_6112	-2.450	42.467	Hap_148	Western Europe
Western Europe	Switzerland_6115	6.067	46.167	Hap_169	Western Europe

Table A.3. Classification of the countries of each sample according to global regions.

Region	Countries/ cities
Central Asia	Tajikistan, Turkmenistan
British Isles	Ireland, England, Northern Ireland
Western Europe	Spain, France, Portugal, Switzerland
Central Europe	Germany, Poland, Czech Republic, Slovakia
Eastern Europe	Ukraine, Russia, Romania
Southern Europe	Greece, Italy, Albania, Sicily, Malta, Corsica
Middle East	Syria, Lebanon, Jordan, Iran, Cyprus
North Africa	Morocco, Algeria, Tunisia
Anatolia Türkiye	Akbez, Antalya, Cappadocia, İzmir, Manisa, Yozgat, Yalova, Çanakkale, Bandırma, Bursa
European Türkiye	Edirne, Kıyıköy, Tayakadın, Tekirdağ

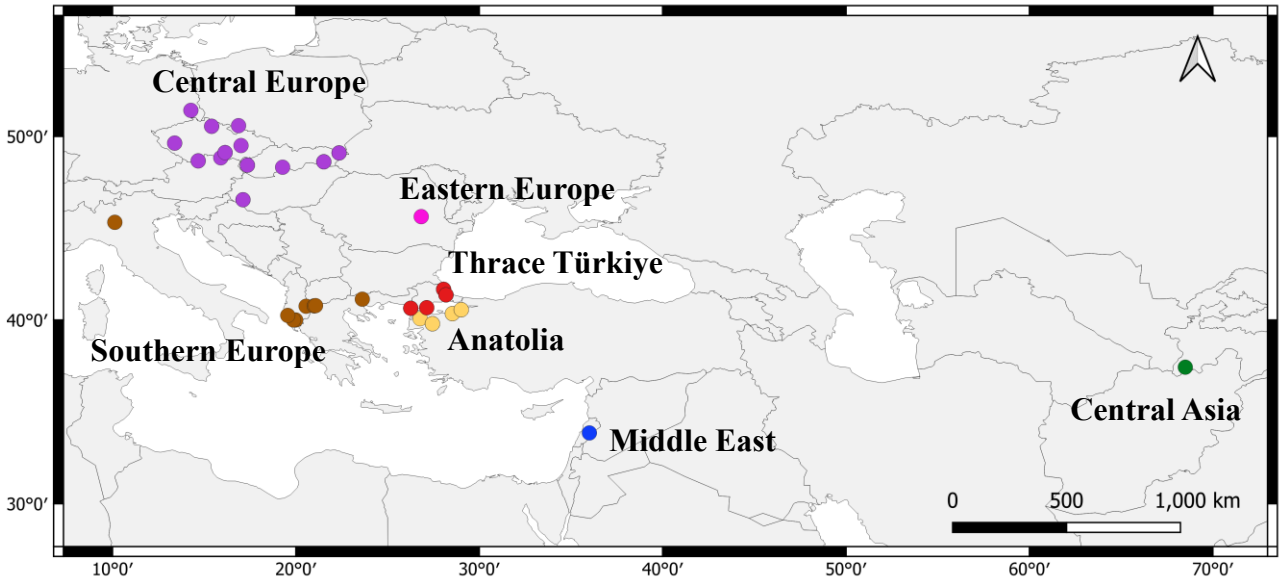


Figure A.1. Geographic distribution of mtDNA haplotypes of the Mixed cluster. Sampling localities are color-coded by geographic region: orange = Anatolia, red = European (Thrace) Türkiye, brown = Southern Europe, pink = Eastern Europe, purple = Central Europe, dark blue = Middle East, and dark green = Central Asia.

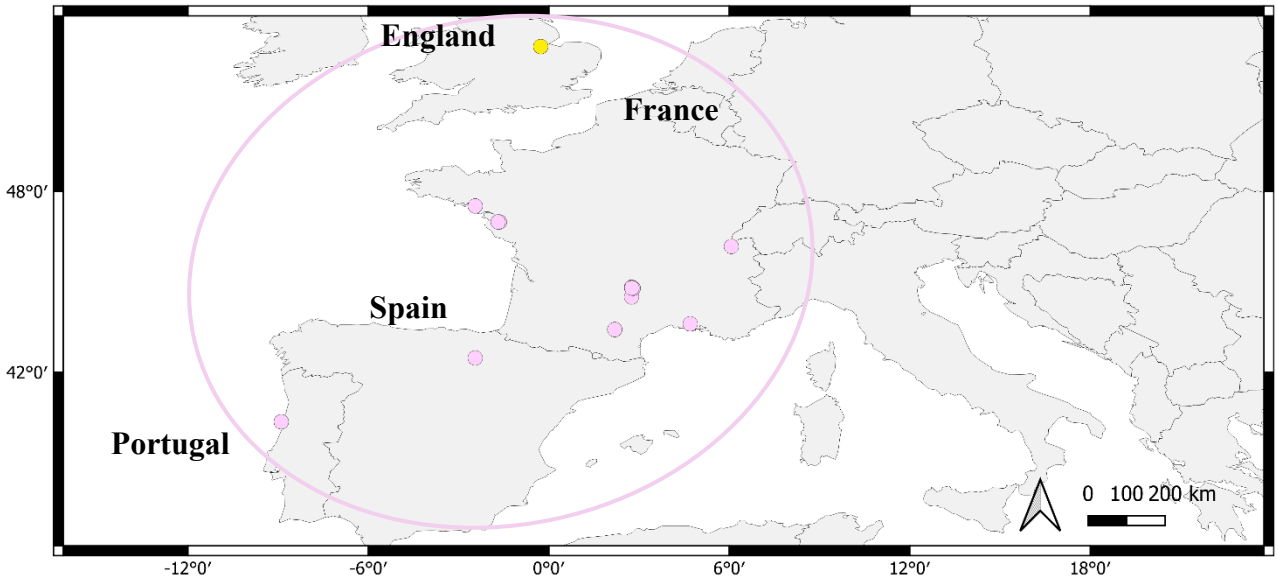


Figure A.2. Geographic distribution of mtDNA haplotypes of the Western Europe cluster. Samples originate from France, Spain, Portugal, and England.

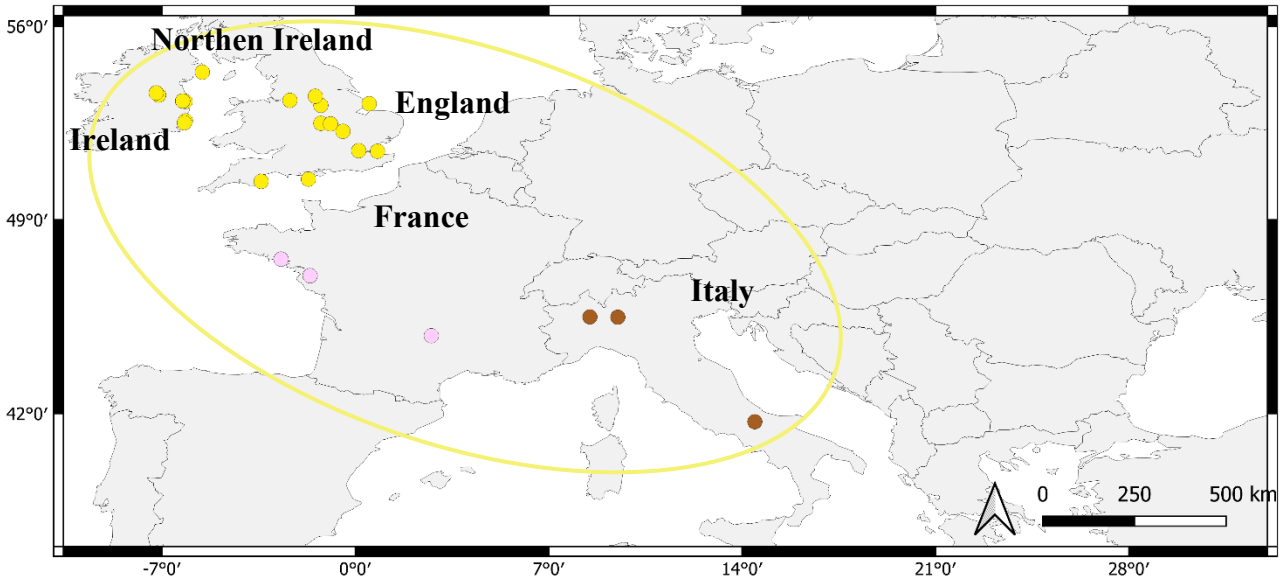


Figure A.3. Geographic distribution of mtDNA haplotypes of the British Isles cluster, including samples from France, Italy, Northern Ireland, Ireland and England.

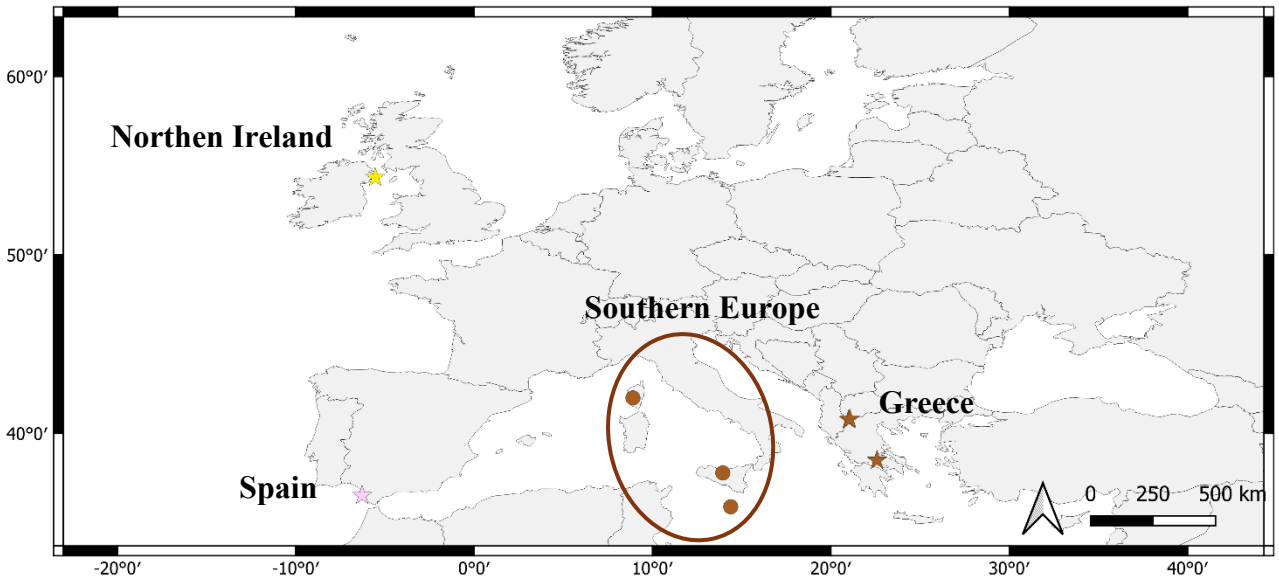


Figure A.4. Geographic distribution of mtDNA haplotypes of the Southern Europe cluster. Samples originate from Sicily, Corsica, and Malta. Star-shaped symbols indicate samples that did not cluster and originate from Greece, Northern Ireland, and Spain.

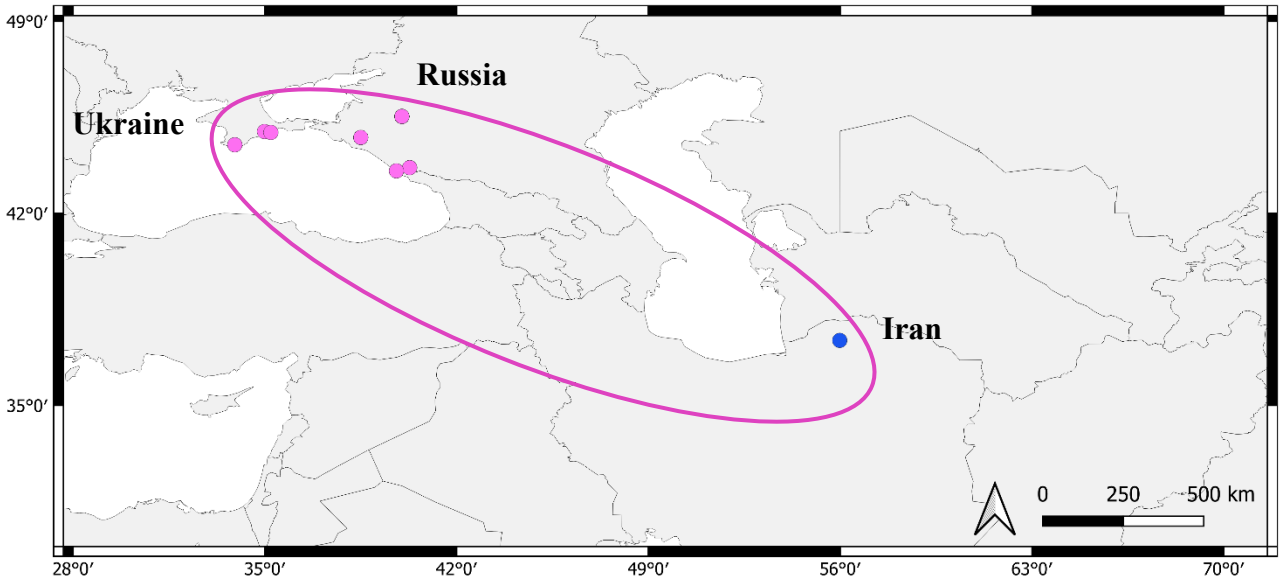


Figure A.5. Geographic distribution of mtDNA haplotypes of the Eastern Europe cluster. Samples originate from Ukraine, Russia and Iran.

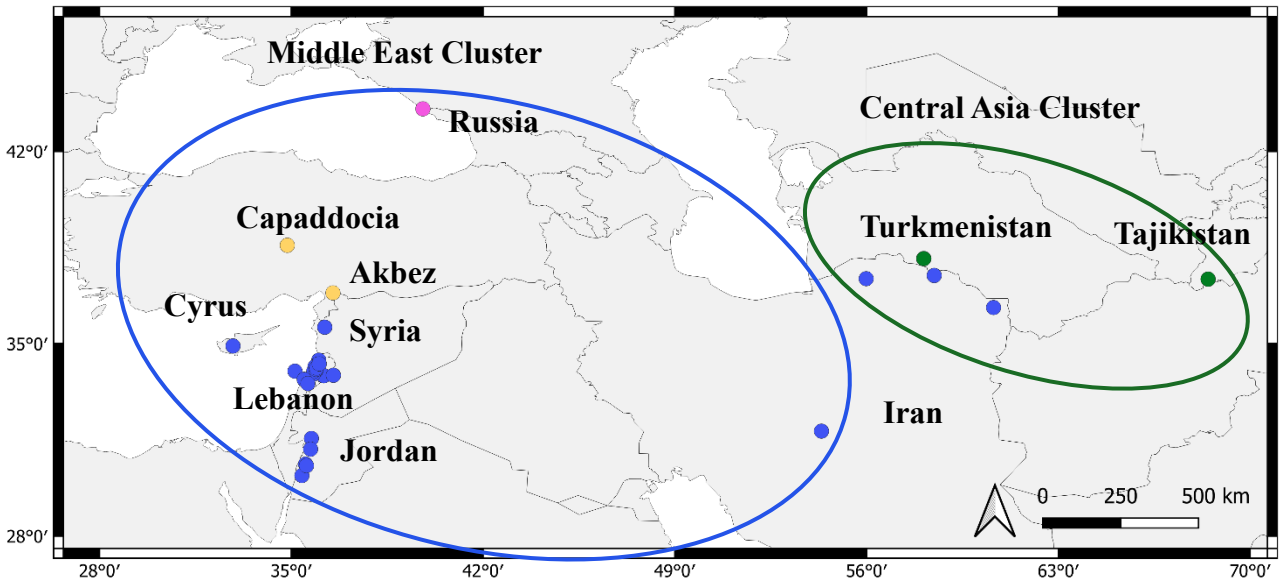


Figure A.6. Geographic distribution of mtDNA haplotypes of the Central Asia and Middle East clusters. The Central Asia cluster (green) includes samples from northeastern Iran, Turkmenistan, and Tajikistan. The Middle East cluster (dark blue) comprises samples from Anatolia, Russia, Cyprus, Lebanon, Syria, Jordan, and one sample from central Iran.

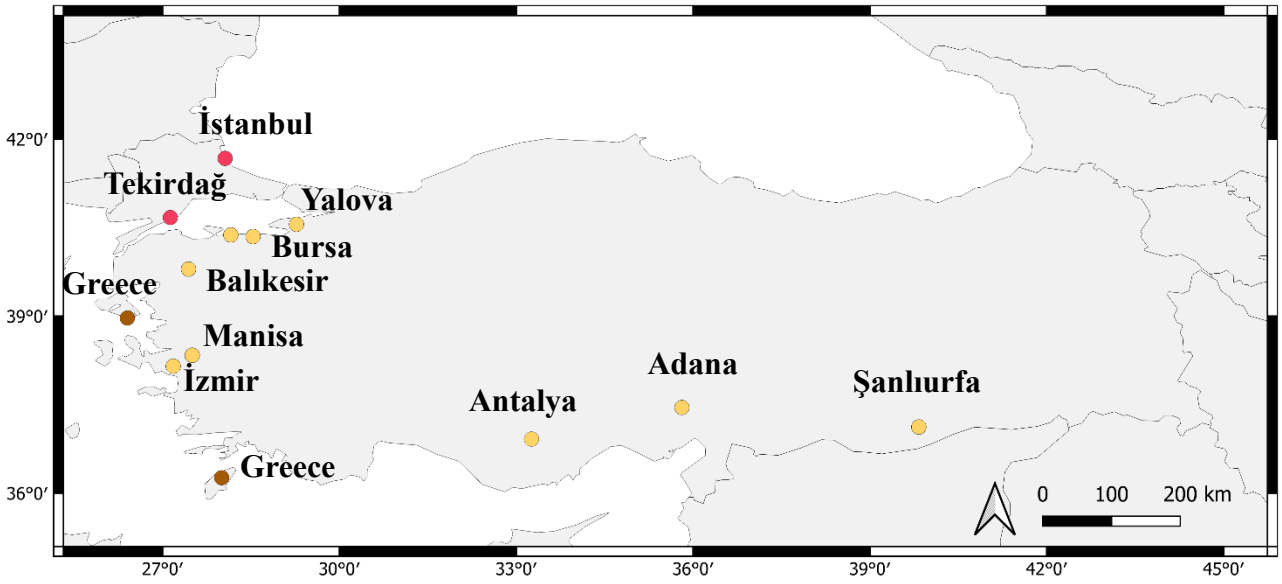


Figure A.7. Geographic distribution of mtDNA haplotypes of the Anatolia cluster.

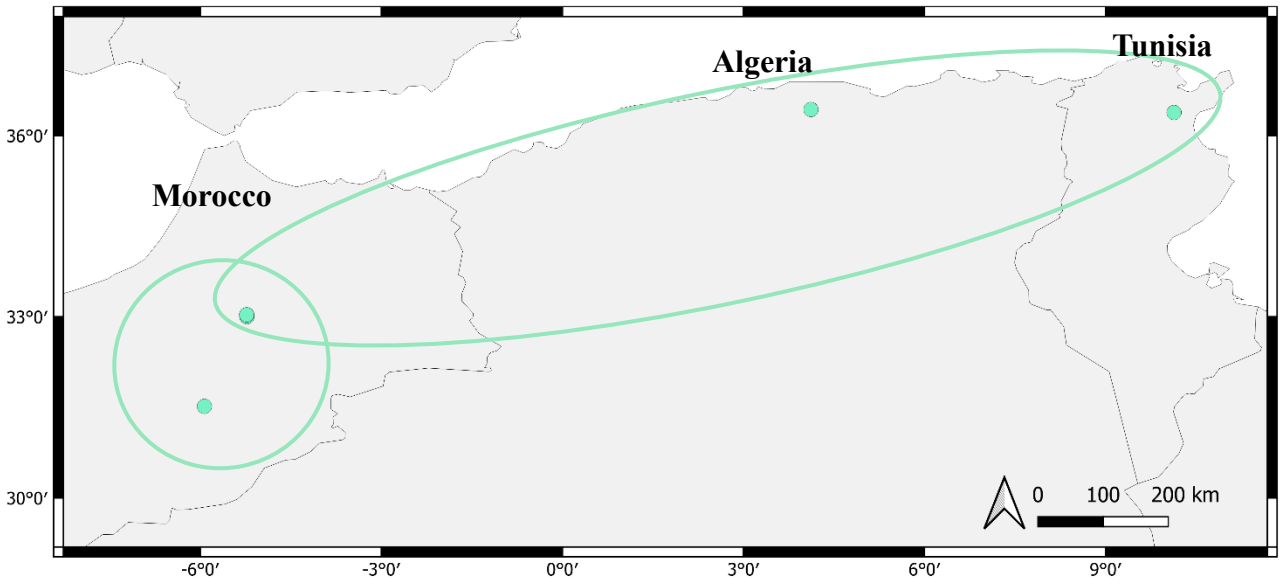


Figure A.8. Geographic distribution of mtDNA haplotypes within the North African clusters. Cluster 1 includes samples from Tunisia, Algeria, and Morocco, whereas Cluster 2 comprises two closely located samples from Morocco.

Table A.4. Nuclear DNA haplotypes (*COPS7A* and *ABHD11*) and sampling coordinates of analyzed individuals.

Geographic region	**Sample name**	**Longitude**	**Latitude**	***COPS7A* haplotype**	***ABHD11* haplotype**
Anatolia	109 Bandirma	28.532	40.348	Hap_1	Hap_14
Anatolia	115 Bandirma	28.532	40.348	Hap_6	Hap_15/ Hap_6

Geographic region	**Sample name**	**Longitude**	**Latitude**	***COPS7A* haplotype**	***ABHD11* haplotype**
Middle East	12 Jordan	35.383	30.200	Hap_1	Hap_6
Middle East	13 Jordan	35.516	30.616	Hap_1	Hap_6
Central Asia	2 Tajikistan	68.467	37.350	Hap_1	Hap_4/ Hap_6
Central Asia	20 Tajikistan	69.867	37.917	Hap_1	Hap_11/ Hap_6
Anatolia	213 Bursa	28.156	40.375	Hap_3/ Hap_1	Hap_4/ Hap_6
Southern Europe	23 Greece	28.117	36.250	Hap_1	Hap_4, Hap10
Central Asia	3 Tajikistan	68.467	37.350	Hap_1	Hap_4
Middle East	30 Lebanon	36.000	34.400	Hap_1	Hap_4/ Hap_6
Anatolia	301 Çanakkale	27.439	39.795	Hap_1	Hap_4/ Hap_6
Anatolia	309 İzmir	27.501	38.335	Hap_1	Hap_6
Anatolia	315 Çanakkale	27.439	39.795	Hap_1	Hap_4
Anatolia	327 Çanakkale	27.439	39.795	Hap_1	Hap_8/ Hap_9
Southern Europe	4 Albania	19.983	40.002	Hap_1	Hap_2
European Türkiye	416 Kiyikoy	28.050	41.670	Hap_1	Hap_16/ Hap_9
European Türkiye	420 (Kiyikoy)	28.050	41.670	Hap_1	Hap_4/ Hap_6
Middle East	48 Jordan	35.550	30.560	Hap_1	Hap_4
Middle East	51 Iran	58.467	37.483	Hap_1	Hap_6
North Africa	56 Morocco	-5.230	33.001	Hap_1	Hap_12 / Hap_13
Anatolia	602 Çannakale	27.439	39.795	Hap_1	Hap_9
Anatolia	611 Çanakkale	27.439	39.795	Hap_6/ Hap_1	Hap_3
European Türkiye	620 Tayakadin	28.180	41.370	Hap_1	Hap_7
European Türkiye	622 (Tayakadin)	28.180	41.370	Hap_1	Hap_4
Anatolia	711 Yalova	29.270	40.555	Hap_1	Hap_4
Anatolia	714 Bursa	28.156	40.375	Hap_1	Hap_6
Anatolia	730 Izmir	27.501	38.335	Hap_2/Hap_1	Hap_4
Eastern Europe	74 Ukraine	33.900	44.500	Hap_4/ Hap_1	Hap_4
European Türkiye	856 (Tekirdag)	27.130	40.670	Hap_6/ Hap_1	Hap_4/ Hap_6
European Türkiye	878 (Tekirdag)	27.130	40.670	Hap_1	Hap_6

Geographic region	Sample name	Longitude	Latitude	*COPS7A* haplotype	*ABHD11* haplotype
Anatolia	İzmir 307	27.501	38.335	Hap_1	Hap_4
Anatolia	İzmir 731	27.501	38.335	Hap_5/ Hap_1	Hap_4
Southern Europe	46 Albania	19.867	40.067	Hap_1	Hap_1

Table A.5. Neutrality test results (Tajima's D and Fu's Fs) based on nuDNA sequences of the intron 4 of the *COPS7A* gene by region.

Region	n	Tajima's D	P-value	Fu's Fs statistic	P-value
Anatolia	28	−1.566	P > 0.10 (ns)	−3.135	P > 0.10 (ns)
Thrace Türkiye	12	−1.141	P > 0.10 (ns)	−0.476	P > 0.10 (ns)
Southern Europe	6	—	No polymorphism	—	No polymorphism
Middle East	10	—	No polymorphism	—	No polymorphism
Central Asia	6	—	No polymorphism	—	No polymorphism

Table A.6. Summary of the species of bat carcasses collected from under different Turbines between March and November (Chapter 2).

Date	Turbine	Species identification	Forearm (mm)	Sample No
2024-03-28	T24	Negative PCR result	32.50	400
2024-03-28	T24	Negative PCR result	32.50	401
2024-03-30	T33	*Pipistrellus nathusii*	35.50	402
2024-04-01	T29	*Pipistrellus nathusii*	34.65	403
2024-04-01	T05	*Pipistrellus nathusii*	31.35	404
2024-04-19	T17	*Pipistrellus nathusii*	36.45	409
2024-04-19	T30	*Pipistrellus nathusii*	33.40	410
2024-04-19	T30	*Pipistrellus nathusii*	34.65	413
2024-04-21	T33	Species not identified	31.45	405
2024-04-27	T25	*Nyctalus leiserii*	44.30	407
2024-04-27	T30	*Pipistrellus nathusii*	34.65	414
2024-04-27	T30	*Nyctalus leiserii*	-	417
2024-04-27	T30	Negative PCR result	30.15	415
2024-04-29	T29	Species not identified	35.60	418
2024-05-08	T15	*Nyctalus leiserii*	45.35	411
2024-07-20	T22	*Nyctalus leiserii*	43.40	422
2024-07-22	T05	*Pipistrellus pipistrellus*	29.90	406
2024-08-10	T31	*Pipistrellus nathusii*	32.80	423
2024-08-11	T21	*Nyctalus leiserii*	42.40	419
2024-08-22	T20	*Pipistrellus nathusii*	33.50	420
2024-08-22	T20	*Pipistrellus nathusii*	34.45	421
2024-08-22	T20	*Nyctalus leiserii*	45.55	424
2024-08-23	T23	*Pipistrellus nathusii*	31.55	426

Date	Turbine	Species identification	Forearm (mm)	Sample No
2024-08-23	T23	*Pipistrellus nathusii*	33.95	427
2024-08-23	T23	*Pipistrellus nathusii*	34.40	428
2024-08-23	T25	*Pipistrellus nathusii*	34.35	425
2024-08-25	T32	*Pipistrellus nathusii*	33.50	431
2024-08-25	T32	*Nyctalus leiserii*	43.55	432
2024-08-25	T31	Species not identified	46.40	416
2024-08-25	T31	*Nyctalus leiserii*	41.65	429
2024-08-25	T31	*Pipistrellus nathusii*	31.60	430
2024-08-26	T07	*Pipistrellus nathusii*	33.90	433
2024-08-26	T03	*Pipistrellus nathusii*	33.80	437
2024-08-28	T17	*Pipistrellus nathusii*	31.80	441
2024-08-28	T18	*Pipistrellus nathusii*	34.10	439
2024-08-28	T18	*Pipistrellus nathusii*	33.10	440
2024-08-28	T18	*Pipistrellus nathusii*	34.10	438
2024-08-28	T18	*Pipistrellus nathusii*	34.00	495
2024-08-28	T16	*Pipistrellus nathusii*	33.90	434
2024-08-31	T34	*Pipistrellus nathusii*	33.35	408
2024-09-04	T27	*Pipistrellus nathusii*	33.85	435
2024-09-05	T16	*Pipistrellus nathusii*	33.30	445
2024-09-09	T06	Negative PCR result	32.75	498
2024-09-09	T06	*Pipistrellus nathusii*	34.10	497
2024-09-09	T01	*Pipistrellus nathusii*	33.70	446
2024-09-09	T20	*Pipistrellus nathusii*	33.00	436
2024-09-11	T16	*Nyctalus leiserii*	42.80	447
2024-09-13	T28	*Pipistrellus nathusii*	32.80	442
2024-09-14	T14	*Pipistrellus nathusii*	33.10	448
2024-09-17	T10	*Pipistrellus nathusii*	33.15	443
2024-09-17	T10	*Pipistrellus nathusii*	32.90	449
2024-09-22	T31	*Pipistrellus nathusii*	32.85	450
2024-09-22	T20	*Nyctalus leiserii*	43.40	452
2024-10-04	T34	*Pipistrellus nathusii*	34.50	454
2024-10-24	T19	*Pipistrellus nathusii*	34.15	457
2024-10-24	T19	*Pipistrellus nathusii*	32.55	458
2024-10-24	T20	*Pipistrellus pipistrellus*	34.15	549
2024-10-24	T20	*Pipistrellus nathusii*	32.50	460
2024-10-24	T20	*Pipistrellus nathusii*	34.10	461
2024-10-24	T20	*Pipistrellus nathusii*	33.40	451
2024-10-24	T20	*Pipistrellus nathusii*	34.50	497
2024-10-24	T20	*Pipistrellus nathusii*	33.10	499
2024-10-24	T20	Negative PCR result	33.40	463
2024-10-24	T17	*Pipistrellus nathusii*	34.10	474
2024-10-24	T17	*Pipistrellus nathusii*	32.55	473
2024-10-24	T24	*Pipistrellus nathusii*	33.85	453
2024-10-24	T24	*Pipistrellus nathusii*	33.90	455
2024-10-24	T24	*Nyctalus leiserii*	44.00	456
2024-10-24	T17	*Pipistrellus nathusii*	34.00	464

Date	Turbine	Species identification	Forearm (mm)	Sample No
2024-10-24	T17	*Pipistrellus nathusii*	34.40	465
2024-10-24	T17	*Pipistrellus nathusii*	33.55	466
2024-11-02	T34	Negative PCR result	42.30	468